

The unusual NF $\kappa$ B inhibitor I $\kappa$ B<sub>NS</sub> regulates Foxp3 expression

**Dissertation**

zur Erlangung des akademischen Grades

**doctor rerum naturalium**

**(Dr. rer. nat.)**

genehmigt durch die Fakultät für Naturwissenschaften  
der Otto-von-Guericke-Universität Magdeburg

von	Dipl.-Biol. Marc Patrick Schuster
geb. am	2. Juli 1982 in Wuppertal
Gutachter	Prof. Dr. Ingo Schmitz PD Dr. Immo Prinz

eingereicht am	24. Februar 2012
verteidigt am	13. September 2012

#### Acknowledgements:

I want to thank my supervisor, Professor Dr. Ingo Schmitz for the interesting and challenging project, a solid introduction in scientific work and our kind and productive relationship. Thanks to my colleagues Tanja, Frida, Michaela, Sabrina, Yvonne, Ralf, Dominique and Carlos, the practical work in the lab was sweetend by a joyful and efficient atmosphere.

I am deeply gratefully to my mother Christa, my brother Frank and my sister Dana for their heartily support and interest in my work. My biggest thank goes to my beloved girlfriend Sabine, who endured a long-distance relationship, which allowed me to finish my thesis at the university of Magdeburg and the HZI in Braunschweig.

## Content

<b>1. Introduction</b> .....	6
1.1 Abstract .....	6
1.2 How the immune system tolerates self.....	7
1.3 Establishing central tolerance in the thymus .....	8
1.4 Peripheral tolerance is maintained by regulatory T cells.....	10
1.5 Suppressor mechanisms of Foxp3 <sup>+</sup> Treg cells.....	12
1.6 Thymus-derived natural regulatory T cells .....	14
1.7 Peripheral and TGF- $\beta$ -induced Tregs.....	16
1.8 Conserved non coding sequences regulate Foxp3 expression .....	18
1.9 Signalling of Nuclear Factor $\kappa$ B.....	19
1.10 Atypical BCL-3 type I $\kappa$ B proteins.....	23
1.11 Identification and function of I $\kappa$ B <sub>NS</sub> .....	25
1.12 The regulation of Foxp3 by NF $\kappa$ B signalling .....	26
1.13 Aims .....	29
<b>2. Materials</b> .....	30
2.1 Chemicals.....	30
2.2 Cell culture material and devices .....	30
2.2.1 Cell culture media and supplements .....	31
2.2.2 Medium for <i>in vitro</i> differentiation and expansion of primary T cells .....	31
2.2.3 Cytokines and chemicals used for T cell stimulation.....	31
2.2.4 Antibodies and reagents used in cell culture.....	32
2.3 Materials and reagents for flow cytometry.....	32
2.3.1 Devices.....	32
2.3.2 Fluorescent dyes .....	32
2.3.3 Fluorochrome-labeled antibodies .....	33
2.4 Mouse strains .....	34
2.5 Reagents and Materials used for Western blotting .....	34
2.5.1 Primary antibodies.....	34
2.5.2 Horseradish peroxidase-conjugated secondary antibodies .....	35
2.6 Oligonucleotides.....	36
2.6.1 Oligonucleotides for GST-DNA-pulldown .....	36
2.6.2 Oligonucleotides for PCR .....	37
2.7 Frequently used buffers.....	38

<b>3. Experimental Procedures</b> .....	39
3.1 Molecular biology methods.....	39
3.1.1 Isolation of eukaryotic RNA.....	39
3.1.2 Preparation of eukaryotic chromosomal DNA .....	39
3.1.3 Photometric determination of DNA/RNA concentration.....	39
3.1.4 Reverse transcription .....	39
3.1.5 Polymerase chain reaction .....	40
3.1.6 Analytic agarose gels .....	41
3.1.7 DNA methylation analyses .....	41
3.1.8 DNA pulldown.....	41
3.1.9 Luciferase-Assays .....	41
3.2 Proteinbiochemical procedures .....	42
3.2.1 Cell Lysis .....	42
3.2.2 Fractionised cell lysis .....	42
3.2.3 Determination of protein concentration by bicinchoninic acid .....	43
3.2.4 Determination of protein concentration by Bradford.....	43
3.2.5 Immunoprecipitation .....	44
3.2.6 SDS-PAGE.....	44
3.2.7 Western blotting .....	44
3.3 Cellular and mouse surgical methods .....	45
3.3.1 Isolation of lymphoid organs from mice.....	45
3.3.2 Flow cytometry analysis .....	45
3.3.3 Cell isolation via flow cytometry .....	45
3.3.4 Expansion of CD4 <sup>+</sup> CD25 <sup>-</sup> T cells <i>in vitro</i> .....	45
3.3.5 <i>In vitro</i> Treg suppression assay .....	46
3.3.6 Generation of iTregs via TGF- $\beta$ <i>in vitro</i> .....	46
3.3.7 Proliferation analyses via 5' bromodeoxyuridine .....	46
3.3.8 Generation of mixed bone-marrow chimeric mice.....	46
3.3.9 IL-2 mediated expansion of regulatory T cells <i>in vivo</i> .....	47
3.3.10 Adoptive transfer colitis .....	47
3.3.11 Colon organ cultures .....	48
3.4 Statistics .....	48

<b>4 Results</b> .....	49
4.1 I $\kappa$ B <sub>NS</sub> deficiency intrinsically causes reduced Foxp3 <sup>+</sup> cells <i>in vivo</i> and <i>in vitro</i> .....	49
4.2 Functionality of Tregs from I $\kappa$ B <sub>NS</sub> -deficient mice is not altered .....	56
4.3 I $\kappa$ B <sub>NS</sub> -deficient Treg cells display enhanced proliferation but normal apoptosis .....	63
4.4 Followed from defective Foxp3 induction thymic Treg precursor cells accumulate in I $\kappa$ B <sub>NS</sub> -deficient mice.....	69
4.5 I $\kappa$ B <sub>NS</sub> is expressed during thymic Treg development and interacts with p50 and c-Rel at the regulatory elements CNS2 and CNS3 within the <i>Foxp3</i> gene .....	74
4.6 Adoptively transferred I $\kappa$ B <sub>NS</sub> -deficient T cells fail to differentiate in a protective Treg compartment, whereby chronic gut inflammation is exacerbated .....	81
<b>5 Discussion</b> .....	87
5.1 I $\kappa$ B <sub>NS</sub> deficiency results in a massively reduced Treg compartment, comparable to c-Rel deficiency .....	87
5.2 Treg precursor accumulation follows from delayed Foxp3 induction .....	89
5.3 I $\kappa$ B <sub>NS</sub> –deficient Tregs undergo enhanced proliferation .....	90
5.4 Nuclear p50 and c-Rel interacts with 70 kDa and 35 kDa I $\kappa$ B <sub>NS</sub> .....	91
5.5 CNS2 and CNS3 are targeted by I $\kappa$ B <sub>NS</sub> .....	93
5.6 I $\kappa$ B <sub>NS</sub> deficiency does not alter Treg functioning, but affects Treg generation during chronic gut inflammation .....	95
5.7 Concluding remarks and model.....	97
<b>6. Abbreviations</b> .....	99
<b>7. References</b> .....	102
<b>8. Declaration of originality</b> .....	113
<b>9. Curriculum vitae</b> .....	114

---

# 1. Introduction

## 1.1 Abstract

This study demonstrates that the unusual NF $\kappa$ B inhibitor I $\kappa$ B<sub>NS</sub> is a novel regulator of the forkhead box P3 transcription factor 3 (Foxp3). Foxp3 entirely governs the development and functioning of immune suppressive regulatory T cells (Tregs). Flow cytometrical analyses uncovered a reduction of regulatory T cells by 50% in I $\kappa$ B<sub>NS</sub>-deficient mice. Nevertheless, mature Tregs, although reduced in number, displayed a normal phenotype and suppressive functioning. The generation of mixed bone marrow chimeric mice demonstrated that I $\kappa$ B<sub>NS</sub> must control Treg development by an intrinsic mechanism. This effect was proven to be distinct from reduced proliferation or enhanced apoptosis.

Analyses of Treg precursor cells from the thymus of I $\kappa$ B<sub>NS</sub>-deficient mice revealed their reduced transition from the immature Foxp3<sup>-</sup> precursor into the mature Foxp3<sup>+</sup> Treg state, followed from delayed Foxp3 induction. In contrast to studies using other NF $\kappa$ B-compromised mice, which display reduction of regulatory T cells as well, generation of thymic Treg precursor cells was not affected in I $\kappa$ B<sub>NS</sub>-deficient mice. On the molecular level, I $\kappa$ B<sub>NS</sub> expression was found in these Treg precursor cells in the thymus, but also by other thymic subsets. Using CD4<sup>+</sup>CD25<sup>-</sup> T cells as a model system, interaction of I $\kappa$ B<sub>NS</sub> with p50 and c-Rel on the molecular level was detected. Within the Foxp3 locus I $\kappa$ B<sub>NS</sub> bound to the conserved non-coding sequences CNS2 and CNS3 and luciferase constructs containing CNS2 expressed in primary T cells from I $\kappa$ B<sub>NS</sub>-deficient mice showed reduced transcriptional activity.

The *in vivo* relevance of impaired Treg generation was analysed by a transfer colitis model. I $\kappa$ B<sub>NS</sub>-deficient T cells adoptively transferred into RAG-deficient mice developed to a weaker extent in Foxp3<sup>+</sup> Treg cells compared to wildtype controls. Thereby colitis was exacerbated in recipients of I $\kappa$ B<sub>NS</sub>-deficient T cells.

---

## 1.2 How the immune system tolerates self

The immune system permanently encounters self and foreign antigens and is thereby challenged to specify its response on harmful pathogens and cancer cells and to tolerate self antigens and commensal microbial environments (Gregersen and Behrens, 2006; Kyewski and Klein, 2006; Liston et al., 2005; Sakaguchi et al., 2006b). As the immune system consists of innate and adaptive immune cells, separate tolerance mechanisms have developed. Innate immune cells, like macrophages and dendritic cells (DCs) recognize specific microbial motifs, the pathogen associated molecular patterns (PAMPs) (Boller and Felix, 2009). PAMPs are vital components of the bacterial cell physiology, like lipopolysaccharides (LPS) and mannose, which are integrated in the bacterial cell wall or microbial-specific nucleic acids like double-stranded ribonucleic acid (dsRNA) (Raetz and Whitfield, 2002; Stewart et al., 2006). In contrast to innate immune cells the pathogen-specificities of adaptive immune cells, most prominently  $\alpha\beta$ T and B cells, derive from stochastic rearrangement processes of the gene segments encoding the chains of the T cell receptor (TCR) and the immunoglobulin (Ig) (Davis et al., 1993; Germain, 2002; Zuniga-Pflucker, 2004). Due to the random rearrangement process of the TCR autoreactive T cell clones are regularly generated (Sprent and Kishimoto, 2001; von Boehmer et al., 1989). Their apoptosis in the last maturation steps in the thymus, which is called negative selection, prevents autoimmunity and specifies the reactivity of the T cell compartment towards foreign antigens (Sprent and Kishimoto, 2001; von Boehmer et al., 1989). Elimination of self reactive B cells by apoptosis or receptor editing takes place in the bone marrow, lymph nodes and the spleen (Sandek et al., 1999). The depletion of autoreactive cells from the adaptive immune compartment is the basis of so the called central tolerance (Hogquist et al., 2005; Lederberg, 1959). A minority of the autoreactive cells, however, escape their apoptotic deletion and migrate into the peripheral lymphoid organs. Their activation is inhibited by a second mechanism, the peripheral tolerance, which is achieved by Treg-mediated immune suppression.

---

### 1.3 Establishing central tolerance in the thymus

At the beginning of  $\alpha\beta$ T cell development haematopoietic precursor cells enter the thymus at the cortical-medullary border (Germain, 2002; Schwarz and Bhandoola, 2006). In this stage, their developmental fate in  $CD4^+$  helper or  $CD8^+$  cytotoxic T cells is not yet determined and they appear as  $CD4^-CD8^-$  double negative cells (Liston et al., 2005). Within the outer cortex, the gene segments of the  $\alpha$ - and  $\beta$ -chain of the T cell receptor (TCR) are stochastically rearranged in a process termed V(D)J-recombination (Davis and Bjorkman, 1988; Tonegawa, 1983). The stages of gene-rearrangement in DN cells are associated with sequential expression of CD25 and CD44 and results in the assembly of a pre TCR (Fig. 1) (Pearse et al., 1989; Shortman, 1992). If signalling via the pre TCR is malfunctioning, cells die by neglect (von Boehmer et al., 1989). The remaining cells upregulate the co-receptors CD4 and CD8 (Alam et al., 1999). These double positive cells make up about 85% of the thymocytes and are exposed to self-peptides by the major histocompatibility complexes (MHCs) of medullary thymic epithelial cells (mTECs) (Alam et al., 1996; Kyewski and Klein, 2006; Sprent and Kishimoto, 2001; von Boehmer, 1991; von Boehmer et al., 1989; Zuniga-Pflucker, 2004). mTECs express a transcription factor, termed autoimmune regulator (AIRE), which induces promiscuous expression of proteins from different tissues, whose fragments are presented to DP cells via MHC class I and MHC class II after proteolytical degradation (Heino et al., 1996). If the T cell receptor of DP cells strongly recognizes presented self-peptides the DP cell undergoes apoptosis (Alam et al., 1996; Kyewski and Klein, 2006; Sprent and Kishimoto, 2001; von Boehmer, 1991; von Boehmer et al., 1989; Zuniga-Pflucker, 2004). Non-autoreactive T cells are positively selected, develop into  $CD4^+$  or  $CD8^+$  single positive cells, depending on their binding to MHC class II or MHC class I, respectively, are again checked for their autoreactivity and leave the thymus (Goldrath and Bevan, 1999). The mechanism, which decides about a CD4 or CD8 fate is not completely understood. Loss of central tolerance, for example due to functional loss of AIRE, leads to the autoimmune polyendocrinopathy syndrome type-1 (APS-1), as autoreactive T cells are not deleted from the repertoire (Bensing et al., 2007a; Bensing et al., 2007b; Ramsey et al., 2002).

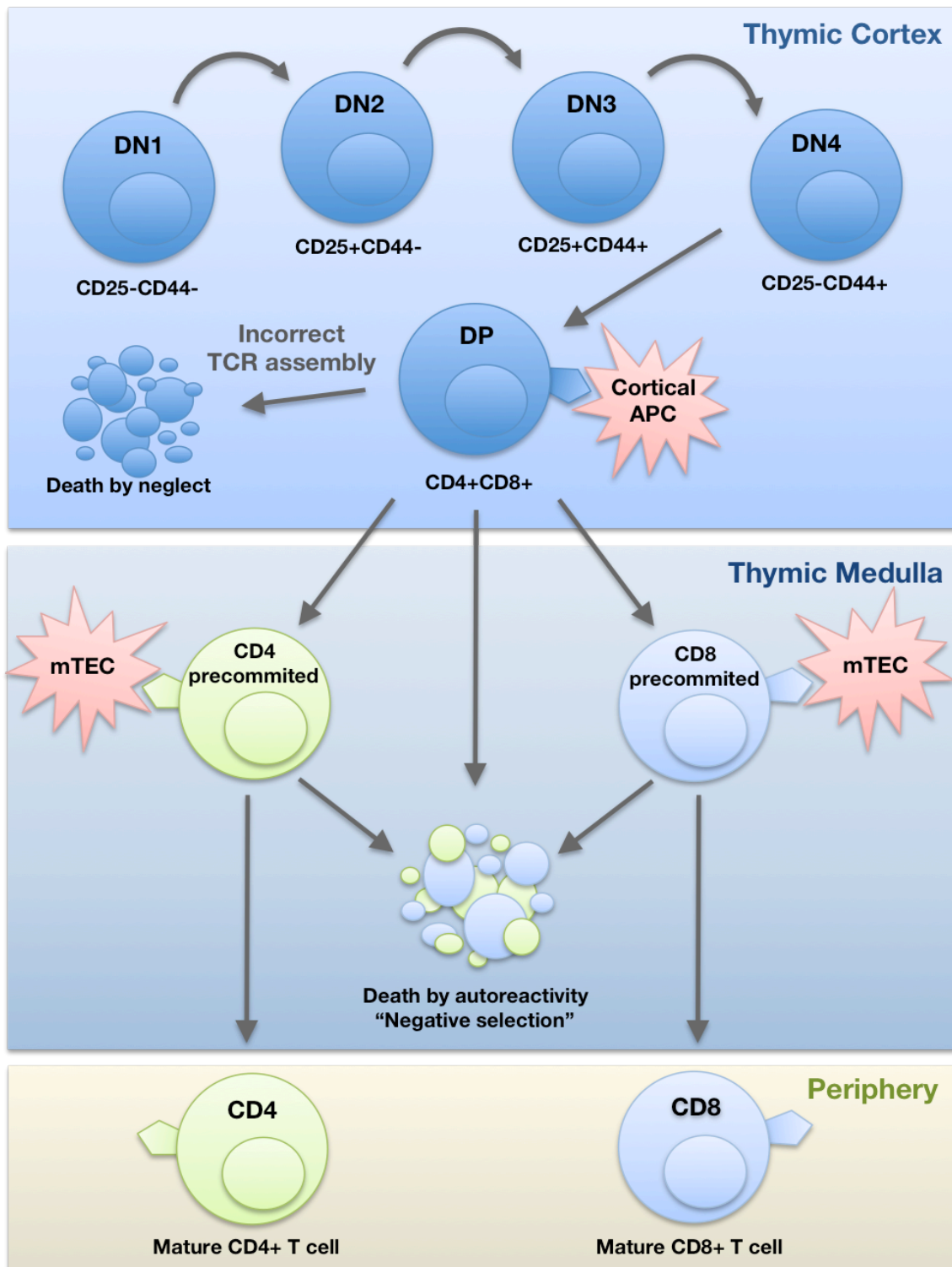


**Figure 1: Maturation and selection of thymic T cells**

CD4<sup>+</sup>CD8<sup>-</sup> stem cell precursors enter the thymus in the outer cortex. Within, they develop from DN1 CD25<sup>-</sup>CD44<sup>+</sup> to DN2 CD25<sup>+</sup>CD44<sup>+</sup> and to DN3 CD25<sup>+</sup>CD44<sup>-</sup> and finally to DN4 CD25<sup>-</sup>CD44<sup>-</sup> cells, associated with the stages of  $\alpha\beta$ TCR recombination. Once TCR is assembled it turns into a CD4<sup>+</sup>CD8<sup>+</sup> double positive cell. Functionality of TCRs is controlled, thought by cortical APCs, whereby defective signalling leads to death by neglect. The autoreactivity is controlled in the CD4<sup>+</sup>CD8<sup>+</sup>, CD4<sup>+</sup>CD8<sup>-</sup> and CD4<sup>-</sup>CD8<sup>+</sup> stages, whereby T cells detecting self-peptides undergo apoptosis, so called negative selection. If cells are not detecting self peptides they leave the thymus as CD4<sup>+</sup> or CD8<sup>+</sup> cells and migrate into the periphery.

---

Even if negative selection is not perturbed by AIRE mutations, a minority of autoreactive T cells escapes negative selection, develop in mature CD4<sup>+</sup> or CD8<sup>+</sup> cells and emigrates the thymus (Mueller, 2010). As negative selection does not completely exclude development of autoreactive cells, a peripheral tolerance mechanism is essential to prevent autoimmunity.

#### **1.4 Peripheral tolerance is maintained by regulatory T cells**

The simplest way to guarantee peripheral tolerance is compartmentalization of critical tissues containing self-antigens from circulating autoreactive cells. The blood-brain barrier separates most immune from neuronal cells and the epithelial barriers in the gut, lung and oral cavity isolate the microbial microflora from immune recognition (Siddiqui and Powrie, 2008; Waubant, 2006). Another way of peripheral tolerance represents so called immune privileged areas, like the testes and the placenta. Expression of the indolamine 2,3 dioxygenase (IDO) in the placenta cleaves L-tryptophan to N-formylkynurenine leading to a microenvironment insufficient for L-tryptophan-dependent lymphocyte proliferation (Munn et al., 1998; Takikawa, 2005). Anergy of T cells, occurring after TCR triggering without costimulation of inflammatory signals, which indicate an infection, inactivates autoreactive T cells as well (Schwartz, 2003). However, the key mechanism of peripheral tolerance is the generation of a threshold of T cell activation by suppressive immune cells (Sakaguchi et al., 1995; Sakaguchi et al., 2007). Tr1 and T<sub>H</sub>3 cells secreting the immunosuppressive cytokines interleukin-10 (IL-10) and transforming growth factor  $\beta$  (TGF- $\beta$ ) are most prominent in the intestine. The vast majority of suppressor cells, which make up to 10-15% of the CD4<sup>+</sup> T cell compartment are Tregs, which express the forkhead box P3 transcription factor, Foxp3, and interleukin-2 receptor  $\alpha$  chain (CD25) (Sakaguchi et al., 2006a; Sakaguchi et al., 1995). Whereas Tr1 and T<sub>H</sub>3 cells are restricted to the gut, Foxp3<sup>+</sup> Tregs can be found throughout all lymphoid tissues. Remarkably, their pure existence was for a long time controversially discussed (Sakaguchi et al., 1995).

A suppressive regulatory T cell (Treg) compartment restricts induction, strength and duration of an immune response by generating a threshold for the activation of immune effector cells,

---

thereby causing peripheral tolerance (Hori et al., 2003; Mueller, 2010; Sakaguchi et al., 2007). The established threshold protects the host from autoimmunity due to inhibition of peripheral autoreactive T cells, which escaped negative selection. Therefore, compromised Treg development and function are associated with autoimmune diseases like multiple sclerosis and diabetes mellitus (Sakaguchi et al., 2001). The complete loss of a protective Treg compartment peaks in a fatal systemic autoimmune disease, termed idiopathic polyendocrinopathy X-linked (IPEX) syndrome and the corresponding murine phenotype *scurfy* (Bennett et al., 2001; Bennett and Ochs, 2001; Brunkow et al., 2001; Lahl et al., 2007; Wildin et al., 2001). On the other hand, accumulation of Tregs in the vicinity of solid tumours causes their protection from recognition and elimination by the immune system as a reason of localized immune suppression (Crimeen-Irwin et al., 2005; Klages et al., 2010). Therefore, dysregulation of the regulatory T cell compartment can cause autoimmune diseases or carries tumor protection, underlining the importance of the balance between suppressor and effector cells for immune homeostasis (Crimeen-Irwin et al., 2005). Thus, the modulation of Treg development or Treg suppressor strength represents a promising approach for the treatment of autoimmunity and cancer (Crimeen-Irwin et al., 2005). It is also considered to use adoptive transfer of antigen-specific Tregs to increase the acceptance of transplanted organs by the host immune system (Huehn et al., 2009; Sakaguchi et al., 2001).

The development of those Treg-based therapies needs an understanding of Treg differentiation and suppressor mechanisms. Therefore, the underlying molecular signalling events are in the focus of current research. Substantial progress was reported in the understanding of suppressor mechanisms, which either interfere directly with effector cell activity or influence T cell maturation at antigen presenting cells (APCs) (Vignali, 2008; Vignali et al., 2008). It is also widely accepted, that the stability of a mature Treg compartment is guaranteed by epigenetic regulation (Floess et al., 2007; Huehn et al., 2009; Toker and Huehn, 2011). However, the orchestration of environmental and molecular signals, which force Treg development remain marginally understood and require further investigation to understand immune tolerance entirely.

---

Taken together, central tolerance means the restriction of T cell specificity to foreign antigens by elimination of autoreactive cells, whereas Treg-mediated peripheral tolerance thresholds T cell activation by suppressor mechanisms.

### **1.5 Suppressor mechanisms of Foxp3<sup>+</sup> Treg cells**

Regulatory T cells do not inhibit effector cell activation by a single mechanism (Vignali, 2008; von Boehmer, 2005). The cooperation between the different suppressor mechanisms is not completely understood, but it is likely, that the environmental conditions, the target cell type and the hosts immune condition determine the most effective suppressor mechanism *in vivo*. Treg suppression occurs in a contact-dependent as well as -independent fashion. Among the secretory mechanisms, release of the cytokines transforming growth factor  $\beta$  (TGF- $\beta$ ), interleukin-10 (IL-10) and interleukin-35 (IL-35) reduces effector cell activity (Fig. 2a) (Asseman et al., 1999; Collison et al., 2007; Nakamura et al., 2001). However to which extent these cytokines contribute to the suppressive capacity of Treg cells is still a matter of debate (Pillai et al., 2011). Usage of unresponsive cells or blocking antibodies, which neutralized soluble TGF- $\beta$  or IL-10 *in vitro* did not sufficiently impair Treg-mediated suppression (Pillai et al., 2011). However, IL-10 secretion was essential to prevent exacerbated colitis in mouse models of inflammatory bowel disease (IBD) and concanavalin—A induced hepatitis (Hawrylowicz and O'Garra, 2005). Although the role of soluble TGF- $\beta$  seems to be less important, membrane-bound TGF- $\beta$  suppressed allergic responses and colitis in IBD models in a cell contact-dependent manner (Nakamura et al., 2001). It was also shown that membrane-bound TGF- $\beta$  in tumor-associated Tregs enhances tumor immuno-surveillance (Liu et al., 2007). IL-35 is a heterodimer composed of Epstein-Barr virus-induced gene 3 (*Ebi3*) and Interleukin-12a (IL-12a), whose expression in regulatory T cells was suggested as a central suppressive cytokine (Collison et al., 2007; Pillai et al., 2011). Deficiency of *Ebi3* or *IL-12a* significantly reduces the suppressive capacity of Tregs *in vitro* and *in vivo* in IBD, underlining its role as a key cytokine in Treg function (Collison et al., 2007; Didierlaurent et al., 2005; Pillai et al., 2011). Another route of contact-

independent suppression is effector cell cytolysis or cell death as a result of cytokine deprivation (Fig. 2b). Tregs have been reported to secrete the serine proteases Granzyme A and Granzyme B, to interfere with the viability of target cells and release of perforin results in the formation of a lysis pore in the targeted effector cell and subsequently in apoptotic cell death (Gondek et al., 2005; Grossman et al., 2004). A remarkable way to interfere with effector cell viability is consumption of Interleukin-2 (IL-2) (Duthoit et al., 2005; Fontenot et al., 2005). Via CD25, Treg cells are able to bind large amounts of IL-2, which usually promotes activation and clonal expansion of activated effector T cells, whereby cytokine deprivation leads to effector cell death (Fig. 2c) (Duthoit et al., 2005; Fontenot et al., 2005).

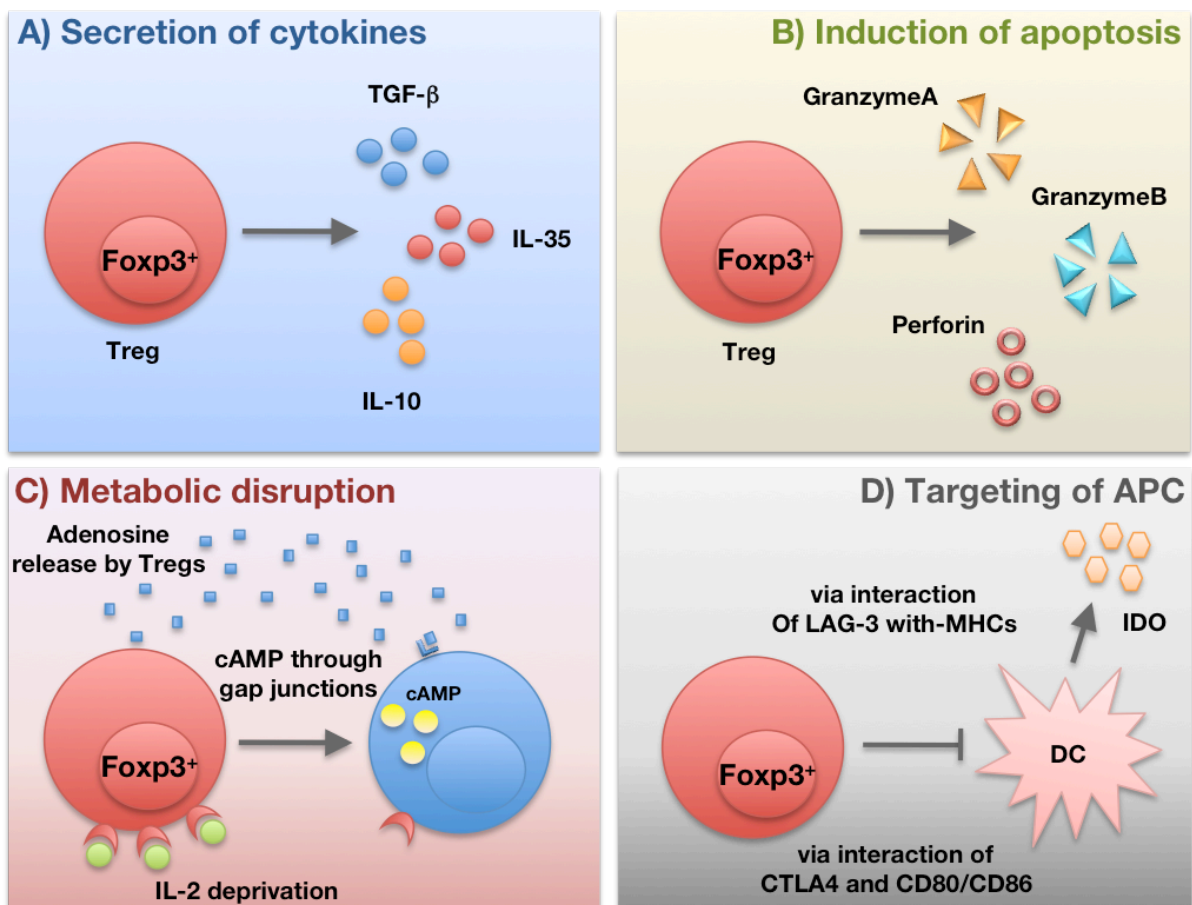


**Figure 2: Examples of suppressor mechanisms used by regulatory T cells**

(a) Secretion of inhibitory cytokines IL-10, IL-35 and TGF- $\beta$  directly reduce effector T cell activity. Membrane-anchored TGF- $\beta$  serves as an additional source of suppression. (b) Cytolysis of effector cells by granzyme A and granzyme B leads to cell death. Generation of a perforine pore induces apoptosis of effector cells. (c) Tregs interfere with the metabolism of effector cells via transfer of cyclic AMP through gap junctions. Alternatively, Tregs consume IL-2 via CD25 from activated effector T cells reducing their proliferation and survival. (d) CTLA-4 and the CD4-homolog LAG3 are expressed on T cells, leading to competition with activation of effector cells via binding of CD80/CD86 and MHC class II. CD80/CD86 engagement can induce IDO-release, resulting in tryptophane deprivation.

---

It has also been shown that IL-2 signaling is important for Treg maintenance, as it ensures Treg survival and forces expression of the transcription factor Foxp3 via signal transducer and activator of transcription 5 (STAT5) (Burchill et al., 2007). Therefore, IL-2 consumption appears not only as a mechanism to suppress effector cells, but also to ensure Foxp3 maintenance. However, the mechanisms described above interfere directly with activated effector cell function or viability, but Tregs are also reported to inhibit T cell activation by targeting MHCs and the costimulatory proteins CD80/CD86 expressed by DCs (Tang et al., 2006). For this reason Tregs express high amounts of cytotoxic T-lymphocyte antigen-4 (CTLA-4), the interaction partner of CD80/CD86 and lymphocyte activation gene 3 (Lag-3), a CD4 homolog reported to associate with MHC class II (Fig. 2d) (Fallarino et al., 2003; Read et al., 2000).

Manipulation of the described suppressor mechanisms represents one hypothetical way of using Tregs in therapy. Another idea is the modulation of the quantity of the Treg compartment. This requires understanding of the regulation of the master transcription factor Foxp3, which controls Treg development. Of note, the Treg pool consists of cells originating from the thymus and the peripheral lymphoid organs (Fig. 3) (Huehn et al., 2009).

### **1.6 Thymus-derived natural regulatory T cells**

Comparison of TCR specificities between regulatory and conventional T cells revealed only minimal overlap in their antigen recognition (Aschenbrenner et al., 2007). Surprisingly, the majority of TCRs expressed by Treg cells detected self-peptides, indicating that T cells, which escaped negative selection in the thymus are partially converted into Tregs to prevent their activation as autoreactive effector cells (Apostolou et al., 2002; Hsieh et al., 2004). One of the current models of thymic nTreg development suggests commitment of autoreactive T cells to the Treg lineage prior to negative selection (van Santen et al., 2004). The more accepted alternative model predicts that combined TCR- and cytokine-mediated signals during negative selection protect Treg precursors from apoptosis and lead to Foxp3 induction (Lio and Hsieh, 2008).

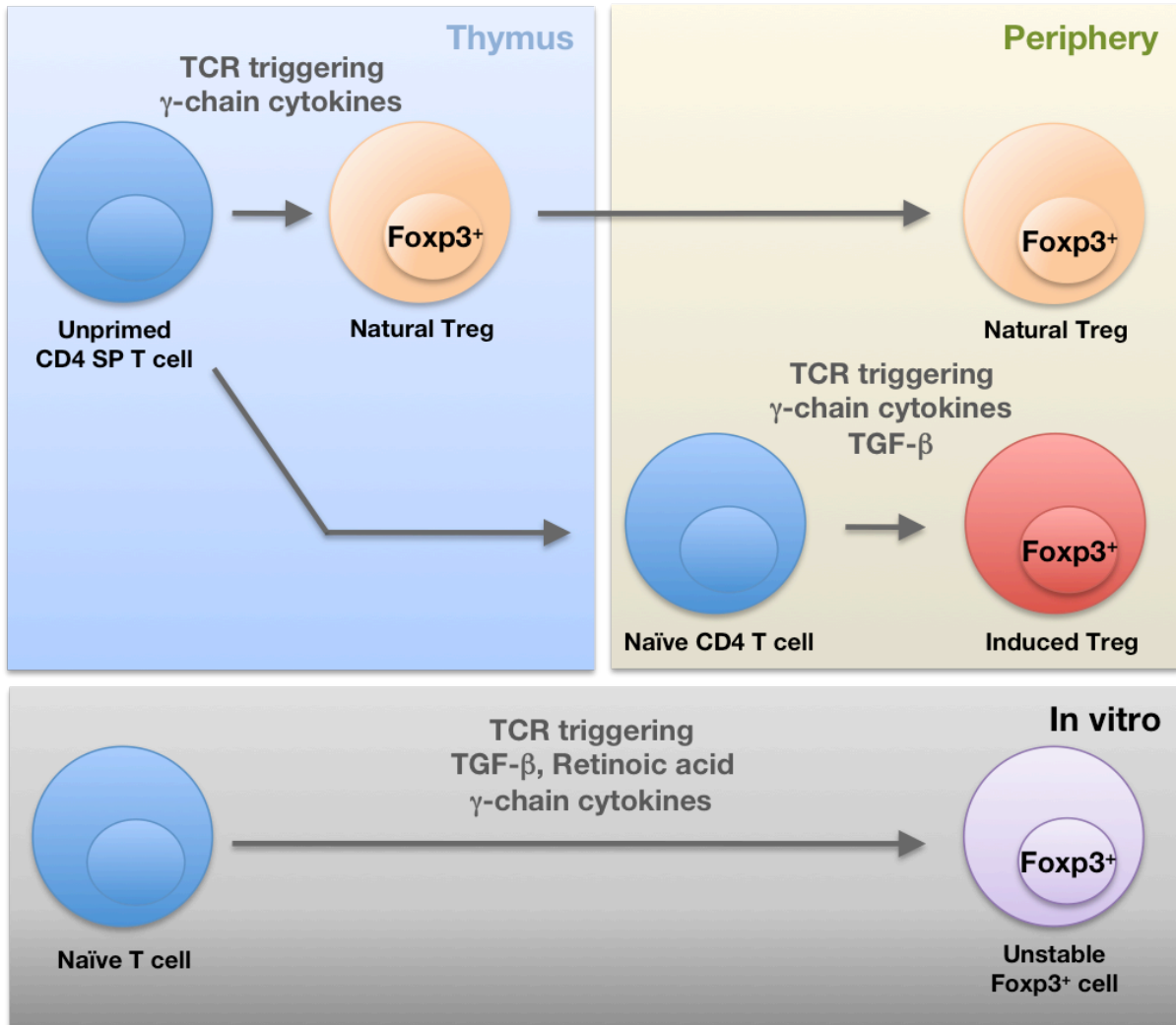


**Figure 3: Foxp3 induction during nTreg and iTreg development and *in vitro***

nTreg cells originate from autoreactive cells in the thymus, whose transition into Foxp3<sup>+</sup> cells is induced by common γ-chain cytokine signaling. After leaving the thymus, these cells undergo homeostatic proliferation in an IL-2-dependent manner and circulate to the periphery. iTreg cells develop in the periphery from Foxp3<sup>-</sup> naïve CD4<sup>+</sup> T cells in an antigen-induced fashion. Their generation is usually occurring in tissues, which require an increased tolerogenic compartment, like the Gut-Associated Lymphoid Tissues (GALT). Their differentiation appears to depend on TGF-β and possibly retinoic acids. *In vitro* Foxp3<sup>+</sup> cells are induced by TGF-β treatment and TCR-triggering, but Foxp3 expression is not maintained, upon removal of TGF-β.

Experimental data favours the second model, since a population of thymic nTreg precursors was identified, which is induced by TCR triggering and converted into Foxp3<sup>+</sup> Tregs by common γ-chain cytokine signalling (γc) (Lio and Hsieh, 2008; Vang et al., 2008). The latter, also referred as “two-step” model argues, that CD4<sup>+</sup>GITR<sup>+</sup>CD25<sup>+</sup>Foxp3<sup>-</sup> cells represent regulatory T cell precursors. By the expression of GITR and CD25 these precursors are already positive for two key markers of mature Treg cells, but negative for Foxp3. Its

---

upregulation is induced by the  $\gamma$ -cytokines IL-2 and IL-15 and to a weaker extent by IL-7 (Vang et al., 2008). The generated mature Foxp3<sup>+</sup> nTregs leave the thymus, undergo IL-2-mediated proliferation and migrate to the periphery (Toker, 2011).

### **1.7 Peripheral and TGF- $\beta$ -induced Tregs**

Peripheral tissues displaying a microenvironment, which favours Foxp3 induction are the gut-associated lymphoid tissues (GALT), the mesenteric and celiac lymph nodes and Peyer's patches (Siddiqui and Powrie, 2008; Sun et al., 2007). Enhanced Treg induction in the GALT is emphasised by minimal increased Treg frequencies compared to other peripheral tissues like the spleen and cervical lymph nodes (Sun et al., 2007). Treg generation in the GALT is essential to generate a tolerogenic environment to prevent an immune reaction towards and food antigens and PAMPs, which cross the epithelial border in the gut. Moreover, it has been shown that Treg induction in the GALT depends on TGF- $\beta$  and occurs in an antigen-dependent manner (Harada et al., 1995). Thus, both nTreg and iTreg generation depends on TCR triggering. Oral feeding of OT-II mice with ovalbumine (OVA) represents a suitable method to study generation of iTregs in the GALT (Mucida et al., 2005). Since TCR transgenic mice do not endogenously develop any Treg cells, contamination with thymus-derived nTregs is excluded (Mucida et al., 2005). Another mode of studying iTreg generation is transfer of CD4<sup>+</sup> Treg-depleted cells into mice deficient for the recombination activating genes 1 and 2 (RAG1, or RAG2) (Leithauser et al., 2002; Ostanin et al., 2009). This leads to the development of an iTreg compartment in the gut and at the same time to a so called transfer colitis, since the adoptively transferred cell population develops into a large amount of T<sub>H</sub>1 effector cells, which cause severe inflammation (Leithauser et al., 2002). In contrast to the OT-II model, transfer colitis does not depend on a single TCR specificity, but occurs in a polyclonal background.

So far, no satisfying marker exists, which allows to distinguish between nTregs and iTregs in the peripheral lymphoid organs. First, the zinc-finger transcription factor Helios was suggested to be a protein, which is exclusively expressed on nTregs as it is induced in the

---

thymus (Thornton et al., 2010; Verhagen and Wraith, 2010). Most importantly, nTregs maintain its expression after migrating to the periphery (Verhagen and Wraith, 2010). In contrast, iTregs generated by oral tolerance do not induce Helios. Although those were promising data, a recent report demonstrated that *in vitro* induced Foxp3<sup>+</sup> cells express Helios as well, when they were activated by APCs instead of anti-CD3 (Gottschalk, 2012). Moreover, adoptively transferred TCRtg Foxp3<sup>-</sup>CD4<sup>+</sup> T cells express Helios and Foxp3, when they are activated in recipient mice after i.v. injection of the cognate antigen (Gottschalk, 2012). Therefore, it is unlikely that Helios represents a suitable marker for nTregs. It is currently investigated, whether the surface protein neuropilin-1 (NP-1) is an exclusive marker of thymus-derived nTregs (unpublished study), but so far, there exist not enough data to make any conclusions about the potential of this marker.

Transfer of *in vitro* generated Tregs into patients suffering from autoimmune diseases was as an early idea in the research of Treg-based therapies. Foxp3 expression can be induced after TCR triggering in the presence of TGF- $\beta$ , which signals via the transcription factor mothers against decapentaplegic homolog 3 (Smad3) (Chen et al., 2003; Fu et al., 2004; Park et al., 2004). Unfortunately, *in vitro*-induced Foxp3 expression in these cells is lost, when the TGF- $\beta$  stimulus is removed. The signals of the microenvironment *in vivo* leading to stable Foxp3 expression are so far not known (Floess et al., 2007; Huehn et al., 2009; Toker and Huehn, 2011). Thus, TGF- $\beta$ -induced Tregs cannot be used in therapy as stability *in vivo* is not guaranteed. A common feature of all routes, which lead to Foxp3 induction, either during nTreg or iTreg development or by TGF- $\beta$  induction, is initial TCR triggering (Huehn et al., 2009; Mantel et al., 2006; Tran et al., 2007). Of the signalling cascades induced after TCR engagement Nuclear Factor  $\kappa$  B (NF $\kappa$ B) signalling represents the most important one for Foxp3 induction (Kanno and Siebenlist, 1996; Kingeter et al., 2010).

---

## 1.8 Conserved non coding sequences regulate Foxp3 expression

The development and maintenance of regulatory T cells is entirely governed by the Foxp3 transcription factor (Brunkow et al., 2001; Hori et al., 2003). Its forkhead box is a DNA binding motif of about 100 amino acids and a variant of the helix-turn-helix domain. Foxp3 forms homodimers or associates with the activator protein 1 (AP-1) or nuclear factor of activated T-cells (NFAT) to force Treg differentiation and maintenance (Chen et al., 2006; Marson et al., 2007). Remarkably, Foxp3 downregulates numerous genes mediating T cell activation like IL-2 and Zap70, but induces CD25, the glycocorticoid induced TNF receptor (GITR) and Ly6a (Marson et al., 2007). The regulation of Foxp3 itself, however, is just partially uncovered. A major breakthrough in the investigation of Foxp3 regulation was the identification of three species-conserved non-coding DNA sequences (CNS) in the *Foxp3* locus, which display enhancer functions (Fig. 4) (Toker and Huehn, 2011; Zheng et al., 2010). CNS1, the TGF- $\beta$  sensor, is located in intron 2 and is preferentially active upon generation of Foxp3 by TGF- $\beta$  *in vitro* (Floess et al., 2007; Zheng et al., 2010). Thereby, the downstream transcription factor Smad3 binds to CNS1 (Marie et al., 2005). The second regulatory sequence CNS2, also termed Treg specific demethylation region (TSDR), is located in intron 2 as well and a segment of epigenetic regulation, as it is methylated in conventional T cells (Tcon) to silence the *Foxp3* locus (Floess et al., 2007; Huehn et al., 2009; Polansky et al., 2008). Thus, its demethylation is essential to ensure a stable expression of Foxp3 (Toker and Huehn, 2011). It is hypothesized, that the stabilization of Foxp3 expression by demethylation of CNS2 occurs during peripheral proliferation immediately after Tregs leave the thymus (Toker and Huehn, 2011). However, it needs to be experimentally validated, whether methyl groups are actively removed from the DNA by so far undefined methylases or whether the new DNA-strand does not become methylated during mitosis. Of note, CNS2 does not undergo demethylation by TGF- $\beta$  treatment and, therefore, *in vitro* generated Tregs are not stable as described above. The last sequence, CNS3, is located in intron 4, downstream of the first coding exon of Foxp3 (Zheng et al., 2010). Current models argue that initial binding of an enhanceosome to CNS3 remodels the

locus to an open conformation by the recruitment of histone modifying enzymes via the NF $\kappa$ B subunit c-Rel, thereby regulating the degree of DNA condensation (Hsieh, 2009; Ruan et al., 2009). This last element is termed, with respect to its initial usage, pioneer element. Since only an opened locus is accessible for the induction of *Foxp3* it is speculated that via CNS3 chromatin condensation of the locus is regulated (Zheng et al., 2010). However, the signalling networks leading to the usage of one particular site depend on the environmental conditions of the tissues, where Tregs develop.

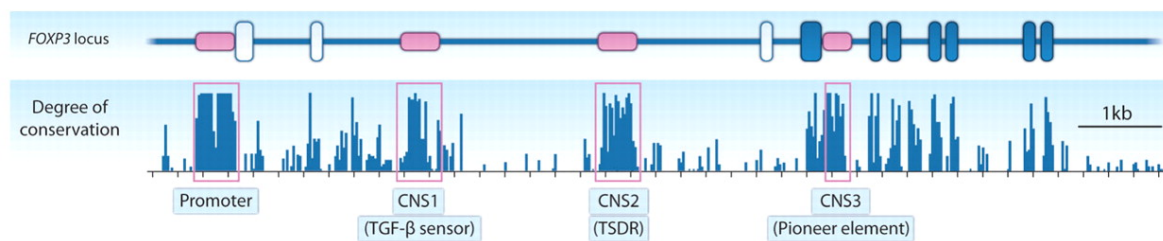


**Figure 4: Conserved non-coding Sequences (CNS) in the *Foxp3* locus**

Schematic overview of the *Foxp3* locus. Open boxes in the upper panel represent the localisation of non-coding exons, blue filled boxes coding exons. Regulatory sequences are indicated by red boxes. The lower panel displays the degree of evolutionary conservation. Sizes of blue peaks correlate with their interspecies conservation. Figure taken from Toker, 2011.

### 1.9 Signalling of Nuclear Factor $\kappa$ B

NF $\kappa$ B was initially identified as a key transcription factor controlling the expression of the  $\kappa$  light chain immunoglobulin gene in mature B and plasma cells (Sen and Baltimore, 1986). By now, it is known that NF $\kappa$ B represents one of the most important signalling networks in the immune system (Ghosh and Hayden, 2008; Hayden and Ghosh, 2011). It is induced by a variety of stimuli, like LPS, Interleukin-1 (IL-1) and tumor necrosis factor- $\alpha$  (TNF- $\alpha$ ), and forces T and B cell development (Claudio et al., 2006; Schmitz and Krappmann, 2006; Siebenlist et al., 2005). Its target genes comprise cytokines like IL-6, antiapoptotic proteins as Bcl-2 and Flip, adhesion molecules ICAM-1 and cyclin-dependent kinases (CDKs), which force proliferation (Claudio et al., 2006; Gerondakis et al., 1999; Pahl, 1999). NF $\kappa$ B transcription factors are dimers formed by two subunits of the REL protein family, which consists of p50, p52, p65/Rel-A, c-Rel and Rel-B (Fig. 5). Their common structural motif is

the REL-homology domain, which contains the dimerisation motif, the nuclear localisation signal (NLS) and the DNA-binding domain (Hayden and Ghosh, 2008; May and Ghosh, 1998). p65/Rel-A, c-Rel and Rel-B contain a transactivation domain (TAD), whereby NF $\kappa$ B dimers containing one of these subunits induce transcription of their target genes (Ghosh and Hayden, 2008). Since p50 and p52 do not contain a TAD, homo- and heterodimers of those two subunits act as transcriptional inhibitors. Of note, p50 and p52 originate from proteasomal cleavage of the precursors p105 and p100, respectively (Li and Verma, 2002).

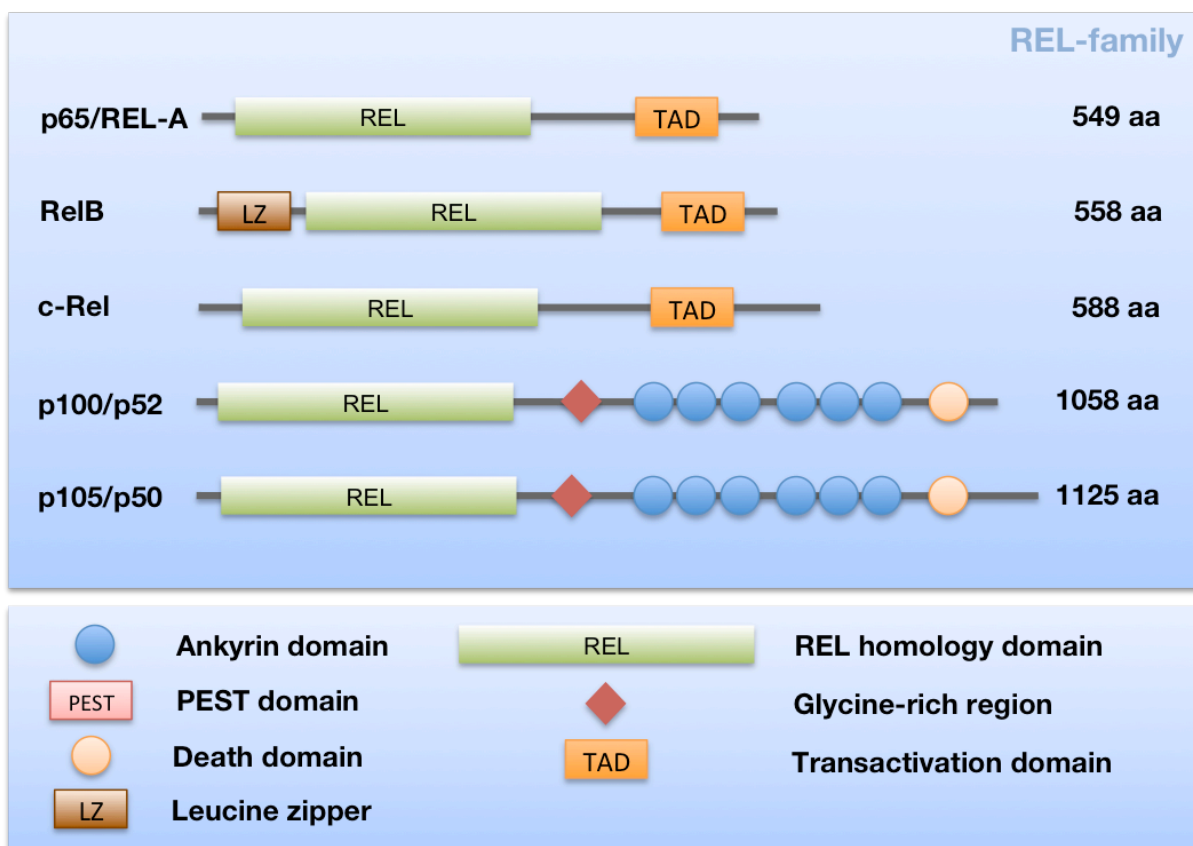


**Figure 5: The REL protein family**

The NF $\kappa$ B family, also called REL protein family, consists of the five members p65/Rel-A, Rel-B, c-Rel, p50 and p52. The common structural motif is the REL-homology domain (RHD), located at the N-terminal part of the proteins. This domain contains the nuclear localisation signal, the DNA-binding site and the dimerisation motif. p65/Rel-A, Rel-B and c-Rel display a C-terminal transactivation domain (TAD), leading to the recruitment of components enhancing gene transcription. p52 and p50 derive from the precursor proteins p100 and p105, respectively. Both precursor proteins display Ankyrin-repeats, the inhibitory motif of I $\kappa$ B proteins, leading to intramolecular masking of the nuclear localisation signal. Cleavage of the isoforms occurs at a glycine-rich region between the RHD- and Ankyrin-domains.

*In vivo*, all dimer combinations are observed, although Rel-B preferentially interacts with p52 (Hayden and Ghosh, 2008). Due to minimal differences in the sequences of their DNA binding domains, NF $\kappa$ B dimers associate to nucleotide sequences, which are not identical. Therefore, each dimer combination displays affinity to a slightly different target sequence resulting in a magnitude of possible  $\kappa$ B binding sites (Ghosh and Hayden, 2008; Hayden and Ghosh, 2008).

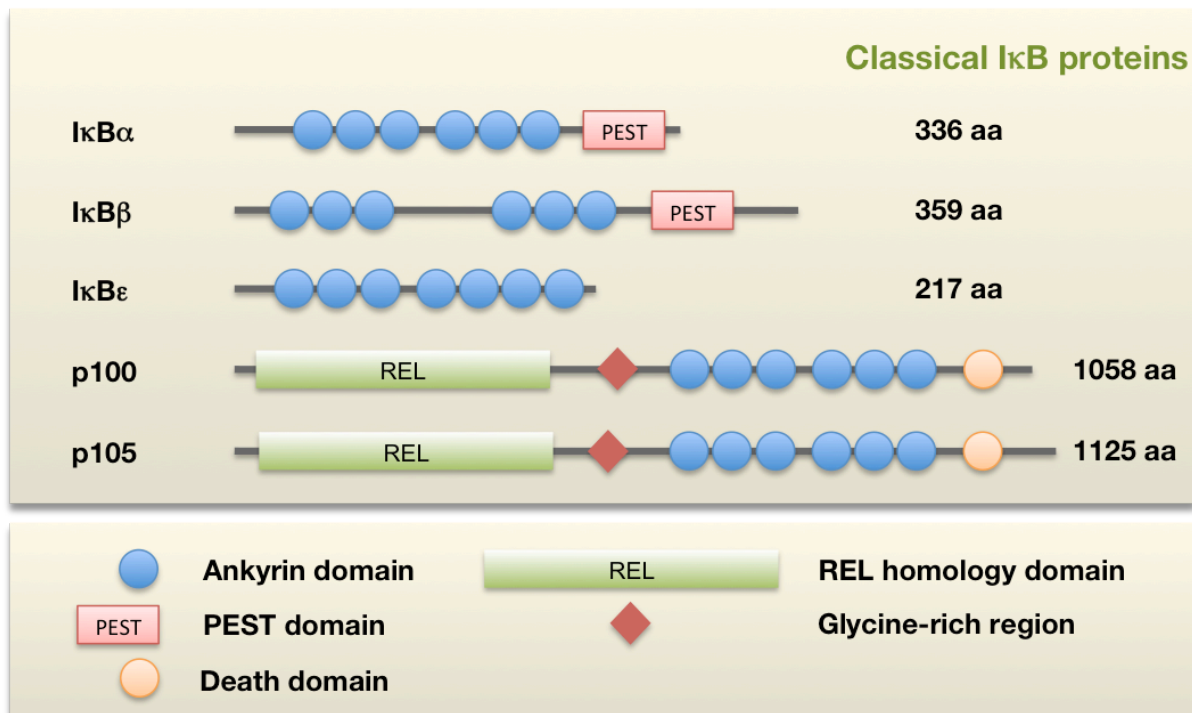


**Figure 6: Inhibitor of NF $\kappa$ B proteins**

The classical I $\kappa$ B-family is formed by the members I $\kappa$ B $\alpha$ , I $\kappa$ B $\beta$  and I $\kappa$ B $\epsilon$ . Their common structural motifs are the Ankyrin repeats, by which I $\kappa$ Bs interact with REL-proteins in the cytoplasm, sequestering them inactive due to masking of the nuclear localisation signal. The proline-glutamic acid-serine-threonine (PEST)-sequence at the C-terminal end mediates proteasomal recruitment and, therefore, serves as a signaling peptide for protein degradation. As p100 and p105 contain Ankyrin-repeats as well, they belong to both the REL- and I $\kappa$ B-family.

NF $\kappa$ B transcription factors are kept inactive in the cytoplasm by binding to cytoplasmic inhibitors of NF $\kappa$ B proteins (I $\kappa$ Bs) (Gerondakis et al., 1999). The largest part of their protein sequences form the Ankyrin-repeats, that are highly conserved among the protein family, which consists of the members I $\kappa$ B $\alpha$ , I $\kappa$ B $\beta$  and I $\kappa$ B $\epsilon$  (Fig. 6) (Chen and Greene, 2004; Chiba et al., 2011b; Yamauchi et al., 2010). The prototypical member of this group is I $\kappa$ B $\alpha$ . Via Ankyrin-repeats I $\kappa$ B $\alpha$  associates to NF $\kappa$ B, masks the NLS within the REL-homology domain

and prevents recognition for nuclear import (Chen and Greene, 2004; Ghosh and Hayden, 2008; Hayden and Ghosh, 2008, 2011). The precursor proteins of p52 and p50, p100 and p105, respectively, consist of an C-terminal Ankyrin domain, which leads to intramolecular masking of the REL-homology domain. Therefore, p100 and p105 formally belong to REL and I $\kappa$ B proteins as well. The C-terminal Ankyrin domain is constitutively cleaved at a glycine-rich region from the REL-homology domain (Perkins, 2007). The common signalling event after NF $\kappa$ B activation is the degradation of cytoplasmic I $\kappa$ B proteins, mostly I $\kappa$ B $\alpha$ , which is induced upon phosphorylation of the serine residues 32 and 36 (Lawrence et al., 2005; Perkins, 2007). The following conformational change results in the dissociation of the I $\kappa$ B/NF $\kappa$ B complex and via the accessible NLS, NF $\kappa$ B translocates into the nucleus and binds to  $\kappa$ B-sites in the DNA. The released phospho-I $\kappa$ B $\alpha$  protein becomes polyubiquitinated and proteasomal degraded (Fig. 7) (Chen, 2005; Pasparakis et al., 2006).

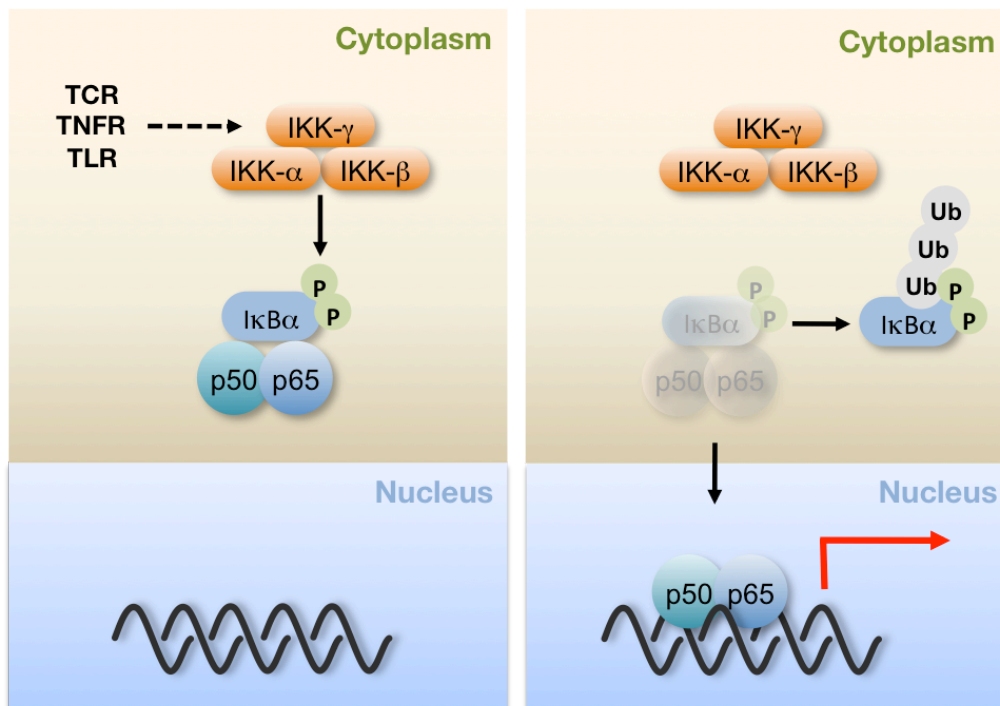


**Figure 7: Schematic overview of NF $\kappa$ B signaling**

The common signalling event in NF $\kappa$ B induction is the activation of the I $\kappa$ B kinase complex, which consists of IKK $\alpha$ , IKK $\beta$  and IKK $\gamma$ . The activating stimuli comprise for example TNF-receptor signalling, TLR engagement and TCR stimulation. Upon IKK activation I $\kappa$ B $\alpha$  is phosphorylated at serines 32/36, released from NF $\kappa$ B transcription factor and subjected to proteasomal degradation. The free transcription factor, here indicated as a p50/p65 heterodimer, is imported into the nucleus and associated to  $\kappa$ B sites on the DNA.

---

Phosphorylation of serines 32/36 of I $\kappa$ B $\alpha$  is induced via the Inhibitor of  $\kappa$ B Kinase complex, a trimeric protein structure consisting of the subunits IKK $\alpha$ , IKK $\beta$  and IKK $\gamma$  (Pasparakis et al., 2006). The enzymatically active subunit IKK $\beta$  mediates the phosphorylation of I $\kappa$ B after its own phosphorylation by IKK $\alpha$  (Pasparakis et al., 2006). IKK $\gamma$ , also called NF $\kappa$ B essential modulator (NEMO) serves as a scaffold protein and platform for adaptor proteins, which modulate NF $\kappa$ B activity (Chen, 2005; Krappmann and Scheidereit, 2005).

### **1.10 Atypical BCL-3 type I $\kappa$ B proteins**

Aside from classical I $\kappa$ B proteins, which sequester NF $\kappa$ B inactive in the cytoplasm, the BCL-3 subfamily, comprising the members BCL-3, I $\kappa$ B $\zeta$ , I $\kappa$ B<sub>NS</sub> and I $\kappa$ B $\eta$ , belongs to the I $\kappa$ B protein family (Fig. 8) (Chen and Greene, 2004; Chiba et al., 2011b; Ghosh and Hayden, 2008; Yamauchi et al., 2010). BCL-3 proteins share the common structural motif of I $\kappa$ B proteins, the Ankyrin domain, whereby they interact with NF $\kappa$ B transcription factors and predominantly with the p50 subunit (Hayden and Ghosh, 2008, 2011). The first remarkable difference to classical I $\kappa$ B proteins is their nuclear localisation (Fiorini et al., 2002; Totzke et al., 2006; Touma et al., 2007; Yamauchi et al., 2010). Moreover, they are induced upon NF $\kappa$ B activation, unlike classical I $\kappa$ Bs, which undergo rapid degradation (Bours et al., 1993). Functionally, they appear as transcriptional modulators of NF $\kappa$ B, by binding to the DNA-associated transcription factor. Thereby, unusual I $\kappa$ Bs modulate the transcription of their target genes either in an inducing or repressing fashion, as reported for the prototypical member of the group, BCL-3 (Dechend et al., 1999). Via its Transactivation Domain (TAD) it induces transcription, when bound to a p50/p50 homodimer (Bours et al., 1993). Upon association to a p50/p65 heterodimer the occurring interference between the two TADs of p65 and BCL-3 leads to repression of transcription (Bours et al., 1993). The exemplary target genes of BCL-3, IL-6 and IP-10, induced after LPS triggering are regulated in that fashion (Bours et al., 1993; Massoumi et al., 2006). I $\kappa$ B $\zeta$  was initially reported to control IL-6 expression in macrophages and DCs, whereby loss of the protein massively reduces release of the cytokine (Kitamura et al., 2000). Of note, I $\kappa$ B $\zeta$  colocalizes with histone deacetylases-4

---

and -5 (HDACs), whose enzymatic activity mediates gene silencing due to chromatin condensation (Totzke et al., 2006). By a reciprocal mechanism, BCL-3 recruits the histone acetyl transferase TIP60 to relax the chromatin to an open conformation (Dechend et al., 1999). Taken together, it appears that chromatin remodelling followed by recruitment of histone modifying enzymes displays one mechanism of unusual I $\kappa$ B functioning (Dechend et al., 1999). Recently, T<sub>H</sub>17-development was reported to depend essentially on I $\kappa$ B $\zeta$ , whereby I $\kappa$ B $\zeta$ -deficient mice are completely protected from experimental induced autoimmune encephalomyelitis (EAE) (Okamoto et al., 2010). I $\kappa$ B $\eta$ , a novel member of the BCL-3 family, is induced after LPS-, zymosan-, CpG oligo- and polyI:C-treatment in macrophages (Yamauchi et al., 2010). Corresponding to I $\kappa$ B $\zeta$ , siRNA mediated knockdown of I $\kappa$ B $\eta$  results in reduced IL-6 expression (Yamauchi et al., 2010). It is controversially discussed, whether two other proteins, I $\kappa$ BL and I $\kappa$ BR, belong to the BCL-3 family (Hayden and Ghosh, 2012). I $\kappa$ BL overexpression was shown to inhibit IL-6 and TNF $\alpha$  expression upon LPS-treatment in macrophages *in vitro* and its transgenic overexpression could suppress the development of experimental induced arthritis (Chiba et al., 2011a; Chiba et al., 2011b). I $\kappa$ BR increased RANTES expression in human lung alveolar epithelial cells (Ray et al., 1997). Despite their sequence homology to BCL-3 proteins and the regulation of the NF $\kappa$ B target genes IL-6, TNF $\alpha$  and RANTES it was not shown that I $\kappa$ BL nor I $\kappa$ BR bind to REL proteins. Thus, it remains unclear whether I $\kappa$ BL and I $\kappa$ BR functionally act as real I $\kappa$ B proteins.

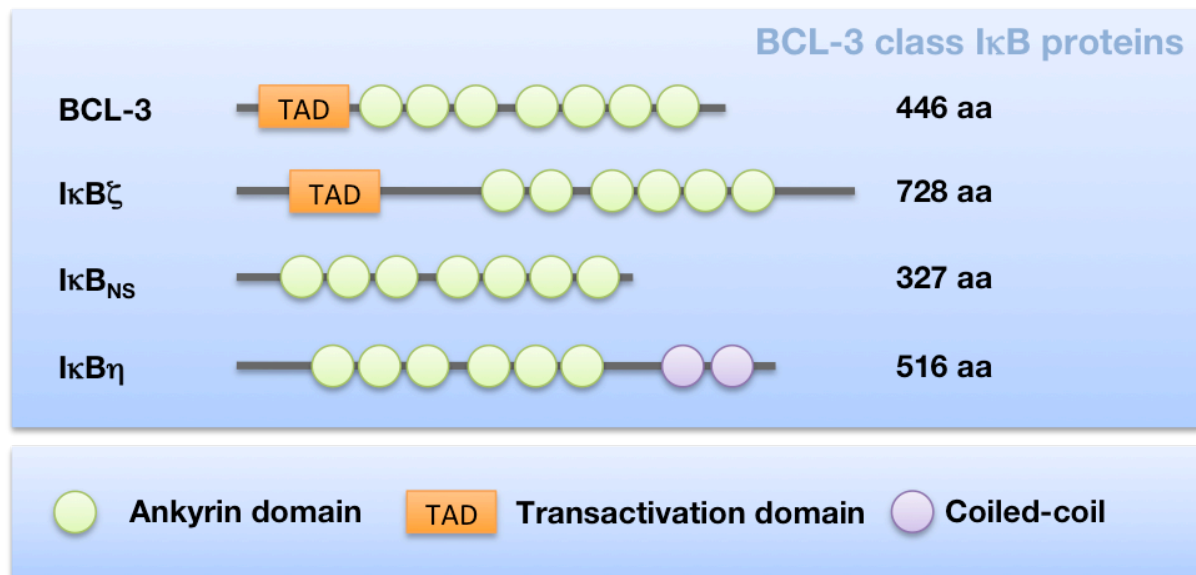


**Figure 8: Unusual I $\kappa$ B-proteins**

The four known members I $\kappa$ B $\zeta$ , BCL-3, I $\kappa$ B<sub>NS</sub> and I $\kappa$ B $\eta$  of the atypical I $\kappa$ B subfamily display the common structural motif, the Ankyrin domains (green circles). BCL-3 and I $\kappa$ B $\zeta$  contain a transactivation domain (TAD), whereby they force gene transcription. A coiled-coil domain in I $\kappa$ B $\eta$  is thought to mediate either dimerisation or DNA-binding.

### 1.11 Identification and function of I $\kappa$ B<sub>NS</sub>

The protein I $\kappa$ B<sub>NS</sub> was initially identified in T cells, undergoing apoptosis in the MHC class I-restricted N15 and MHC class II-restricted 5CC7 mouse models of peptide-induced negative selection (Fiorini et al., 2002). Therefore, it was initially thought that I $\kappa$ B<sub>NS</sub> might contribute to maintenance of central tolerance. I $\kappa$ B<sub>NS</sub>-deficient mice, however, neither developed autoimmune disease nor displayed altered distribution of CD4<sup>+</sup> and CD8<sup>+</sup> cells nor a different V $\beta$  usage followed from impaired negative selection arguing against a distinguished function of I $\kappa$ B<sub>NS</sub> in central tolerance (Touma et al., 2007). An independently generated I $\kappa$ B<sub>NS</sub>-deficient mouse line was also reported not to show autoimmunity, but further analyses demonstrated its induction after TCR triggering in purified peripheral T cells (Hirotsani et al., 2005; Touma et al., 2007). I $\kappa$ B<sub>NS</sub>-deficient CD8<sup>+</sup> T cells displayed reduced proliferation and expression of the cytokines IFN $\gamma$  and IL-2 (Touma et al., 2007). It was recently reported, that B cell function depends on I $\kappa$ B<sub>NS</sub>, as I $\kappa$ B<sub>NS</sub>-deficient mice show reduced serum levels of IgM and IgG3 due to reduced B-cell proliferation (Touma et al.,

---

2011). Remarkably, I $\kappa$ B<sub>NS</sub>-deficient mice do not develop intraperitoneal B1 B-cells (Touma et al., 2011). Its deficiency in innate immune cells prolongs the duration of IL-6 and IL-12 production in macrophages and DCs after LPS-treatment, whereby I $\kappa$ B<sub>NS</sub>-deficient mice are highly susceptible to LPS-induced endotoxic shock (Hirotani et al., 2005). Therefore, I $\kappa$ B<sub>NS</sub> appears to modulate NF $\kappa$ B activity in an opposite manner to I $\kappa$ B $\zeta$ , whose deficiency reduces the IL-6 response (Hirotani et al., 2005; Kuwata et al., 2006). mRNA of I $\kappa$ B<sub>NS</sub> is expressed in thymus, lymph nodes, spleen, heart, muscle cells and the brain indicating that the protein displays different functions (Fiorini et al., 2002). Via its 7 Ankyrin repeats the protein predominantly interacts with p50 and p52 and to a reduced extent with all other members of the REL-family, shown by GST-pulldown analyses (Fiorini et al., 2002). Interestingly, I $\kappa$ B<sub>NS</sub> interacted preferentially with nuclear REL-proteins.

### **1.12 The regulation of Foxp3 by NF $\kappa$ B signalling**

The first proteins of the NF $\kappa$ B pathway described to modulate Foxp3 expression were IKK $\beta$  TAK1, and the matrix-associated guanylate kinase CARMA1, whereby the latter are activators of IKK $\beta$  (Barnes et al., 2009; Sato et al., 2006; Schmidt-Suprian et al., 2003; Wan et al., 2006). CARMA1 serves as a scaffold protein in a complex assembled by the proteins BCL-10 and the paracaspase MALT1 (CBM-complex; Fig. 9) (Barnes et al., 2009; Thome, 2004). CARMA1 consists of an N-terminal Caspase-recruitment domain followed by a coiled-coil motif, a linker region of 3  $\alpha$ -helices, a PSD95/Dlg/ZO-1 (PDZ) homology domain, a src-homology 3 (SH3) domain and at the C-terminal end a guanylate kinase like (GUK) domain (Fig. 9) (Thome, 2004). Its expression is restricted to lymphocytes. The CBM-complex assembles through the interaction between the CARD-domains of CARMA1 and BCL-10, with BCL-10 consisting almost entirely of a single CARD domain (Tavares et al., 2001). The para-caspase MALT-1 displays two N-terminal Ig-domains, which bind to BCL-10 outside of its CARD-domain and to CARMA-1 at the coiled-coil domain (Tavares et al., 2001). The C-terminal caspase-like domain of MALT-1 was reported to mediate IKK complex activation.

Knockout of CARMA1, BCL-10 and MALT1 leads to a nearly complete loss of NF $\kappa$ B activation resulting in impaired B-cell activation after LPS-stimulation and reduced T cell proliferation and IL-2 expression upon TCR triggering (Ruefli-Brasse et al., 2003; Ruland et al., 2001; Tavares et al., 2001; Uren et al., 2000). Remarkably, NFAT and MAPK activation are not affected by deficiencies or mutations of CBM complex proteins underlining its selectivity for NF $\kappa$ B activation (Thome, 2004). Complete or functional loss of CARMA1 as seen in knockout and *king*-mutant mice leads to virtually complete loss of regulatory T cells (Barnes et al., 2009). *King*-mutant mice harbour a point mutation in the  $\alpha$ -helical linker region between the coiled-coil domain and the PDZ-homology region of CARMA1. The few generated Tregs display normal suppressor function, but increased TGF- $\beta$  secretion. Most importantly, the loss of regulatory T cells originates from impaired development of thymic CD25<sup>+</sup>GITR<sup>+</sup>Foxp3<sup>-</sup> nTreg precursors (Molinerio et al., 2009). Therefore, CARMA1 activity appears to essentially regulate the responsiveness to TCR triggering, as the first step in nTreg generation (Long et al., 2009).

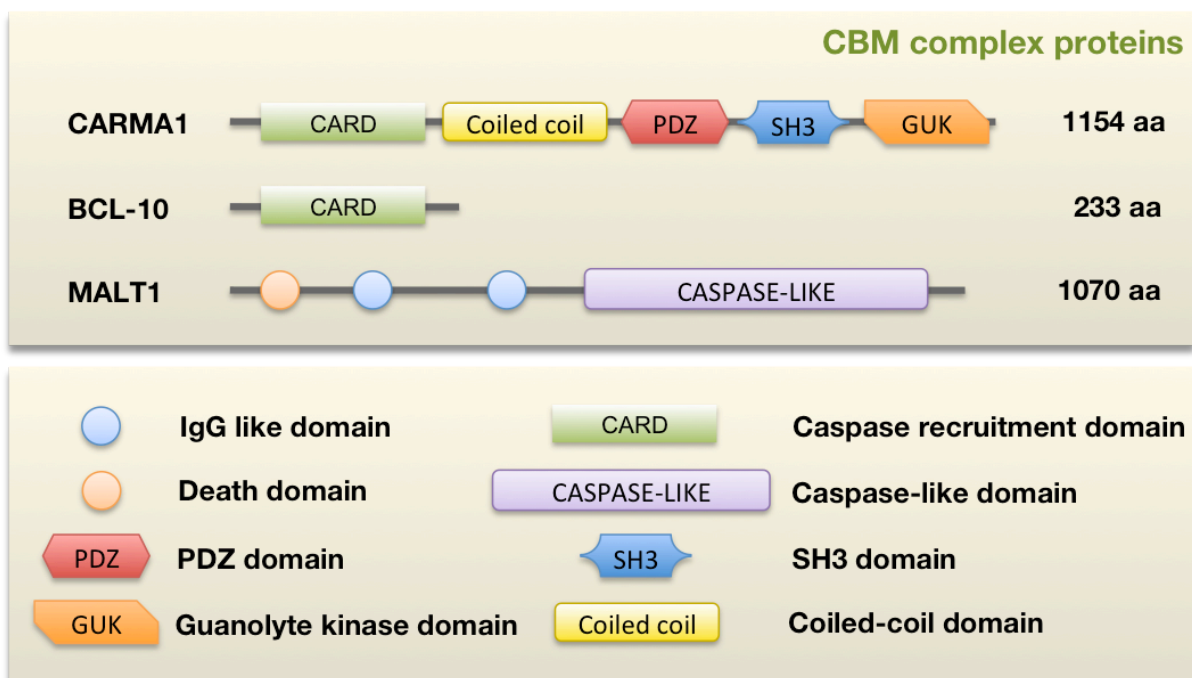


**Figure 9: Structures of CARMA1, BCL-10 and MALT1**

The matrix-associated guanylate kinase CARMA1 consists of a N-terminal caspase-recruitment domain (CARD), a coiled-coil structure, a PSD95/Dlg/ZO-1 (PDZ) homology domain, a src-homology 3 (SH3) domain and a guanylate-kinase like (GUK) domain. BCL-10 consists almost of one CARD-domain. The para-caspase MALT1 consists of a N-terminal death-domain (DD), two Immunoglobulin-like (Ig) domains and a caspase-like domain.

---

By breeding of mice, which ectopically overexpress Bcl-2 it was shown that CARMA1 does not modulate nTreg precursor apoptosis (Molinero et al., 2009). Up to now, the only nuclear protein described to modulate Foxp3 expression is the NF $\kappa$ B subunit c-Rel (Hsieh, 2009; Isomura et al., 2009; Long et al., 2009; Ruan et al., 2009). Its deficiency was shown to abolish production of IL-2 and to reduce proliferative capacity of T cells *in vitro* (Liou et al., 1999). The Treg compartment of c-Rel-deficient mice displayed a reduction of 50% compared to wildtype mice in contrast to CARMA1-deficient mice, which lost almost the complete Treg compartment (Isomura et al., 2009). Similar to Tregs derived from CARMA1-deficient mice, c-Rel deficiency did not affect Treg suppressive capacity indicating that Treg functioning does not depend on NF $\kappa$ B activity (Isomura et al., 2009). So far, the molecular mechanism leading to induction of Foxp3 remains incompletely understood. The most accepted model is Foxp3 regulation via the c-Rel enhanceosome (Hsieh, 2009). According to this theory, initial binding of c-Rel leads to the recruitment of acetyl transferases, which relax the chromatin surrounding the *Foxp3* locus to an open conformation, whereby c-Rel allows binding of other transcription factors like STAT5, which force Foxp3 induction (Hori, 2010; Hsieh, 2009). This model is emphasised by the binding of c-Rel to the CNS3 region, which serves as a pioneer element during *de novo* Foxp3 expression (Zheng et al., 2010). However, the molecular composition of the enhanceosome remains unknown, especially it is still unclear which histone modifying enzymes are recruited to the Foxp3 locus. As unusual I $\kappa$ B proteins are thought to recruit histone modifying enzymes those proteins might represent an important part of the enhanceosome as well. c-Rel does not only bind to the CNS3 element in the Foxp3 locus. Another study could show its binding to two NFAT sites in the Foxp3 promoter (Ruan et al., 2009). Furthermore, binding of c-Rel to kB-sites within the CNS2 was shown to enhance transcriptional activity (Long et al., 2009). Both studies indicated that c-Rel regulates Foxp3 induction by direct transcriptional activation at the promoter and CNS2 as well.

---

### 1.13 Aims

Previous reports demonstrated that I $\kappa$ B<sub>NS</sub> does not modulate thymic negative selection despite its strong expression in T cells, which express self-reactive TCRs (Fiorini et al., 2002; Touma et al., 2007). The only reported T cell phenotype was reduced expression of IL-2 and impaired proliferation after activation of thymic and peripheral T cells from I $\kappa$ B<sub>NS</sub>-deficient mice (Touma et al., 2007). Natural regulatory T cells (nTregs) develop from autoreactive cells, which are prevented from thymic negative selection and, moreover, consume large amounts of IL-2 to maintain Foxp3 expression and peripheral functioning (Aschenbrenner et al., 2007; Huehn et al., 2009). These observations emphasised that I $\kappa$ B<sub>NS</sub> expression in developing autoreactive T cells might be important for their commitment to the Treg lineage or for the maintenance of a protective Treg compartment via modulation of IL-2 levels. Supporting this hypothesis are similarities between I $\kappa$ B<sub>NS</sub> and c-Rel-deficient mice, such as reduced IL-2 secretion, abolishment of intraperitoneal B1 cells and reduced proliferation of T cells (Liou et al., 1999; Touma et al., 2007; Touma et al., 2011). Importantly, c-Rel deficiency results in a massive reduction of regulatory T cells, which follows from defective generation of thymic nTreg precursor cells (Grigoriadis et al., 2011; Isomura et al., 2009). Therefore, the aim of this thesis was to address, whether or not I $\kappa$ B<sub>NS</sub> is important for the development or functional maintenance of regulatory T cells and whether a presumable Treg phenotype is the result of an intrinsic or extrinsic effect. If the Treg compartment was altered by I $\kappa$ B<sub>NS</sub> deficiency, Treg apoptosis, proliferation and binding of I $\kappa$ B<sub>NS</sub> to the Foxp3 locus should be analysed to uncover the mechanism of impaired Treg development. Finally, it should be tested, whether or not I $\kappa$ B<sub>NS</sub> deficiency in Tregs has any physiological relevance in an animal disease model.

---

## **2. Materials**

### **2.1 Chemicals**

If not mentioned differently, chemicals were obtained from Sigma Aldrich (Munich, Germany), Roth (Karlsruhe, Germany) or Merck (Darmstadt, Germany).

### **2.2 Cell culture material and devices**

Cell culture flasks, 10 cm dishes, 6-well and 12-well plates were obtained from NUNC – Thermo Fisher scientific (Rochester, USA). Sarstedt (Nümbrecht, Germany) provided 10 µl sterile pipette tips, 1.5 ml and 2 ml small reaction tubes. 15 ml and 50 ml reaction tubes were used from Greiner bio-one (Frickenhausen, Germany). 45 µm and 20 µm sterile syringe filters were obtained from Becton, Dickinson (Heidelberg, Germany) and Millipore (Waltham, USA). Sterilin – Thermo Fisher Scientific (Rochester, USA) provided 5 ml, 10 ml and 25 ml pipettes. Sterile 200 µl and 1 ml pipett tips were obtained from Starlab (Ahrensburg, Germany).

Cells were cultured at 37°C at 5% CO<sub>2</sub> and 95% air humidity in a HERAcell 240i from Thermo Scientific. Cells were settled in a 5810R centrifuge from Eppendorf (Hamburg, Germany) and handled in a Sterile Guard III by the Baker Company (Sanford, USA).

## 2.2.1 Cell culture media and supplements

Reagent	Lot	Order-No	Company
RPMI 1640	1003068	41965	GIBCO – life technologies (Grand Island, USA)
Fetal Calf Serum (FCS)	A10108-2367	A15-101	PAA (Pasching, Austria)
Sodium-pyruvate 100 mM	749750	11360	GIBCO – life technologies
Non-essential amino acids 100x	930229	11140	GIBCO – life technologies
Penicillin / Streptomycin 5 µg/ml	918582	15070	GIBCO – life technologies
β-Mercaptoethanol 50 mM	806672	31350	GIBCO – life technologies

## 2.2.2 Medium for *in vitro* differentiation and expansion of primary T cells

If not mentioned differently, primary murine T cells were cultured in RPMI 1640, supplemented with 10% FCS, 1 mM Sodium-pyruvate, 50 ng/ml Penicilline/ Streptomycin, 1x non-essential amino acids and 50 µM β-Mercaptoethanol.

## 2.2.3 Cytokines and chemicals used for T cell stimulation

Reagent	Lot	Order-No	Company
Murine interleukin-2	MX1210031	402-ML	R&D Systems (Minneapolis, USA)
Murine interleukin-2	212-2D12-28	212-12	Pepto Tech (Rocky Hill, USA)
Phorbol 12-myristate 13-acetate (PMA)	16561-29-8	P8139	Sigma Aldrich
Ionomycin (Iono)	56092-82-1	I-0634	Sigma Aldrich
Human transforming growth factor-β	0504S88-1	100-21R	Pepto Tech

## 2.2.4 Antibodies and reagents used in cell culture

Antibody	Lot	Clone	Order-No	Company
Anti-murine CD3	B133074	145-2C11	100314	Biolegend (San Diego, USA)
Anti-murine CD28	E032666	37.51	16-0281-86	eBiosciences (San Diego, USA)
Anti-murine IL-4	-	11B11	-	Self purified
Anti-murine IFN $\gamma$	-	XMG1.2	-	Self purified

## 2.3 Materials and reagents for flow cytometry

### 2.3.1 Devices

Labelled samples were analyzed on FACS Calibur and LSR II by Becton, Dickinson. For cell purification samples were sorted on FACS Aria II (Becton, Dickinson) or Moflo (Beckman Coulter, Indianapolis, USA).

### 2.3.2 Fluorescent dyes

Reagent	Excitation	Emmision	Order-No	Company
Carboxyfluorescein succinimidyl ester (CFSE)	494 nm	530 nm	65-0850	eBiosciences
LIVE/DEAD® Blue cell stain	305 nm	450 nm	L23105	Life technologies
LIVE/DEAD® Far red stain	633/635 nm	665 nm	L10120	Life technologies

### 2.3.3 Fluorochrome-labeled antibodies

Reactivity	Dye	Species	Notation	Order-No	Company
<b>CD4</b>	PE	Rat IgG2A, $\kappa$	L3T4	553048	Becton, Dickinson
<b>CD4</b>	Pacific Blue	Rat IgG2A, $\kappa$	L3T4	100531	Biolegend
<b>CD4</b>	APC	Rat IgG2A, $\kappa$	L3T4	17-0042	eBioscience
<b>CD8</b>	Horizon V500	Rat IgG2A, $\kappa$	53-6.7	560776	Becton, Dickinson
<b>CD8</b>	FITC	Rat IgG2A, $\kappa$	53-6.7	553030	Becton, Dickinson
<b>CD8</b>	eFluor 710	Rat IgG2A, $\kappa$	53-6.7	46-0081	eBioscience
<b>CD25</b>	PerCP eFluor 710	Rat IgG2A, $\lambda$	PC61.5	557192	Becton, Dickinson
<b>CD25</b>	APC	Rat IgG2A, $\lambda$	PC61.5	17-0251	eBioscience
<b>CD25</b>	PE	Rat IgG2A, $\lambda$	PC61.5	553866	Becton, Dickinson
<b>CD25</b>	FITC	Rat IgG2A, $\lambda$	PC61.5	553071	Becton, Dickinson
<b>CD62L</b>	PE	Rat IgG2A, $\kappa$	MEL-14	553151	Becton, Dickinson
<b>CD103</b>	APC	Hamster IgG	2E7	17-1031	eBioscience
<b>CD122</b>	FITC	Rat IgG2A, $\kappa$	5H4	553362	Becton, Dickinson
<b>CTLA-4</b>	PE	Hamster IgG	UC10-4B9	12-1522	Becton, Dickinson
<b>GITR</b>	APC	Rat IgG2B	DTA-1	17-5874	eBioscience
<b>GITR</b>	PE-Cy7	Rat IgG2B	DTA-1	25-5874	eBioscience
<b>Ki67</b>	PE	Mouse IgG1, $\kappa$	B56	556027	Becton, Dickinson
<b>Foxp3</b>	PE	Mouse IgG1	3G3	130-093-014	Miltenyi Biotech (Mönchengladbach, Germany)
<b>Foxp3</b>	APC	Mouse IgG1	3G3	130-093-013	Miltenyi Biotech

## 2.4 Mouse strains

B6.129/SV-NFKBID(tm1Clay)-mice, later referred to as  $I\kappa B_{NS}^{-/-}$  mice were a kind gift of Prof. Dr. Linda Clayton (Harvard Medical School, Boston, USA). B6.PL-Thy1a/CyJ-mice, later referred to as Th1.1-mice were provided by Dr. René Teich (Helmholtz-Centre for Infections Research, Braunschweig, Germany). B6-Tg(Foxp3-DTR/EGFP)23.1Spar/J, later referred to as DEREK mice were a kind gift of Prof. Dr. Tim Sparwasser (Twincore, Hannover, Germany).  $I\kappa B_{NS}^{-/-}$ , Thy1.1- and DEREK mice were kept under specific pathogen free (SPF) conditions in the animal facility of the Helmholtz-Centre for Infections Research. B6.129S7-Rag1<sup>tm1Mom</sup>-mice, later named RAG1-mice were bred at the animal facility of the Charité (Berlin, Germany).

## 2.5 Reagents and Materials used for Western blotting

PVDF membrane and photosensitive Hyperfilms® were obtained from GE Healthcare (Buckinghamshire, UK). SDS-PAGEs and protein transfers were performed using blotting and transfer devices by Bio-Rad Laboratories (Hercules, USA).

### 2.5.1 Primary antibodies

Antibody	Reactivity	Isotype	Species	Clone/Notation	Company
Anti- $\beta$ -Actin	Ms, Hu	IgG2A	Mouse	AC-74	Sigma-Aldrich
Anti-CARMA1	Ms, Hu	IgG	Rabbit	1D12	Cell Signalling (Danvers, USA)
Anti-c-Rel	Ms	IgG2A	Rat	290512	R&D Systems
Anti-c-Rel	Ms, Hu	IgG	Rabbit	SC-71	Santa Cruz (Santa Cruz, USA)
Anti- $I\kappa B_{NS}$	Ms, Hu	IgG2B	Mouse	138	Self-made
Anti- $I\kappa B_{NS}$	Ms, Hu	IgG	Rabbit	G49 & G50	Self-made
Anti-LaminB	Ms, Rt, Hu	IgG	Goat	M-20	Santa Cruz

Antibody	Reactivity	Isotype	Species	Clone/Notation	Company
<b>Anti-p52/p100</b>	Ms, Hu, Rt, Mk	IgG	Rabbit	4882	Cell Signalling
<b>Anti-p50/p105</b>	Ms, Rt	IgG	Rabbit	TF112	Stressgen (San Diego, USA)
<b>Anti-p50/p105</b>	Ms, Hu, Rt	IgG	Rabbit	E381	Epitomics (Burlingame, USA)
<b>Anti-p50/p105</b>	Ms, Hu	IgG1	Mouse	285412	R&D Systems
<b>Anti-p65</b>	Ms, Hu, Rt	IgG	Rabbit	C-20	Santa Cruz
<b>Anti-Rel-B</b>	Ms	IgG	Rabbit	C19	Santa Cruz
<b>Anti-STAT5a</b>	Ms, Hu, Rt	IgG1	Mouse	C-10	Santa Cruz
<b>Anti-STAT5b</b>	Ms, Hu	IgG	Rabbit	S6183	Sigma Aldrich
<b>Anti-pSTAT5a/b</b>	Ms, Hu, Rt, Mk	IgG	Rabbit	D47E7	Cell Signaling

### 2.5.2 Horseradish peroxidase-conjugated secondary antibodies

Reactivity	Species	Clone/Notation	Company
<b>Mouse IgG1</b>	Goat	1070-09	Southern Biotechnology (Birmingham, USA)
<b>Mouse IgG2a</b>	Goat	1080-05	Southern Biotechnology
<b>Mouse IgG2b</b>	Goat	1090-05	Southern Biotechnology
<b>Mouse IgG3</b>	Goat	1100-05	Southern Biotechnology
<b>Mouse IgG</b>	Goat	111-035-068	Dianova (Hamburg, Germany)
<b>Rabbit IgG</b>	Goat	111-035-144	Dianova
<b>Rabbit IgG</b>	Goat	5030-05	Southern Biotechnology
<b>Rabbit IgL</b>	Mouse IgG1, $\kappa$	211-032-171	Jackson ImmunoResearch (Bar Harbor, USA)
<b>Rat IgG</b>	Goat	Sc-2065	Santa Cruz

---

## 2.6 Oligonucleotides

All oligonucleotides were obtained from Eurofins MWG Operon (Ebersberg, Germany) HPLC-purified and lyophilised. Forward DNA oligonucleotides for DNA-pulldown were modified with biotin-TEG (15 atom triethylene glycol spacer) at the 5' end.

### 2.6.1 Oligonucleotides for GST-DNA-pulldown

Name	Sequence 5'→3'
NFκB ctr fwd	AACCA AGAGG GATTT CACCT AAATC CATTG AGTCA
NFκB ctr rev	TGACT GAATG GATTT AGGTG AAATC CCTCT TGGTT
CD28RE ctr fwd	TGTAT GGGGG TTAA AGAAA TTCCA GAGAG TCATC
CD28RE ctr rev	GATGA CTCTC TGGAA TTTCT TAAA CCCCATACA
Prom κB1 fwd	ATTTG ACTTA TTTTC CCTCA GTTTT TTTT TCTGA
Prom κB1 rev	TCAGA AAAAA AAAAC TGAGG GAAAA TAAGT CAAAT
Prom κB2 fwd	TTGTT TAAGA AATTG TGGTT TCTCA TGAGC CCTGT
Prom κB2 rev	ACAGG GCTCA TGAGA AACCA CAATT TCTTA AACAA
Prom κB3 fwd	GTTTT TGATA ATGTG GCAGT TTCCC ACAAG CCAGG
Prom κB3 rev	CCTGG CTTGT GGGAA ACTGC CACAT TATCA AAAAC
Prom κB4 fwd	CCCAC CAGTA CAGCT GGAAA CACCC AGCCA CTCCA
Prom κB4 rev	TGGAG TGGCT GGGTG TTTCC AGCTG TACTG GTGGG
CNS2 κB1 fwd	CAGAG ATGGA CAGGA AGGCC CCTTT GTCCC AAGAG
CNS2 κB1 rev	CTCTT GGGAC AAAGG GGCCT TCCTG TCCAT CTCTG
CNS2 κB2 fwd	TCAGG ACAGT AGAGG GTTTT CCAAT CCTCT GTCAT
CNS2 κB2 rev	ATGAC AGAGG ATTGG AAAAA CCTCT ACTGT CCTGA
CNS2 κB3 fwd	TCCTG GCTTT AGGTG GTTCC CATTG CTTTG GGCTC
CNS2 κB3 rev	GAGCC CAAAG AAATG GGAAC CACCT AAAGC CAGGA

Name	Sequence 5' → 3'
<b>CNS2 κB4 fwd</b>	ATCAC CCTAC CTGGG CCTAT CCGGC TACAG GATAG
<b>CNS2 κB4 rev</b>	CTATC CTGTA GCCGG ATAGG CCCAG GTAGG GTGAT
<b>CNS2 κB5 fwd</b>	ACAGG GCCCA GATGT AGACC CCGAT AGGAA AACAT
<b>CNS2 κB5 rev</b>	ATGTT TTCCT ATCGG GGTCT ACATC TGGGC CCTGT
<b>CNS2 κB6 fwd</b>	AACAG TCAAA CAGGA ACGCC CCAAC AGACA GTGCA
<b>CNS2 κB6 rev</b>	TGCAC TGTCT GTTGG GCGT TCCTG TTTGA CTGTT
<b>CNS3 κB1 fwd</b>	TTGCA GGGCC AAGAA AATCC CCACT CTCCA GGCTT
<b>CNS3 κB1 rev</b>	AAGCC TGGAG AGTGG GGATT TTCTT GGCCC TGCAA

## 2.6.2 Oligonucleotides for PCR

Name	T <sub>M</sub>	Sequence 5' → 3'	Size
<b>RT β-Actin fwd</b>	57.3	TGT TAC CAA CTG GGA CGA CA	312 bp
<b>RT β-Actin rev</b>	59.4	TCT CAG CTG TGG TGG TGA AG	
<b>RT IκB<sub>NS</sub> fwd</b>	66.1	GCT GTA TCC TGA GCC TTC CCT GTC	272 bp
<b>RT IκB<sub>NS</sub> rev</b>	64.4	GCT CAG CAG GTC TTC CAC AAT CAG	
<b>RT Foxp3 fwd</b>	60.4	TTC ATG CAT CAG CTC TCC AC	272 bp
<b>RT Foxp3 rev</b>	60.4	AGA CTC CAT TTG CCA GCA GT	
<b>RT c-Rel fwd</b>	60.4	TGC TGG ACA TTG AAG ACT GC	608 bp
<b>RT c-Rel rev</b>	60.4	GAC CTG GGC ATT TCT GGT AA	
<b>RT CARMA1 fwd</b>	60.4	TGA AGA CGA GGT GCT CAA TG	402 bp
<b>RT CARMA1 rev</b>	60.4	CTG GCC AAA GAA GAA ACT CG	

## 2.7 Frequently used buffers

Group	Buffer	Components
Cellular buffers	PBS	138 mM NaCl
		8.1 mM $\text{Na}_2\text{HPO}_4$
		2.7 mM KCl
		1.5 mM $\text{K}_2\text{HPO}_4$ , pH7.4
	FACS buffer	2% w/v BSA in PBS
MACS buffer	0.2% w/v BSA 1 mM EDTA in PBS	
Lysis buffers and additives	TPNE	300 mM NaCl
		1% v/v Triton X-100
		2 mM EDTA
		in PBS pH 7.4
	Cytoplasm A	10 mM HEPES
		1.5 mM $\text{MgCl}_2$
		10 mM KCl
		300 mM Sucrose 0.5% NP-40 pH 7.9
	Nucleus B	20 mM HEPES
		1.5 mM $\text{MgCl}_2$
		420 mM NaCl
		0.2 mM EDTA 2.5% Glycerol pH 7.9
	Nucleus HGMK	10 mM HEPES
		5 mM $\text{MgCl}_2$
		100 mM KCl
10% Glycerol 1 mM DTT pH 7.9		
100x protease inhibitors	100 $\mu\text{g/ml}$ Apotinin	
	100 $\mu\text{g/ml}$ Leupeptin	
	100 $\mu\text{g/ml}$ Chymostatin	
	100 $\mu\text{g/ml}$ Pepstatin	
Western blot buffers	5x Laemmli	50 mM Tris, pH 8.8
		10% w/v SDS
		25% v/v $\beta$ -Mercaptoethanol
		50% v/v Glycerol 0.25 mg/ml Bromphenolblue
	Running buffer	25 mM Tris, pH 8.0
		192 mM Glycerol 1% v/v SDS
	Transfer buffer	25 mM Tris, pH 8.0
		192 mM Glycerol 20% v/v Methanol
	Blocking buffer	5% w/v non-fat dry milk
		0.2 % v/v Tween-20 in PBS
Wash buffer	0.05% v/v Tween-20	
	in PBS	

---

### 3. Experimental Procedures

#### 3.1 Molecular biology methods

##### 3.1.1 Isolation of eukaryotic RNA

RNA of eukaryotic cells was isolated from purified primary cells using Qiagen RNeasy Kit (Hilden, Germany) according to the protocol provided by the supplier.

##### 3.1.2 Preparation of eukaryotic chromosomal DNA

To determine the methylation status of CNS2/TSDR from the *Foxp3* locus (see 3.1.7) chromosomal DNA of conventional and regulatory T cells was isolated from purified primary cells using NucleoBond kit by Macherey-Nagel (Düren, Germany) according to the protocol provided by the supplier.

##### 3.1.3 Photometric determination of DNA/RNA concentration

DNA/RNA concentrations were determined by Nanodrop 2000c (Thermo Scientific). Absorbance at 260 nm was measured to calculate DNA concentration according to the Lambert-Beer functions:

$$E = c \times \epsilon \times d \Leftrightarrow c = \epsilon \times d \times E^{-1}$$

E = extinction

c = concentration [mol/l]

$\epsilon$  = coefficient of extinction [ $M^{-1} \times cm^{-1}$ ]

d = density of cuvette [cm]

##### 3.1.4 Reverse transcription

Purified RNA was transcribed into copyDNA (cDNA) for PCR analyses (see 3.1.5) using RevertAid™ Premium First Strand cDNA Synthesis Kit (Thermo Scientific). mRNA was specifically transcribed using oligo-dT primers. Reagents were incubated in peqSTAR thermocycler from peqlab (Erlangen, Germany).

### 3.1.5 Polymerase chain reaction

DNA was amplified using ready-to-use 2x KAPA Fast ReadyMix (peqlab) after reverse transcription of mRNA in cDNA as described in 3.1.4. As the Polymerase does not display exonuclease and proof-reading activity the average error rate is  $1 \times 10^{-6}$ .

PCR components were mixed according to the following scheme:

Component	Amount
cDNA template	1 $\mu$ l (~50-100 ng)
2x ready-to-use mix	12.5 $\mu$ l
Forward primer 100 pmol	1 $\mu$ l
Reverse primer 100 pmol	1 $\mu$ l
Dest H <sub>2</sub> O	Adjusted to 25 $\mu$ l total volume

PCRs were incubated in peqSTAR thermocycler (peqlab) according to the program shown below. The temperature chosen for hybridization was 3°C under the  $T_M$  value of the indicated primer combinations.

Time	Temperature	Function	
5 min	94°C	Initial denaturation	
30 sec	94°C	Denaturation	
30 sec	60°C (-/+ x°C)	Hybridisation	25-32 cycles
30 sec	72°C	Elongation	
10 min	72°C	Terminal elongation	

---

### 3.1.6 Analytic agarose gels

DNA fragments were separated according to their size in 1-2% agarose gels in an electric field of 150 mA in the horizontal gel-electrophoresis system perfectBlue M (peqlab) in TAE-buffer (40 mM Tris pH 8, 20 mM acetic acid, 1 mM EDTA) with 0.5 µg/ml ethidiumbromide. The DNA-integrated ethidiumbromide was visualized by UV-light ( $\lambda = 254\text{nm}$ ). As a standard, 1 kB DNA-ladder by peqlab was used.

### 3.1.7 DNA methylation analyses

The CNS2/TSDR of the *Foxp3* locus contains 13 CpG sequences. Their demethylation ensures epigenetically stable *Foxp3* expression. To determine TSDR methylation, purified chromosomal DNA was sent to Biontis (Berlin, Germany) and analyzed by bisulfid sequencing and real-time PCR in cooperation with Dr. Stefan Floess from the department of Experimental Immunology at the HZI (Braunschweig).

### 3.1.8 DNA pulldown

For DNA pulldown, cytoplasmic extracts of  $\text{CD4}^+\text{CD25}^-$  cells were stimulated for 4 hours with 10 ng/ml PMA and 1 µM ionomycin. Nuclear extracts were generated as described in 3.2.2 and incubated overnight with 8 µg DNA-oligo, bound to paramagnetic streptavidin beads (MyOne Streptavidin C1, Life technologies). Unbound proteins were removed and eluates analyzed by SDS-PAGE and Western blotting (see 3.2.6 and 3.2.7). 35 bp DNA-oligos of the promoter, CNS2/TSDR and CNS3/Pioneer elements containing  $\kappa\text{B}$  binding sites were designed according to Genomatix<sup>TM</sup> database analysis and previous studies. A classical  $\kappa\text{B}$ -site and a CD28-responsive element of the IL-2 promoter served as controls. See 2.6.1 for oligo-nucleotide-sequences.

### 3.1.9 Luciferase-Assays

Luciferase constructs, containing the *Foxp3* promoter and conserved non-coding DNA sequences CNS2 and CNS3 (pGL4-Prom, pGL4-CNS2 and pGL4-CNS3), were a kind gift of Dr. Ye Zheng from the Salk Institute for Biological Studies (La Jolla, CA, USA). *In vitro*

---

expanded CD4<sup>+</sup>CD25<sup>-</sup> T cells were stimulated for 3 hours with 10 ng/ml PMA and 1 μM ionomycin. After change of cell culture medium, cells rested for additional 24 hours. Subsequently, 3 μg of the indicated plasmids together with 1.5 μg of Renilla luciferase control vector was nucleofected into 3x10<sup>6</sup> to 5x10<sup>6</sup> cells by Amaxa human T cell nucleofector kit from Lonza (Visp, Switzerland) according to suppliers instructions. Cells were restimulated with the same concentrations of PMA/ionomycin for 16 hours and luciferase activity was determined using Dual-Luciferase Reporter Assay System from Promega according to the protocol of the supplier (Madison, USA). Luciferase assays were performed in cooperation with Dipl.-Biol. Lisa Schreiber from the department of Experimental Immunology at the HZI (Braunschweig).

## **3.2 Proteinbiochemical procedures**

### **3.2.1 Cell Lysis**

For whole cell extracts 1x10<sup>6</sup> to 5x10<sup>6</sup> cells were lysed in 50 μl TPNE lysis buffer (300 mM NaCl, 1% Triton X-100, 2mM EDTA, 1 mM PMSF and 1 μg/ml of Leupeptin, Aprotinin, Chymostatin and Pepstatin A, respectively) for 20 min on ice and centrifuged (15 min, 20,000 g). Supernatant was transferred into a prechilled tube and used for further experiments.

### **3.2.2 Fractionised cell lysis**

To generate cytoplasmic extracts 4\*10<sup>6</sup> T cells were lysed in 250 μl buffer A (10 mM HEPES, pH 7.9, 1.5 mM MgCl<sub>2</sub>, 10 mM KCl, 300 mM sucrose, 0.5% NP-40 supplemented with 1 mM PMSF and 1 μg/ml of leupeptin, aprotinin, chymostatin and pepstatin A, respectively) for 10 min on ice and centrifuged (30 sec, 2500 g). The supernatant, which represents the cytoplasmic fraction, was transferred to a new prechilled tube. The nuclear pellet was washed twice with 500 μl buffer A. After removal of the washing buffer the nuclear pellet was resuspended in buffer B (20 mM HEPES, pH7.9, 1.5 mM MgCl<sub>2</sub>, 420 mM NaCl, 0.2 mM

---

EDTA, 2.5% glycerol with 1 mM PMSF and 1 µg/ml of Leupeptin, Aprotinin, Chymostatin and Pepstatin A, respectively). The resuspended nuclear pellets were sonicated using a Bioruptor™ NextGen (Diagenode, Denville, USA) 3 times for 15 seconds at the highest power setting. Remnants of the nuclear wall were removed by centrifugation (5 min, 10,500 g) and the supernatant containing nuclear proteins was transferred to a new tube. For DNA-pulldown (3.1.8) and co-immunoprecipitations (3.2.5) buffer B was replaced by HGMK buffer (0.1% NP-40, 10 mM HEPES, pH 7.9, 5 mM MgCl<sub>2</sub>, 100 mM KCl, 1 mM DTT, 10% Glycerol with 1 mM PMSF and 1 µg/ml of Leupeptin, Aprotinin, Chymostatin and Pepstatin A, respectively).

### **3.2.3 Determination of protein concentration by bicinchoninic acid**

For TPNE, cytoplasmic buffer A and nuclear buffer B protein concentration from protein extracts as generated in 3.2.1 and 3.2.2 was determined by bicinchoninic acid (BCA) protein assay reagent provided by Pierce – Thermo Fisher Scientific according to the supplier's protocol. The BCA assay is based on the colorimetric detection of a cuprous cation Cu<sup>1+</sup> by bicinchoninic acid. Cu<sup>1+</sup> results from the reduction of Cu<sup>2+</sup> via a chelate complex formed by three or more amino acid residues in alkaline medium, known as biuret reaction. The Cu<sup>1+</sup> forms a complex with two BCA molecules, whose absorption was measured at 562 nm using TECAN infinite 200M (Männedorf, Switzerland).

### **3.2.4 Determination of protein concentration by Bradford**

Protein concentration in HGMK buffer was determined using the Biorad Protein Assay. The Bradford assay uses the complex formation of Coomassie-Brilliant-Blue G-250 with cationic and non-polar amino acids upon acidification. Unbound cationic Coomassie absorbs at 470 nm, whereas complex bound Coomassie absorbs at 595 nm. Absorption was measured using TECAN infinite 200M (Männedorf, Switzerland).

---

### **3.2.5 Immunoprecipitation**

For immunoprecipitation cytoplasmic and nuclear extracts were prepared as described in 3.2.2. Prior to cell lysis 2 µg rabbit polyclonal antibodies detecting IκB<sub>NS</sub>, p50 (StressGen), p65 (Santa Cruz), c-Rel (Santa Cruz) or nonspecific rabbit IgG (Sigma) were labeled to 35 µl 50% slurry Protein A Sepharose CL-4B (Sigma) for 4 hours at 4°C with rotation in 200 µl of buffer A or HGMK. After incubation unbound antibody was removed by washing three times with 500 µl of the corresponding cytoplasmic or nuclear buffer. 200 µg of cytoplasmic or nuclear extracts were added to the antibody-labeled beads filled up to 750 µl with the corresponding buffer and incubated overnight at 4°C with rotation. Unbound proteins were removed by washing three times with 500 µl buffer. The beads were resuspended in 40 µl 1x Laemmli buffer (see 2.7), incubated for 5 min at 95°C and immunoprecipitated proteins analyzed by SDS-PAGE and Western blotting (see 3.2.6 and 3.2.7).

### **3.2.6 SDS-PAGE**

After determination of protein concentration via BCA or Bradford analyses as described in 3.2.3 or 3.2.4, the protein solution was mixed with 5x Laemmli buffer (10% w/v SDS, 24% v/v β-Mercaptoethanol, 50% v/v Glycerol, 0.25 mg/ml Bromphenolblue) to a 1x final concentration and incubated at 95°C for 5 min. 20 µg of protein was separated in a 12% polyacrylamid gel in 1x running buffer (see 2.7) using a Biorad "Tetra cell" at 33 mA per gel and 80 V for the first 10 minutes. SDS page was completed at 195 V.

### **3.2.7 Western blotting**

Proteins from SDS-PAGE were transferred to a PVDF-membrane (GE healthcare) using a Biorad "Criterion Blotter" in 1x transfer buffer (see 2.7) at 500 mA at 80 V for 90 min. The membrane was incubated in blocking buffer (see 2.7) for 1 hour at RT with agitation. Afterwards it was placed in blocking buffer containing primary antibody (see 2.5.1) diluted according to suppliers protocols and incubated overnight in an overhead mixer. Unbound protein was removed by washing 3 times with PBS/Tween and membranes were incubated with secondary antibodies (see 2.5.2) for 1 hour at RT with agitation. Isotype specific anti-

---

mouse antibodies and anti-rabbit antibodies were diluted 1:20000. The other antibodies were used 1:5000. After removal of unbound secondary antibodies by washing 3 times with PBS/Tween proteins were detected by SuperSignal West Dura substrate from PIERCE – Thermo Fisher Scientific.

### **3.3 Cellular and mouse surgical methods**

#### **3.3.1 Isolation of lymphoid organs from mice**

For the analyses of primary cells, thymus, spleen mesenteric and peripheral lymph nodes were removed from mice sacrificed by cervical dislocation or CO<sub>2</sub>. Lymphoid organs were pound through a 45 µm filter and cells were resuspended in 6 ml PBS.

#### **3.3.2 Flow cytometry analysis**

For staining of surface proteins 2\*10<sup>6</sup> primary cells isolated as described in 3.3.1 were washed twice with 1 ml FACS-buffer and resuspended in 250 µl FACS-buffer (see 2.7). Cells were stained with the indicated antibodies according to suppliers dilutions (see 2.3.3) at 4°C in the dark for 15 min. Subsequently, cells were again washed twice with 1 ml of FACS buffer and analysed by a LSRII FACS-device (BD Biosciences). Intracellular staining of Foxp3 was performed using Foxp3 Staining Buffer Set (Miltenyi) according to the providers protocol.

#### **3.3.3 Cell isolation via flow cytometry**

For preparative isolation primary cells were stained as in 3.3.2 and sorted in a FACS Aria II (Abd Elrazek et al.) or Moflo (Beckman and Coulter). Cells were collected in 15 ml tubes filled with 500 µl PBS containing 0.1% BSA. Cells were sorted in cooperation with Dr. Lothar Gröbe from the sorting facility at the HZI (Braunschweig).

#### **3.3.4 Expansion of CD4<sup>+</sup>CD25<sup>-</sup> T cells *in vitro***

After sorting as described in 3.3.3 CD4<sup>+</sup>CD25<sup>-</sup> T cells were expanded *in vitro* for DNA-pulldown (3.1.8) and immunoprecipitation (3.2.5). 4\*10<sup>6</sup> purified T cells were resuspended in 4 ml RPMI (fully supplemented) stimulated with 1 µg/ml plate-bound anti-CD3 and 2 µg/ml

---

soluble anti-CD28 in the presence of 10 ng/ml murine IL-2 in a 6-well plate. On day 3 cells were transferred into a total volume of 15 ml fresh RPMI containing IL-2 without antibodies and transferred into a 10 cm dish. Cells were used on day 6 for further experiments.

### **3.3.5 *In vitro* Treg suppression assay**

CD4<sup>+</sup>CD25<sup>-</sup> (Tcon) and CD4<sup>+</sup>CD25<sup>+</sup> (Treg) T cells were separated using MACS technology (Miltenyi). Tcon cells were labeled with 5 μM CFSE for 15 min in the dark at 37°C and washed twice with fully supplemented RPMI. 2\*10<sup>5</sup> Tcon were activated with 2 μg/ml soluble anti-CD3 and 4 μg/ml soluble anti-CD28. Tregs were coincubated at the indicated ratios with labeled Tcon cells in the presence of 2\*10<sup>5</sup> APCs irradiated with 30 Gy. Proliferation, assessed by loss of the dye signal was analyzed 3 days later by flow cytometry.

### **3.3.6 Generation of iTregs via TGF-β *in vitro***

To induce Foxp3 *in vitro* naïve CD4<sup>+</sup>CD62L<sup>+</sup> T cells were isolated via MACS technology according to the protocol provided by the supplier. Isolated cells were washed twice with fully supplemented RPMI. 5\*10<sup>5</sup> cells were activated with 2 μg/ml plate bound anti-CD3 and 4 μg/ml soluble anti-CD28 in the presence of 2.5 ng/ml TGF-β. After 5 days of cultivation cells were analysed by intracellular staining of Foxp3 as described in 3.3.2.

### **3.3.7 Proliferation analyses via 5' bromodeoxyuridine**

For proliferation analyses, mice were fed orally with 0.8 μg/ml 5'bromodeoxyuridine (BrdU) in the drinking water for 14 days and incorporation was analysed using FITC BrdU Flow Kit (557891, BD Biosciences). As BrdU analysis interferes with Foxp3 staining, we identified Tregs via gating on CD25<sup>high</sup> cells.

### **3.3.8 Generation of mixed bone-marrow chimeric mice**

Bone marrow cells were isolated from femurs and tibias of donor animals (IκB<sub>NS</sub><sup>-/-</sup>Thy1.2<sup>+</sup> and IκB<sub>NS</sub><sup>+/+</sup>Thy1.1<sup>+</sup>). 5\*10<sup>6</sup> cells of each type were coinjected into C57BL/6 wildtype recipient mice 6 hours after sublethal irradiation (9 Gy). 8 weeks later, mice were sacrificed and

---

analysed by flow cytometry for the distribution of Foxp3 positive cells within Thy1.1 and Thy1.2 positive compartments.

### **3.3.9 IL-2 mediated expansion of regulatory T cells *in vivo***

Regulatory T cells were amplified *in vivo* by intravenous injection of a cytokine-antibody complex consisting of murine IL-2 (Peprotech) and anti-IL-2 antibody (JES6-1A12). 2 µg of murine IL-2 and 5 µg of anti IL-2 were mixed in 200 µl PBS and incubated for 30 min at 37°C with agitation. The antibody cytokine complex was injected at three consecutive days in the tail vein. Amplified Tregs were analyzed by intracellular Foxp3 analyses as described in 3.3.2 at day 5.

### **3.3.10 Adoptive transfer colitis**

Freshly isolated CD4<sup>+</sup>CD25<sup>-</sup> T cells ( $5 \times 10^5$ ) from C57BL/6 and I $\kappa$ B<sub>NS</sub>-deficient mice were injected intraperitoneally into RAG1<sup>-/-</sup> mice in 200 µl of PBS. CD4<sup>+</sup>CD25<sup>-</sup> T cells were isolated from murine spleens and lymph nodes by MACS separation (CD4 T Cell Isolation Kit, CD25-PE Kit, Miltenyi) to a purity degree of > 98 % as evaluated by flow cytometry. Wildtype and I $\kappa$ B<sub>NS</sub>-deficient mice were obtained from the animal facility of the Heinrich-Heine-University, Düsseldorf. RAG1<sup>-/-</sup> mice were bred at the animal facility of the Charité Berlin. All mice were kept under specific pathogen-free conditions, and used according to local animal care regulations. Body weight, stool consistency and rectal bleeding were regularly. Stool consistency was scored as follows: 0 - well-formed pellets, 2 - pasty and semi-formed stools which did not adhere to the anus, and 4 - liquid stools that did adhere to the anus. Rectal bleeding was scored as follows: 0 - no hemocult (Beckman Coulter), 2 - positive hemocult and 4 - gross bleeding. Colon length was measured from the caecum to the anus. Colon samples were fixed with 4% paraformaldehyde and embedded in paraffin. 2 µm sections were cut, deparaffinized, stained with hematoxylin and eosin and scored in a blinded manner. The transfer colitis-induced histological colitis score is the sum of individual scores for inflammatory cell infiltration and tissue damage. Colon samples were fixed with 4 % paraformaldehyde and embedded in paraffin. 2 µm sections were cut, deparaffinized, stained

---

with hematoxylin and eosin (H&E), and scored in a blinded manner. The transfer colitis was scored as follows: 0 - no changes, 1 - minimal scattered mucosal inflammatory cell infiltrates  $\pm$  minimal epithelial hyperplasia, 2 - mild scattered to diffuse mucosal cell infiltrates, sometimes extending into the submucosa and associated with erosions, with minimal to mild epithelial hyperplasia, with minimal to mild mucin depletion from goblet cells, 3 - mild to moderate cell infiltrates that were sometimes transmural, often associated with ulceration, with moderate epithelial hyperplasia and mucin depletion, 4 - marked inflammatory cell infiltrates that were often transmural and associated with ulceration, with marked epithelial hyperplasia and mucin depletion 5 - marked transmural inflammation with severe ulceration and loss of intestinal glands. Transfer colitis was performed in cooperation with Dr. Rainer Glauben and Dr. Anja A. Kühl from the Charité (Berlin).

### **3.3.11 Colon organ cultures**

A 1 cm segment of the colon was cut open longitudinally, washed in PBS and incubated over night in serum-free medium. Protein concentrations were determined (Bradford, BioRad) and cytokine concentrations of the supernatants analyzed via bead-based assays (CBA Flex Sets, BD Biosciences). Colon organ cultures were performed in cooperation with Dr. Rainer Glauben and Dr. Anja A. Kühl from the Charité (Berlin).

### **3.4 Statistics**

All statistical analyses were performed using Graph Pad Prism Software from Graph-Pad-Software Inc (La Jolla, CA, USA). Statistical significance was calculated by two-tailed Mann-Whitney-tests. Standard deviation (s.d.) and standard error of the mean (s.e.m.) were represented as error bars.

## 4 Results

### 4.1 $I\kappa B_{NS}$ deficiency intrinsically causes reduced $Foxp3^+$ cells *in vivo* and *in vitro*

Previous studies demonstrated, that  $I\kappa B_{NS}$  deficiency does not affect negative selection, whereby the composition of the T cell compartment in the thymus and  $V\beta$  usage remained unchanged, despite the massive induction of the protein in autoreactive developing T cells (Touma et al., 2007). Initially, the described phenotype was confirmed by the analyses of the percentages and total numbers of  $CD4^+CD8^-$ ,  $CD4^-CD8^+$  and  $CD4^+CD8^+$  T cells in the thymus. Corresponding to the literature these T cell populations were not altered in  $I\kappa B_{NS}^-$  deficient mice as judged by flow cytometry (Fig. 10a).

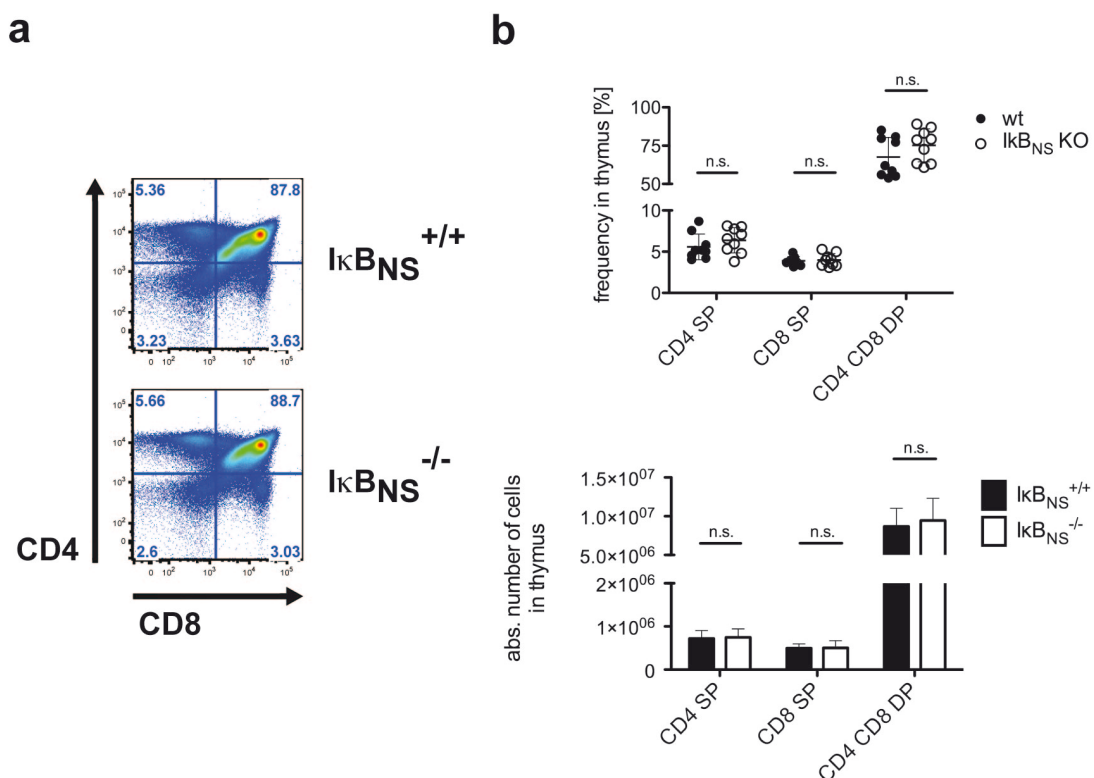


**Figure 10: Thymic distribution of CD4 and CD8 cells is not affected by  $I\kappa B_{NS}$  deficiency**  
(a) Representative pseudo-color dotplot analyses of  $CD4^-CD8^-$ ,  $CD4^+CD8^-$ ,  $CD4^-CD8^+$  and  $CD4^+CD8^+$  cells in thymi from wildtype and  $I\kappa B_{NS}$ -deficient 6 week old gender matched mice. Quadrant numbers indicate the percentages of double negative, single positive and double positive T cells. (b) Scatter dotplot diagram of percentages (upper panel) and bars of the absolute numbers (lower panel) of  $CD4^+CD8^-$ ,  $CD4^-CD8^+$  and  $CD4^+CD8^+$  cells in thymi from wildtype and  $I\kappa B_{NS}$ -deficient 6 week old gender matched mice. Statistical significances were calculated by two-tailed Mann-Whitney tests ( $n=9$ , mean  $\pm$  s.d.; n.s. = not significant).

Independent repetitions did not uncover any difference between wildtype and  $\text{I}\kappa\text{B}_{\text{NS}}$ -deficient mice regarding the percentages and total numbers of  $\text{CD4}^+\text{CD8}^-$ ,  $\text{CD4}^-\text{CD8}^+$  and  $\text{CD4}^+\text{CD8}^+$  T cells within their thymi, statistically verifying that  $\text{I}\kappa\text{B}_{\text{NS}}$  does not have an impact on T cell maturation in terms of negative selection (Fig. 10b).

Since  $\text{I}\kappa\text{B}_{\text{NS}}$  was expressed in autoreactive T cells in the thymus, it was investigated whether  $\text{I}\kappa\text{B}_{\text{NS}}$  contributes to their commitment to the Treg lineage. This idea followed from a recent study, which reported only minimal overlapping TCR specificities between  $\text{Foxp3}^-$  and  $\text{Foxp3}^+$  cells and found self-reactive TCRs expressed by the majority of the Treg cells (Aschenbrenner et al., 2007).

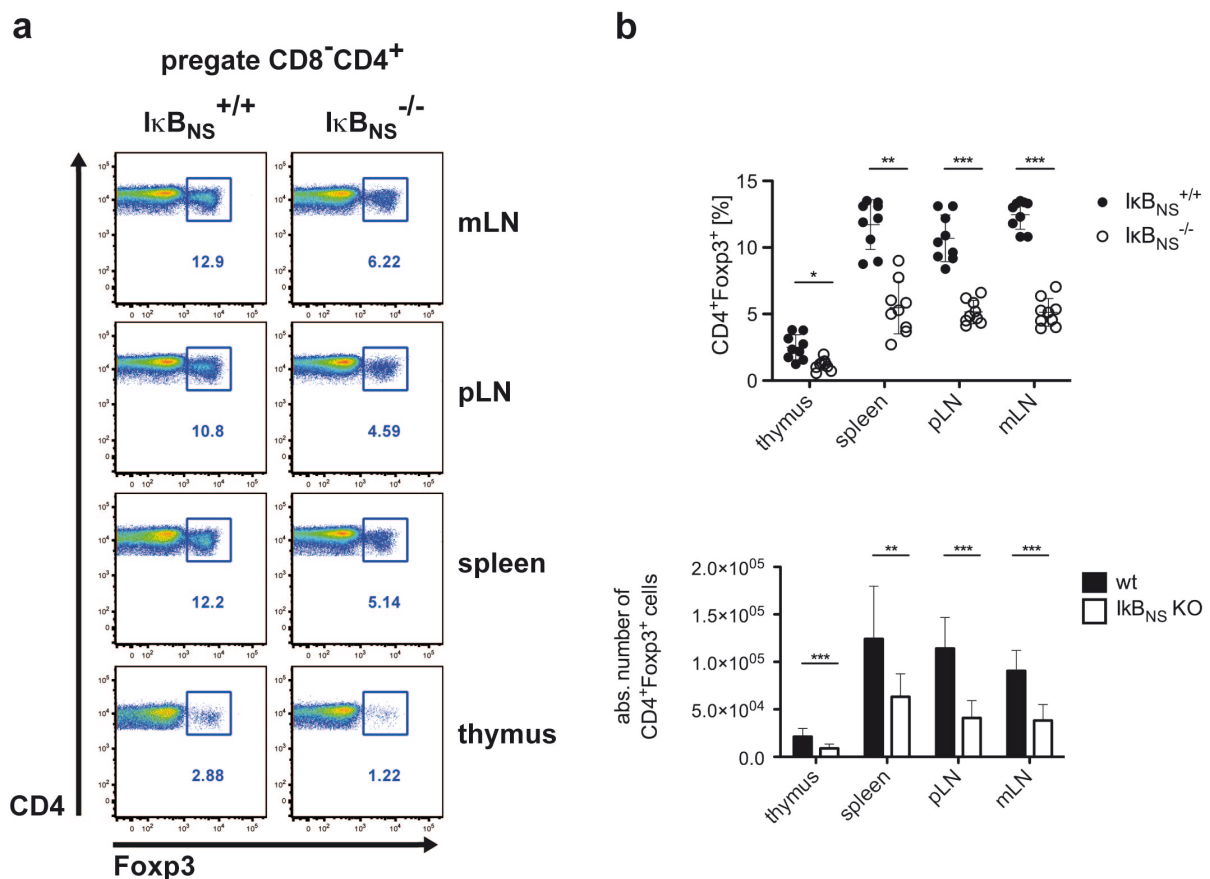


**Figure 11:  $\text{Foxp3}^+$  regulatory T cells are reduced in  $\text{I}\kappa\text{B}_{\text{NS}}$ -deficient mice**

(a) Representative pseudo-color dotplots of CD4 and Foxp3 positive cells in mesenteric and peripheral lymph nodes, spleens and thymi from wildtype and  $\text{I}\kappa\text{B}_{\text{NS}}$ -deficient 6 week old gender matched mice. Numbers indicate the percentages of  $\text{CD4}^+\text{Foxp3}^+$  Treg cells. (b) Scatter dotplot diagram of percentages (upper panel) and bars of the total numbers (lower panel) of  $\text{CD4}^+\text{Foxp3}^+$  Tregs in mesenteric and peripheral lymph nodes, spleens and thymi from wildtype and  $\text{I}\kappa\text{B}_{\text{NS}}$ -deficient 6 week old mice. Statistical significances were calculated by two-tailed Mann-Whitney tests ( $n=9$ , mean  $\pm$  s.d.; n.s. = not significant).

Therefore, autoreactive T cells, which are committed to the Treg lineage, are protected from negative selection in the thymus, although they express TCRs, which recognize self-peptides (Apostolou et al., 2002; Aschenbrenner et al., 2007; Hsieh et al., 2004). Flow cytometrical analyses of the frequencies of CD4<sup>+</sup>Foxp3<sup>+</sup> cells revealed a Treg reduction of about 50% in thymus, spleen, mesenteric and peripheral lymph nodes of I $\kappa$ B<sub>NS</sub>-deficient mice compared to sex- and age-matched wildtype controls (Fig.11a). Independently repeated experiments confirmed the reduction of the Treg compartment to a highly statistical significant extent (Fig.11b). Corresponding to the percentages, the absolute numbers of CD4<sup>+</sup>Foxp3<sup>+</sup> cells were significantly reduced as well (Fig.11b).

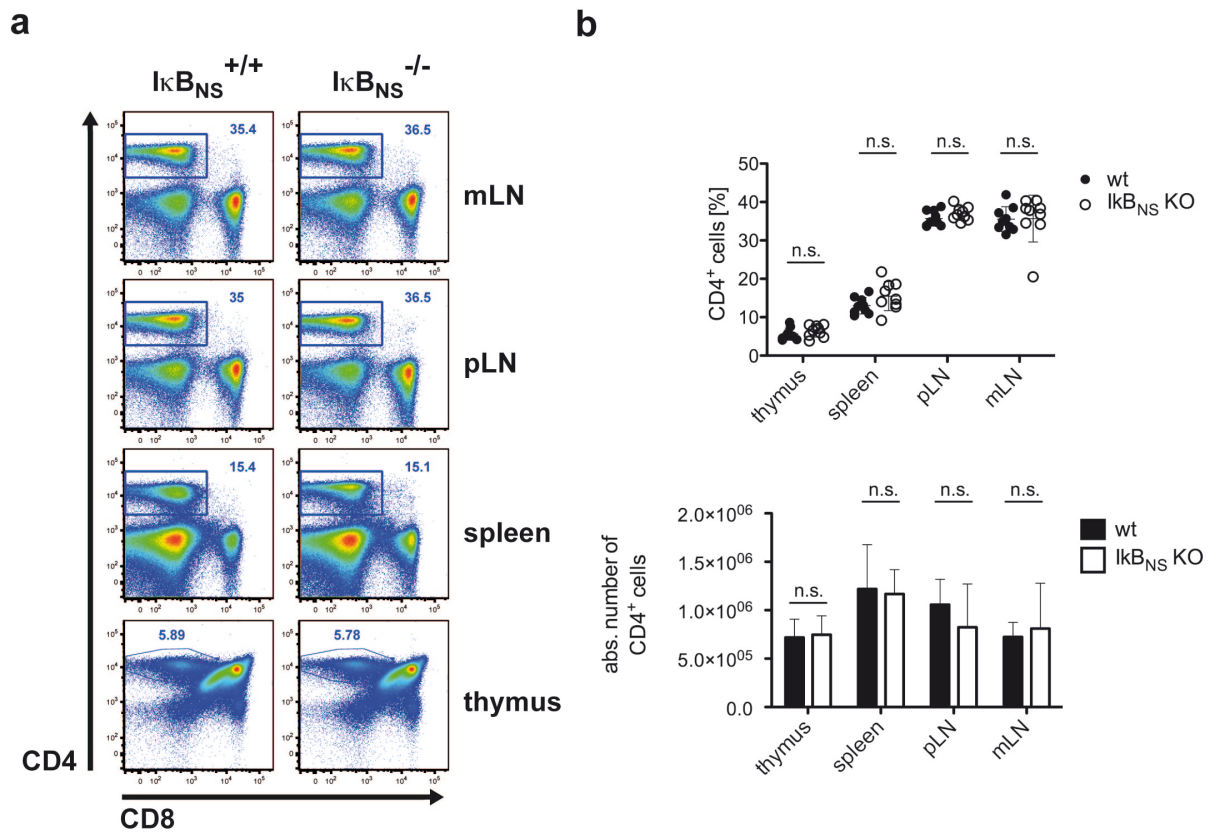


**Figure 12: T cell reduction is restricted to the Foxp3<sup>+</sup> Treg compartment**

**(a)** Representative pseudo-color dotblots of CD4<sup>+</sup> and CD8<sup>+</sup> T cells in mesenteric and peripheral lymph nodes, spleens and thymi from wildtype and I $\kappa$ B<sub>NS</sub>-deficient 6 week old gender matched mice. Numbers indicate the percentages of CD8<sup>-</sup>CD4<sup>+</sup> single positive cells. **(b)** Scatter dotblot diagram of percentages (upper panel) and bars of the total numbers (lower panel) of the entire CD4<sup>+</sup> T cell compartment in mesenteric and peripheral lymph nodes, spleens and thymi from wildtype and I $\kappa$ B<sub>NS</sub>-deficient 6 week old mice. Statistical significances were calculated by two-tailed Mann-Whitney tests (n=9, mean  $\pm$  s.d.; n.s. = not significant).

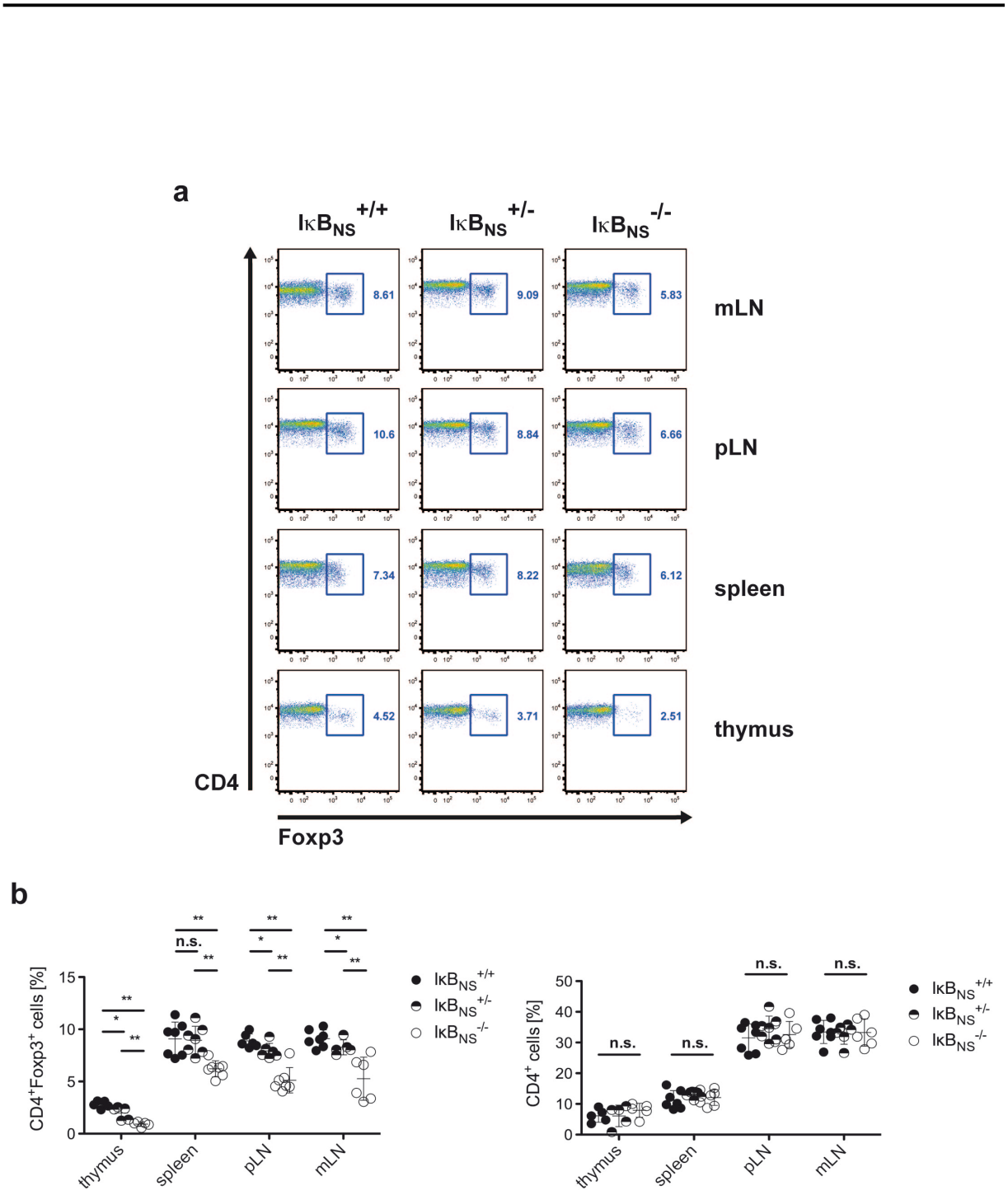


**Figure 13:  $IkB_{NS}$  regulates Treg development in a dose-dependent manner**

**(a)** Representative pseudo-color dotplots of CD4<sup>+</sup>Foxp3<sup>-</sup> and CD4<sup>+</sup>Foxp3<sup>+</sup> T cells in mesenteric and peripheral lymph nodes, spleens and thymi from wildtype, heterozygous and  $IkB_{NS}$ -deficient 6 week old littermate mice. Numbers indicate percentages of CD4<sup>+</sup>Foxp3<sup>+</sup> Tregs. **(b)** Scatter dotplot diagram of the percentages of CD4<sup>+</sup>Foxp3<sup>+</sup> Tregs (left panel) and the CD4<sup>+</sup> T cell compartment (right panel) in mesenteric and peripheral lymph nodes, spleens and thymi from wildtype, heterozygous and  $IkB_{NS}$ -deficient 6 week old littermate mice. Statistical significances were calculated by two-tailed Mann-Whitney tests (n=6, mean ± s.d.; n.s. = not significant; \* p<0.05; \*\* p<0.01).

---

As I $\kappa$ B<sub>NS</sub> deficiency might also have affected the entire CD4<sup>+</sup> T cell compartment the percentages of CD8<sup>-</sup>CD4<sup>+</sup> cells were determined by flow cytometry, accordingly (Fig.12a). There was no statistical significant difference detected, neither in percentages nor absolute cell numbers of CD8<sup>-</sup>CD4<sup>+</sup> cells in thymus, spleen, mesenteric and peripheral lymph nodes of I $\kappa$ B<sub>NS</sub>-deficient compared to wildtype mice (Fig.12a and 12b). Thus, it appeared that I $\kappa$ B<sub>NS</sub> upregulation in autoreactive cells in the thymus participates in directing these cells to the Treg lineage, rather than negative selection of thymocytes. Moreover, I $\kappa$ B<sub>NS</sub> deficiency did not appear to influence the total amount of CD8<sup>-</sup>CD4<sup>+</sup> T cells. To exclude that the observed differences were a result of unequal breeding conditions of wildtype and I $\kappa$ B<sub>NS</sub>-deficient mice and to determine whether I $\kappa$ B<sub>NS</sub> modulates Treg development in a dose dependent manner, the percentages of CD4<sup>+</sup>Foxp3<sup>+</sup> Tregs and of the CD8<sup>-</sup>CD4<sup>+</sup> compartment in littermate mice were determined by flow cytometry (Fig. 13a). The differences in the percentages between wildtype and heterozygous mice was minimal, but statistical significant in thymus, mesenteric and peripheral lymph nodes (Fig. 13a and 13b). In the spleen, however, no difference was detected between wildtype and heterozygous littermate mice (Fig. 13a and 13b). I $\kappa$ B<sub>NS</sub>-deficient mice displayed a reduction of Tregs of about 50% in thymus and peripheral lymphoid organs when compared to wildtype littermate controls while the amount of the entire CD8<sup>-</sup>CD4<sup>+</sup> compartment remained unaffected as seen before in sex- and age-matched mice (Fig. 13a and 13b). As the development of regulatory T cells *in vivo* was impaired by I $\kappa$ B<sub>NS</sub> deficiency, it was tested, whether induction via TGF- $\beta$  *in vitro* in CD8<sup>-</sup>CD4<sup>+</sup>CD62L<sup>+</sup>CD25<sup>-</sup> naive T cells affected Foxp3 induction as well. As costimulation with IL-2 was reported to massively enhance Foxp3 expression via STAT5 it was used in combination with TGF- $\beta$  (Fu et al., 2004). Remarkably, Foxp3 was only minimally induced by TGF- $\beta$  without the addition of exogenous IL-2 to a percentage of about 5% in both wildtype and I $\kappa$ B<sub>NS</sub>-deficient naive cells (Fig. 14a and 14b). Exogenous IL-2 exacerbated Foxp3 expression to about 35% in wildtype cells, but had no effect on I $\kappa$ B<sub>NS</sub>-deficient cells (Fig. 14a and 14b). Thus, Foxp3 induction *in vivo* and *in vitro* appeared to directly depend on I $\kappa$ B<sub>NS</sub>.

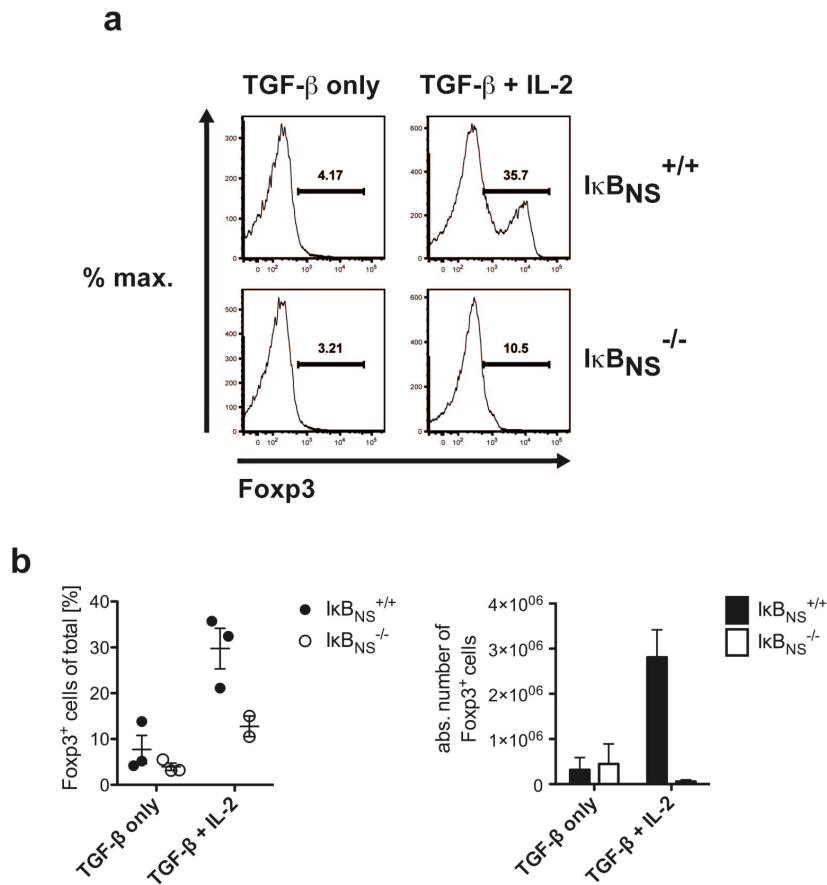


**Figure 14:  $\text{IkB}_{\text{NS}}$  deficiency affects Foxp3 induction by TGF- $\beta$  *in vitro***

**(a)** Representative histogram analysis of Foxp3 expression in purified  $\text{CD4}^+\text{CD62L}^+\text{CD25}^-$  naïve peripheral T cells, isolated from wildtype and  $\text{IkB}_{\text{NS}}$ -deficient 6 week old mice of matched gender and age, incubated with TGF- $\beta$  (5 ng/ml) alone or TGF- $\beta$  combined with IL-2 (10 ng/ml) for 6 days. **(b)** Scatter dotplot diagram of the percentages (left panel) and bars of the total numbers (right panel) of Foxp3<sup>+</sup> cells (n=3, mean  $\pm$  s.d.).

The observation that  $\text{IkB}_{\text{NS}}$  deficiency affected Foxp3 induction *in vitro* suggested that the protein intrinsically modulates Treg generation. The commonly used experiment to proof this is the generation of mixed-bone marrow chimeric mice. To this end, T cell depleted bone marrow cells from  $\text{Thy1.1}^+$  wildtype and  $\text{Thy1.2}^+$   $\text{IkB}_{\text{NS}}$ -deficient mice were adoptively transferred in 1:1 ratio into sublethally irradiated acceptor mice (Fig. 15a) (Isomura et al., 2009). The immune system is completely regenerated by the transferred bone marrow cells. This technique allowed the analysis of Treg generation in  $\text{IkB}_{\text{NS}}$ -deficient cells in a competitive situation with wildtype cells *in vivo*. If the reduced Treg compartment of  $\text{IkB}_{\text{NS}}$ -deficient mice resulted from deprivation of a soluble factor, it would have been compensated by the wildtype cells and led to normal Treg generation. In the generated bone

marrow chimeric mice the CD8<sup>+</sup>CD4<sup>+</sup> compartment approximately consisted to the same extent of Thy1.1<sup>+</sup> wildtype and Thy1.2<sup>+</sup> I $\kappa$ B<sub>NS</sub> deficient T cells (Fig. 15b and 15c). The Treg compartment within the wildtype CD4<sup>+</sup>Thy1.1<sup>+</sup> subset developed to an extent of about 11% comparable to Tregs in wildtype mice (Fig. 15b and 15c). Virtually none F $\kappa$ p3<sup>+</sup> Tregs were detectable in the I $\kappa$ B<sub>NS</sub>-deficient CD4<sup>+</sup>Thy1.2<sup>+</sup> subset demonstrating that the protein modulates Treg development in an intrinsic fashion (Fig. 15b and 15c).

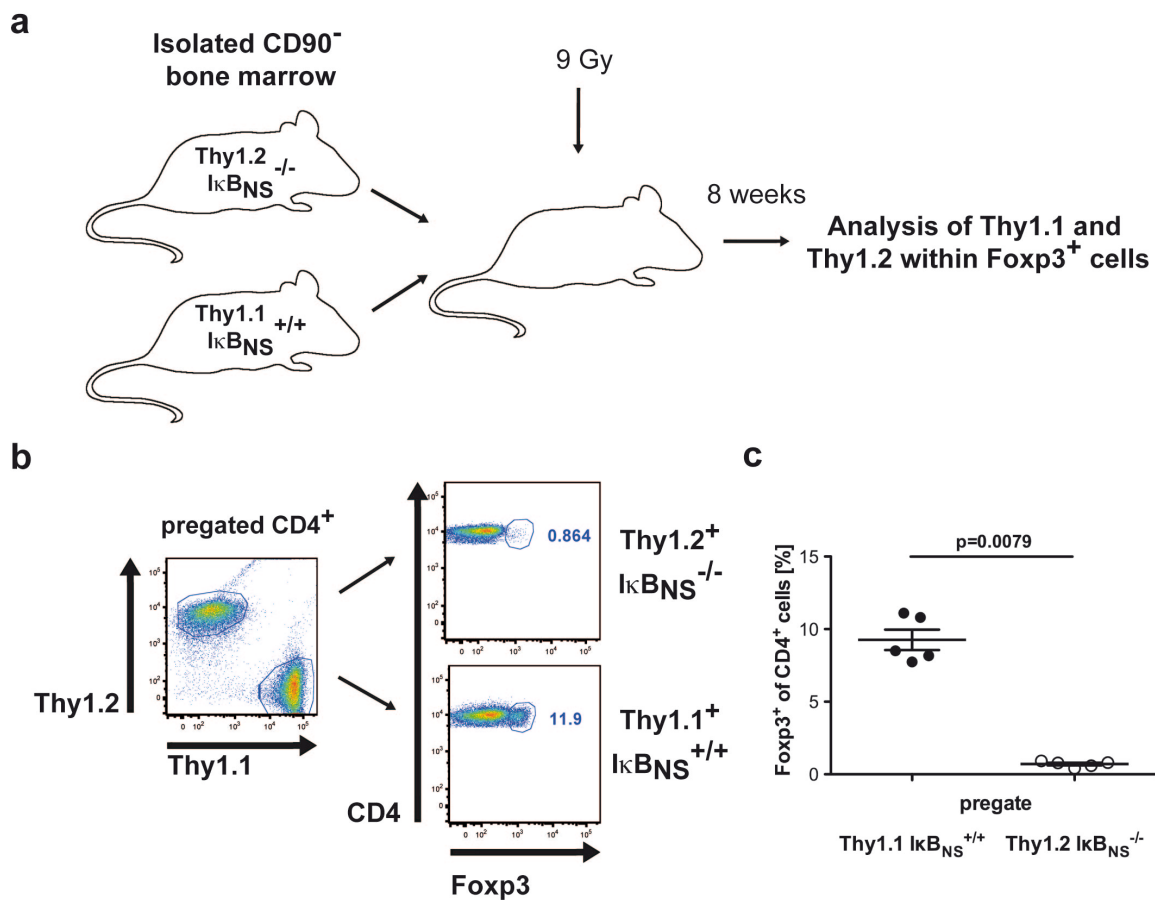


**Figure 15: I $\kappa$ B<sub>NS</sub> regulates Treg development in an intrinsic manner**

**(a)** Schematic overview of the generation of mixed-bone-marrow chimeric mice. To control Treg generation upon I $\kappa$ B<sub>NS</sub>-deficiency in a competitive situation  $5 \times 10^6$  purified bone-marrow cells of I $\kappa$ B<sub>NS</sub><sup>-/-</sup>Thy1.2<sup>+</sup> mice and wildtype Thy1.1<sup>+</sup> mice were co-injected into wildtype mice, which were sublethally irradiated with 9 Gray. After 8 weeks the distribution of Thy1.1<sup>+</sup> to Thy1.2<sup>+</sup> cells within the Treg compartment was analysed. **(b)** Representative pseudo-color dotplots of percentages of F $\kappa$ p3<sup>+</sup> cells pre-gated to Thy1.1<sup>+</sup>I $\kappa$ B<sub>NS</sub><sup>+/+</sup> or Thy1.2<sup>+</sup>I $\kappa$ B<sub>NS</sub><sup>-/-</sup> CD4<sup>+</sup> T cells. Numbers indicate the percentages of CD4<sup>+</sup>F $\kappa$ p3<sup>+</sup> Tregs. **(c)** Scatter dotplot diagram of the percentages of CD4<sup>+</sup>F $\kappa$ p3<sup>+</sup> cells originated from Thy1.1<sup>+</sup>I $\kappa$ B<sub>NS</sub><sup>+/+</sup> or Thy1.2<sup>+</sup>I $\kappa$ B<sub>NS</sub><sup>-/-</sup> bone marrow. Statistical significances were calculated by two-tailed Mann-Whitney tests (n=5, mean  $\pm$  s.d.).

---

Taken together,  $\text{I}\kappa\text{B}_{\text{NS}}$ -deficiency causes a systemic reduction of the  $\text{CD4}^+\text{Foxp3}^+$  Treg compartment *in vivo* and impairs Foxp3 induction by TGF- $\beta$  *in vitro*. The observed differences were proved to be the result of a Treg intrinsic developmental defect demonstrated by the analyses of mixed bone marrow chimeric mice.

#### **4.2 Functionality of Tregs from $\text{I}\kappa\text{B}_{\text{NS}}$ -deficient mice is not altered**

Regulatory T cells suppress the activity of effector T cells. As the regulatory T cell compartment in  $\text{I}\kappa\text{B}_{\text{NS}}$ -deficient mice is massively reduced it might affect the activation status of Foxp3 $^-$  conventional T cells. Commonly, CD62L and CD44 are used to describe the T cell activation status, whereby CD62L expression is restricted to naive cells resting in the lymphoid organs and CD44 $^+$  to non-resting activated cells. Comparison of activated CD62L $^-$ CD44 $^+$  cells among Foxp3 $^-$ CD8 $^-$ CD4 $^+$  Tcon cells in thymus, spleen, peripheral and mesenteric lymph nodes did not reveal any differences between wildtype, heterozygous and  $\text{I}\kappa\text{B}_{\text{NS}}$ -deficient littermate mice (Fig.16a and 16b). The subset of naive CD62L $^+$ CD44 $^-$  cells was most prominent in the spleen, mesenteric and peripheral lymph nodes with about 85%. In the thymus the CD62L $^-$ CD44 $^-$  subset displayed a percentage of about 60% and CD62L $^+$ CD44 $^-$  cells about 30%, but no statistical significant differences between the three genotypes were detected (Fig.16a and 16b). In conclusion, the reduction of the Treg compartment does not lead to increased activated CD62L $^-$ CD44 $^+$ Foxp3 $^-$  Tcon cells or decreased CD62L $^+$ CD44 $^-$  naive cells.

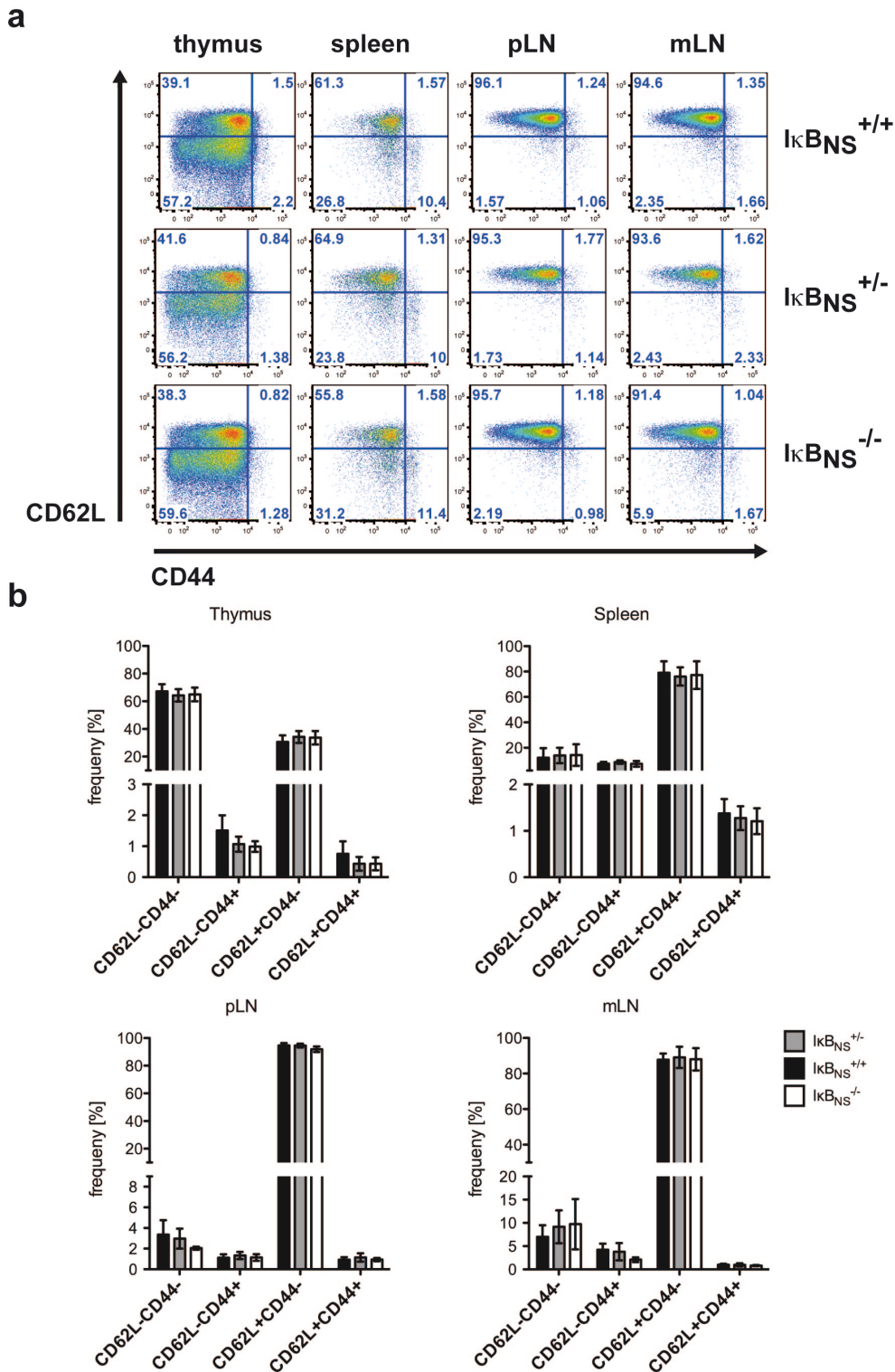


**Figure 16: IκBNS deficiency does not cause enhanced T<sub>eff</sub> activation**

(a) Representative pseudo-color dotblots of CD62L and CD44 expression in CD4<sup>+</sup>Foxp3<sup>-</sup> T cells in mesenteric and peripheral lymph nodes, spleens and thymi from wildtype, heterozygous and IκBNS<sup>-</sup> deficient 6 week old littermate mice. Numbers indicate percentages of the corresponding populations. (b) Bars of the percentages of CD62L<sup>-</sup>CD44<sup>-</sup>, CD62L<sup>+</sup>CD44<sup>-</sup> and CD62L<sup>+</sup>CD44<sup>+</sup> in CD4<sup>+</sup>Foxp3<sup>-</sup> T cells in mesenteric and peripheral lymph nodes, spleens and thymi from wildtype, heterozygous and IκBNS<sup>-</sup> deficient 6 week old littermate mice. (n=3, mean ± s.d).

---

To physiologically characterise regulatory T cells, the expression of CD25 (IL2-R $\alpha$ ), CD122 (IL7-R), GITR, Foxp3 and intracellular CTLA-4 in Tregs and Tcon cells from thymus, spleen, mesenteric and peripheral lymph nodes was compared in wildtype, heterozygous and I $\kappa$ B<sub>NS</sub>-deficient littermate mice. Of note CD25, CD122 and CTLA-4 are strongly induced in Foxp3<sup>+</sup> Tcon cells after activation and to a weaker extent GITR as well. As most of the Tcon cells are not activated (Fig. 16), these proteins can be used to characterise Treg cells under basal conditions. Comparison of the mean fluorescent intensities (MFI) of the indicated proteins did not uncover any difference between wildtype, heterozygous and I $\kappa$ B<sub>NS</sub>-deficient animals (Fig. 17a and 17b). However, Foxp3<sup>-</sup> Tcon cells of each genotype displayed a markedly decreased expression of the analysed proteins compared to Foxp3<sup>+</sup> Treg cells (Fig. 17a), reflecting that most of them are CD62L<sup>+</sup>CD44<sup>-</sup> naive cells (Fig. 16). The expression of CD122 in Treg cells of each genotype was only marginally increased compared to Tcon cells indicating that its basal expression is minimal (Fig. 17a). So, I $\kappa$ B<sub>NS</sub> appeared not to modulate the maintenance of mature Foxp3<sup>+</sup> Treg cells.

It was previously reported that stability of Foxp3 expression is epigenetically regulated by demethylation of 11 CpG sites located within the *Foxp3* locus (Floess et al., 2007; Polansky et al., 2008). As these CpG sites are localised in close vicinity this DNA segment was termed Treg specific demethylation region (TSDR) (Huehn et al., 2009). As mentioned above, the TSDR is part of a group of three conserved non-coding DNA sequences (CNS), which are localised downstream of the *Foxp3* promoter and regulate Foxp3 expression (Toker and Huehn, 2011; Zheng et al., 2010). Thus, the TSDR is referred to as CNS2 as it is the second regulatory sequence downstream of the promoter. To analyse, whether the reduced Treg compartment of I $\kappa$ B<sub>NS</sub>-deficient mice results from impaired stability of Foxp3 expression, the methylation status of CNS2 was analysed. To this end, CD8<sup>-</sup>CD4<sup>+</sup>CD25<sup>-</sup> Tcon and CD8<sup>-</sup>CD4<sup>+</sup>CD25<sup>+</sup> Treg cells were purified from the peripheral lymphoid organs of male wildtype and I $\kappa$ B<sub>NS</sub>-deficient mice of matched age (Fig. 18a). The isolated populations were stained for intracellular Foxp3 to confirm their purity (Fig. 18a).

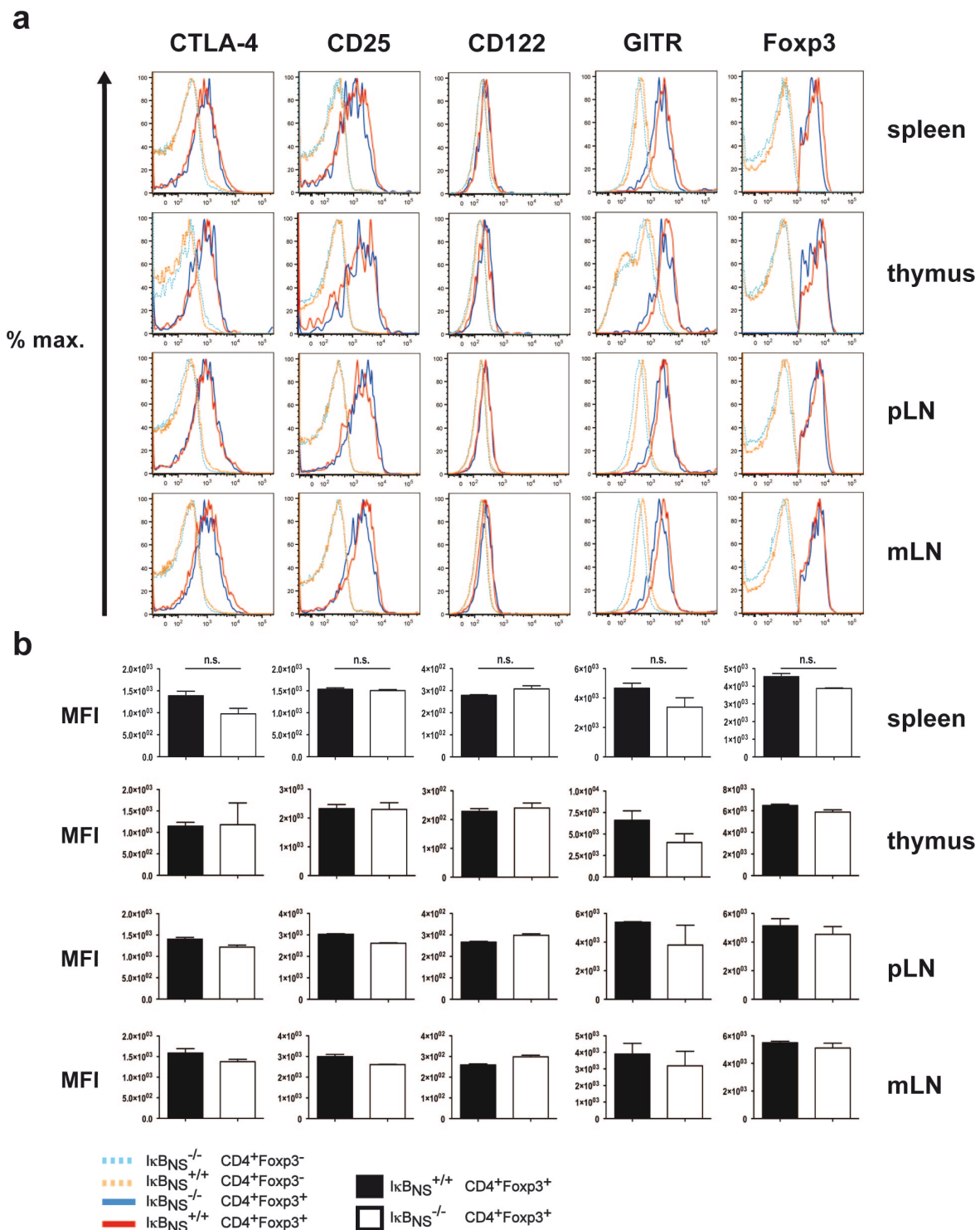


**Figure 17: Tregs of  $I\kappa BNS$ -deficient mice display normal expression of Treg marker proteins**

**(a)** Representative histogram analysis of expression of CTLA-4, CD25, CD122, GITR and Foxp3 in  $CD4^{+}Foxp3^{-}$  and  $CD4^{+}Foxp3^{+}$  cells from mesenteric and peripheral lymph nodes, spleens and thymi from wildtype and  $I\kappa BNS$ -deficient 6 week old mice of matched gender. **(b)** Bars of the mean fluorescent intensities (MFI) of CTLA-4, CD25, CD122, GITR and Foxp3 in  $CD4^{+}Foxp3^{+}$  cells from wildtype and  $I\kappa BNS$ -deficient 6 week old mice. Statistical significances were calculated by two-tailed Mann-Whitney tests ( $n=3$ , mean  $\pm$  s.d).

---

Since the *Foxp3* gene is localised at ChrX:7.16-1.17 Mb and the second X-chromosome is silenced by methylation in female vertebrates only male mice can be used to study epigenetic regulation of *Foxp3* via CNS2. The percentage of cells, which displayed a methylated CNS2 was assessed by bisulfid sequencing in cooperation with Dr. Stefan Floess from the department of Experimental Immunology at the HZI (Braunschweig). 100% of the isolated CD25<sup>-</sup>*Foxp3*<sup>-</sup> cells from both genotypes showed a methylated CNS2, reflecting that *Foxp3* is silenced in Tcon cells (Fig. 18b). Only about 15% of the CD25<sup>+</sup>*Foxp3*<sup>+</sup> Treg cells isolated from wildtype and *I $\kappa$ B<sub>NS</sub>*-deficient mice displayed a methylated CNS2 (Fig. 18b and 18c). Thus, the removal of methyl groups from the *Foxp3* locus is mediated independently of *I $\kappa$ B<sub>NS</sub>*, suggesting that instability of *Foxp3* expression is not the reason of impaired Treg development seen in *I $\kappa$ B<sub>NS</sub>*-deficient mice.

Finally, the suppressive capacity of regulatory T cells was determined *in vitro*. Therefore, CFSE-labelled Tcon cells were activated in the presence of Treg cells from wildtype or *I $\kappa$ B<sub>NS</sub>*-deficient mice in ascending ratios. Proliferation of Tcon cells decreased in a dose-dependent manner with increasing amounts of Tregs and was almost completely blocked at a 1:1 ratio (Fig. 19a and 19b). Only a marginal reduced suppressive capacity of *I $\kappa$ B<sub>NS</sub>*-deficient compared to wildtype Tregs was detected at ratios of 1:2 and 1:4, which was not statistical significant (Fig. 19a and 19b). At the other ratios, suppression of Tcon proliferation mediated by wildtype and *I $\kappa$ B<sub>NS</sub>*-deficient Tregs was identical.

Taken together, these analyses did not uncover a difference in functioning between *I $\kappa$ B<sub>NS</sub>*-deficient and wildtype Tregs analysed by the expression of CD25, CD122, CTLA-4, GITR, *Foxp3* and the demethylation of CNS2. Treg suppressive function was only mildly reduced in Tregs isolated from *I $\kappa$ B<sub>NS</sub>*-deficient mice.

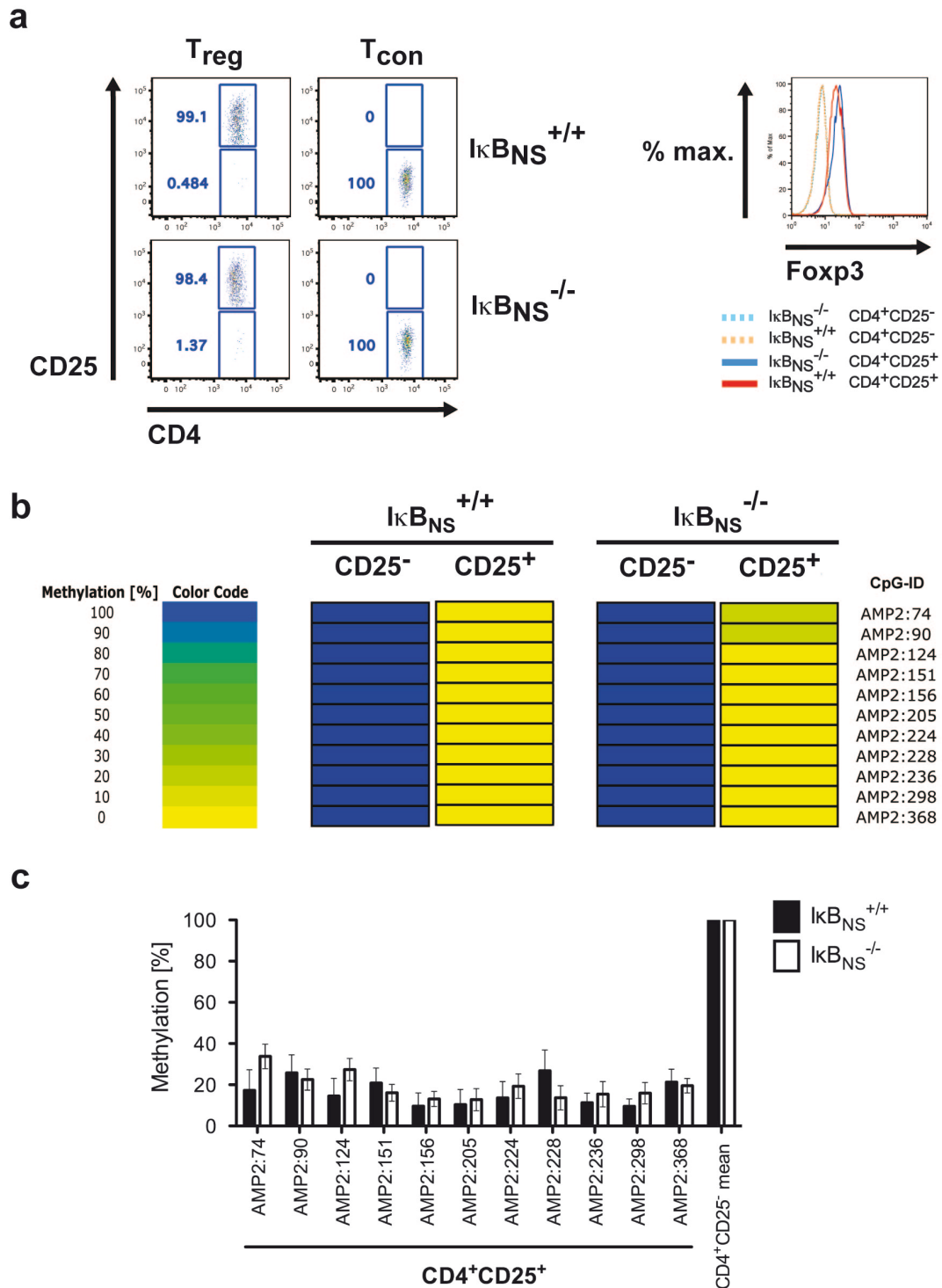


**Figure 18: CNS2 is normally demethylated in  $I\kappa B_{NS}$ -deficient Tregs**

(a) Representative pseudo-color dotplot of sorted  $CD4^+CD25^+$  and  $CD4^+CD25^-$  Tcon cells from the peripheral lymph nodes and spleens from wildtype and  $I\kappa B_{NS}^{-/-}$  8 weeks old male littermate mice (left panel). Representative histogram analysis of Foxp3 stained in the purified populations (right panel). Numbers indicate percentages of the isolated populations. (b) Representative color code analysis of the CNS2 methylation. Color code indicates the percentage of cells displaying a methylated CpG-site at the indicated position. (c) Bars of the percentage of cells displaying methylation of an individual CpG-site at the indicated position (wt: n=8,  $I\kappa B_{NS}^{-/-}$  n=5; mean  $\pm$  s.d.).

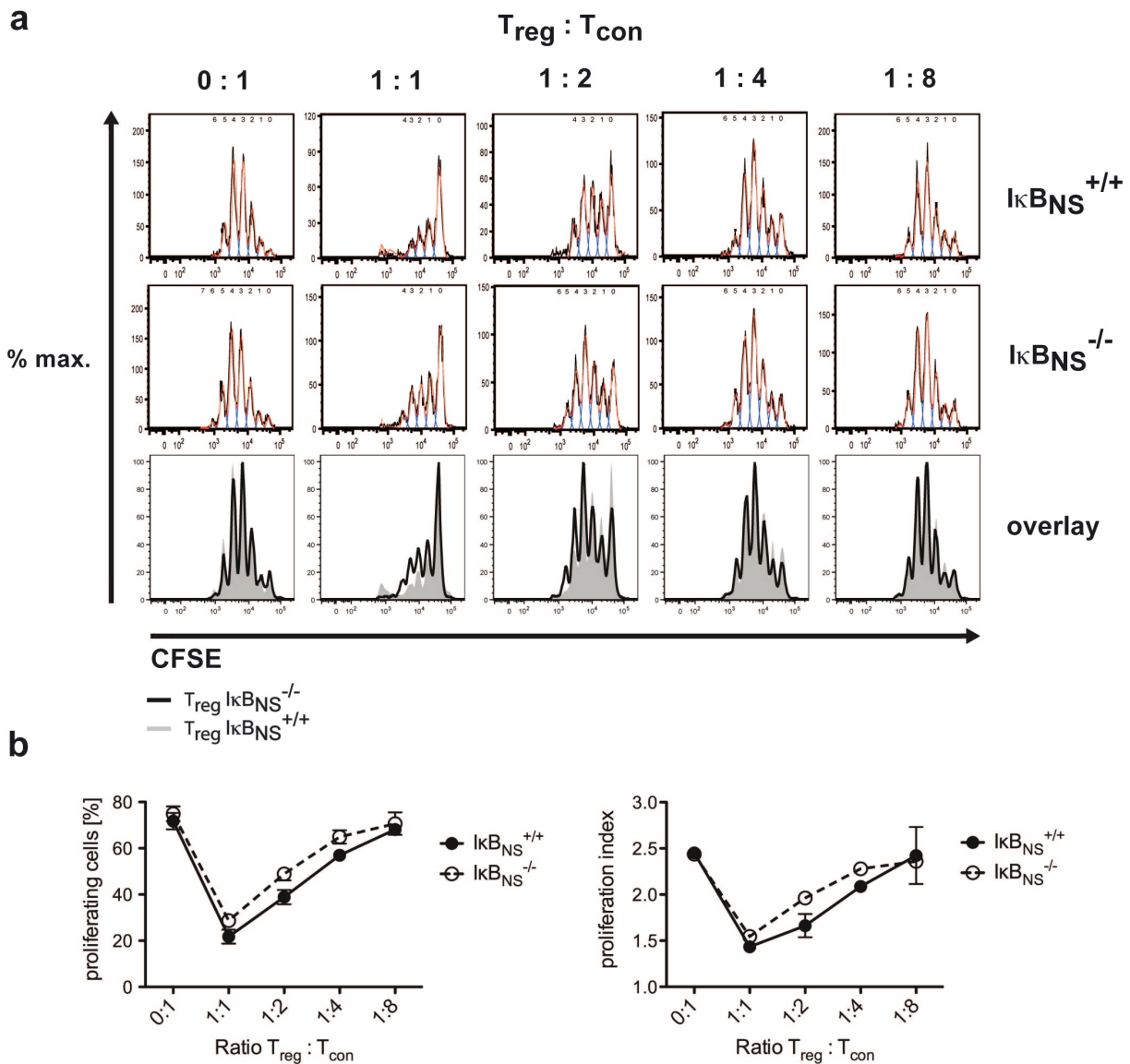


**Figure 19: Suppressive capacity of  $IkB_{NS}$ -deficient Tregs is not impaired**

**(a)** Representative proliferation analyses of CFSE-labelled  $CD4^+Foxp3^-$  wildtype Tcon cells activated in the indicated ratios in the presence of  $CD4^+Foxp3^+$  Tregs isolated from the peripheral lymph nodes and spleens from wildtype and  $IkB_{NS}^{-/-}$  8 weeks old littermate mice. **(b)** Mean of the percentages of proliferating wildtype  $CD4^+Foxp3^-$  cells (left panel) and their average number of cell divisions at the indicated ratios of Treg to Tcon cells calculated by FlowJo® software (right panel; wt: n=9; mean  $\pm$  s.d).

---

### 4.3 I $\kappa$ B<sub>NS</sub>-deficient Treg cells display enhanced proliferation but normal apoptosis

Previous studies demonstrated reduced proliferation of I $\kappa$ B<sub>NS</sub>-deficient CD8<sup>+</sup>CD4<sup>+</sup> and CD8<sup>+</sup>DC4<sup>-</sup> T cells isolated from thymus and spleen after TCR triggering *in vitro* (Touma et al., 2007). To exclude that impaired proliferation *in vivo* causes the reduced Treg compartment found in I $\kappa$ B<sub>NS</sub>-deficient mice, expression of Ki67 was analysed by flow cytometry. Ki67 is a chromosome-associated protein, which is downregulated upon entering the G0-arrest and, thus, a marker for proliferating cells (Schluter et al., 1993; Scholzen and Gerdes, 2000). However, the functional role of Ki67 for cell cycle regulation remains enigmatic. The increased amount of Ki67-positive cells found within Foxp3<sup>+</sup> Tregs from thymus, spleen, mesenteric and peripheral lymph nodes of I $\kappa$ B<sub>NS</sub>-deficient compared to heterozygous and wildtype littermate mice indicated their enhanced proliferation (Fig. 20a and 20b). The increase of Ki67<sup>+</sup> cells was restricted to the Treg compartment and statistically significant compared to wildtype Tregs, but Tcon cells of I $\kappa$ B<sub>NS</sub>-deficient mice did not display enhanced proliferation (Fig. 20a and 20b).

To corroborate these data, wildtype, heterozygous and I $\kappa$ B<sub>NS</sub>-deficient littermate mice were orally fed with 5' bromodeoxyuridine (BrdU) via the drinking water for 14 days. BrdU is integrated into the DNA during the S-phase as a thymidine analog and can be analyzed using a fluorochrome-coupled specific antibody by flow cytometry. I $\kappa$ B<sub>NS</sub>-deficient Tregs in spleen, mesenteric and peripheral lymph nodes, but not in the thymus displayed increased BrdU incorporation compared to heterozygous and wildtype littermate mice (Fig. 21a and 21b). Thus, the corresponding increase in percentages of Ki67<sup>+</sup> and BrdU<sup>+</sup> Tregs demonstrated enhanced proliferation of the Treg compartment in I $\kappa$ B<sub>NS</sub>-deficient mice under basal conditions. Regulatory T cells are shown to proliferate massively upon injection of IL-2/anti-IL-2 (Fig. 22a) (Burchill et al., 2007). According to this protocol, injection of a cytokine antibody complex in 6 week old wildtype and I $\kappa$ B<sub>NS</sub>-deficient mice led to an increase of the Treg compartment in spleen, mesenteric and peripheral lymph nodes (Fig. 22b and 22c). Remarkably, I $\kappa$ B<sub>NS</sub>-deficient mice displayed a 3.5 fold increase of Treg percentages in

the spleen compared to a 2.8 fold increase of wildtype Tregs, whereas proliferation of Tregs in mesenteric and peripheral lymph nodes was not altered between the two genotypes (Fig. 22d). To control, whether increased proliferation of  $\text{I}\kappa\text{B}_{\text{NS}}$ -deficient Tregs represents a compensation of enhanced cell death,  $\text{I}\kappa\text{B}_{\text{NS}}$ -deficient mice were bred with DERE $\text{G}$  ( $\text{Foxp3}^{\text{DTR-eGFP}}$ ) reporter mice (Fig. 23a). The Foxp3 reporter allowed 7AAD/AnnexinV and TMRE stainings of unfixed Tregs.

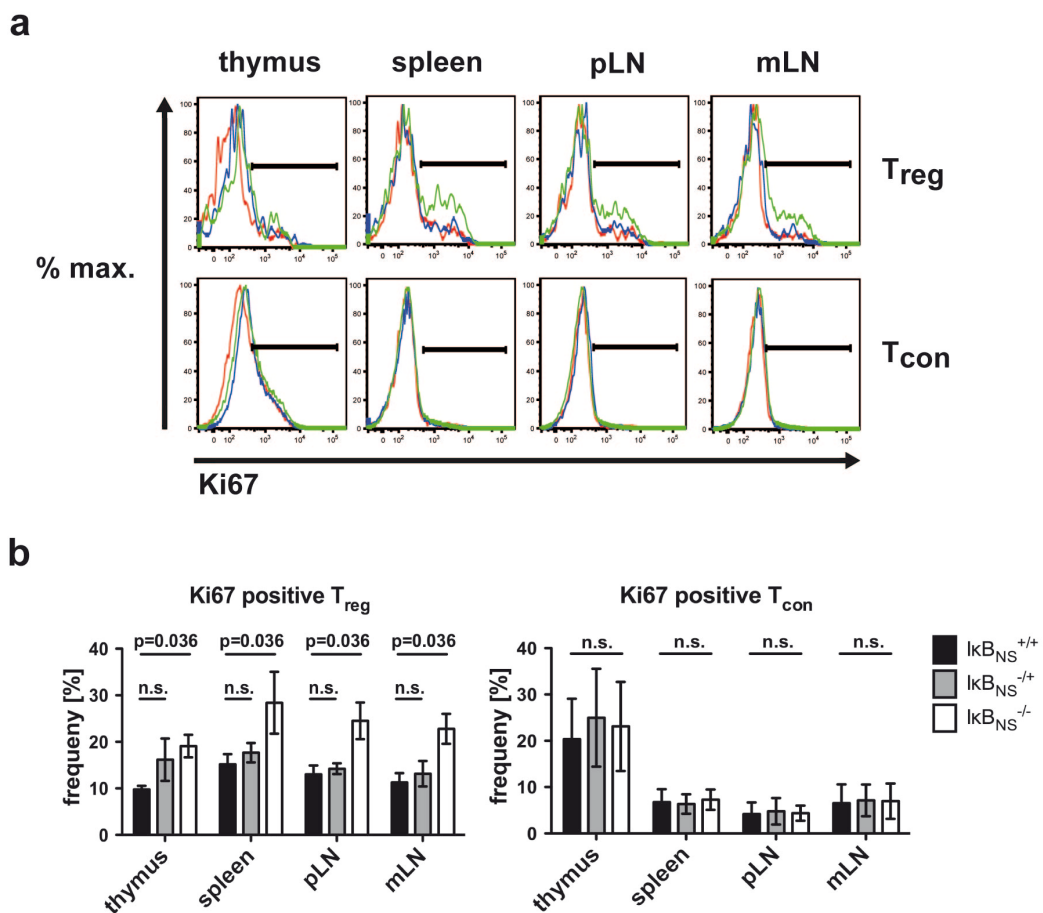


**Figure 20: The Treg compartment of  $\text{I}\kappa\text{B}_{\text{NS}}$ -deficient mice displays more  $\text{Ki67}^+$  cells**

**(a)** Representative histogram analyses of intracellular Ki67 expression in  $\text{CD4}^+\text{Foxp3}^+$  Tregs (upper panel) and  $\text{CD4}^+\text{Foxp3}^-$  Tcon cells (lower panel) in thymi, spleens, peripheral and mesenteric lymph nodes from wildtype, heterozygous and  $\text{I}\kappa\text{B}_{\text{NS}}$ -deficient littermate mice. **(b)** Bars of the percentages of  $\text{Ki67}^+\text{CD4}^+\text{Foxp3}^+$  Tregs (left panel) and  $\text{Ki67}^+\text{CD4}^+\text{Foxp3}^-$  Tcon cells (right panel) in thymi, spleens, peripheral and mesenteric lymph nodes from wildtype, heterozygous and  $\text{I}\kappa\text{B}_{\text{NS}}$ -deficient littermate mice. Statistical significances were calculated by two-tailed Mann-Whitney tests ( $n=9$ ; mean  $\pm$  s.d.; n.s. = not significant).

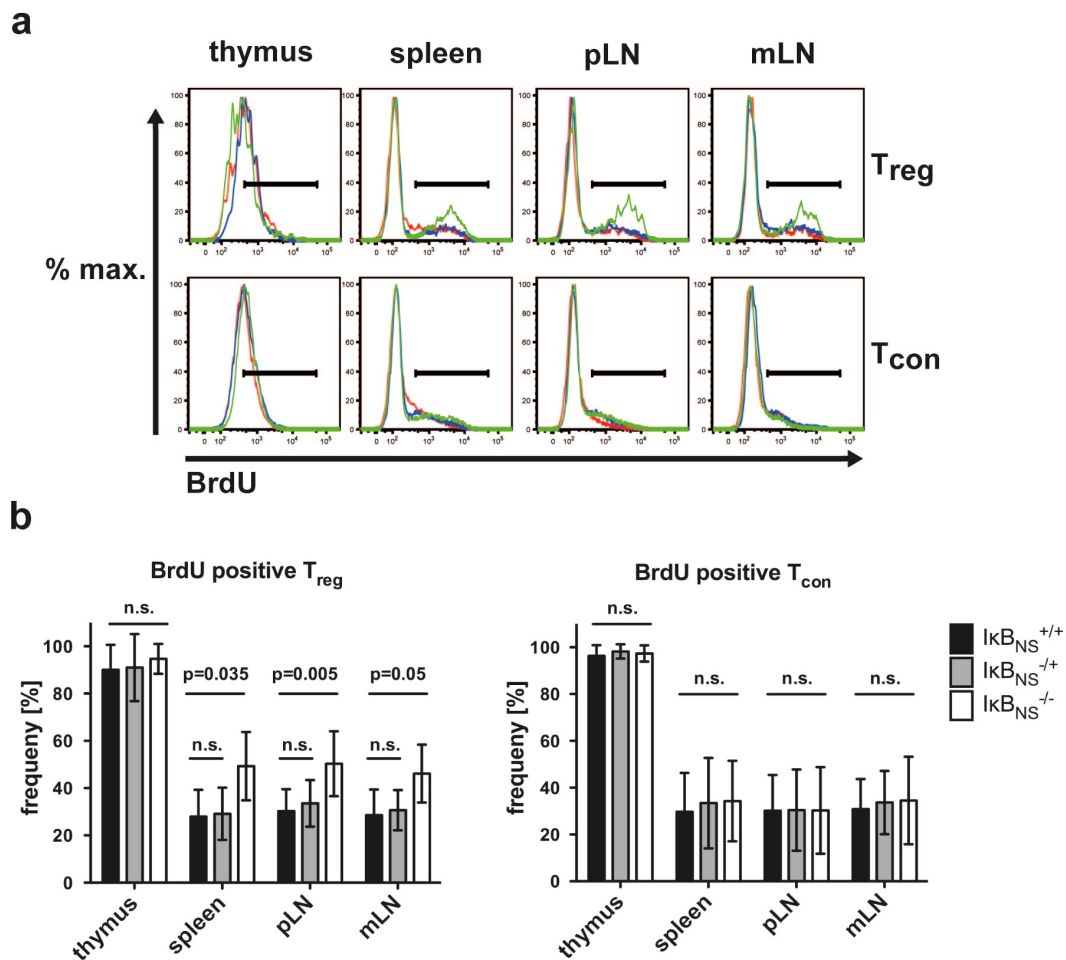


**Figure 21: Tregs of  $\text{IkB}_{\text{NS}}$ -deficient mice undergo enhanced proliferation**

**(a)** Representative histogram analyses of BrdU incorporated by  $\text{CD4}^+\text{Foxp3}^+$  Tregs (upper panel) and  $\text{CD4}^+\text{Foxp3}^-$  Tcon cells (lower panel) in thymi, spleens, peripheral and mesenteric lymph nodes from wildtype, heterozygous and  $\text{IkB}_{\text{NS}}$ -deficient littermate mice fed with 0.8  $\mu\text{g}/\text{ml}$  BrdU in drinking water. **(b)** Bars of the percentages of  $\text{BrdU}^+\text{CD4}^+\text{Foxp3}^+$  Tregs (left panel) and  $\text{BrdU}^+\text{CD4}^+\text{Foxp3}^-$  Tcon cells (right panel) in thymi, spleens, peripheral and mesenteric lymph nodes from wildtype, heterozygous and  $\text{IkB}_{\text{NS}}$ -deficient littermate mice. Statistical significances were calculated by two-tailed Mann-Whitney tests ( $n=9$ ; mean  $\pm$  s.d.; n.s. = not significant).

Tetramethylrhodamine ethyl ester (TMRE) is used to determine cells, which lost mitochondrial membrane potential as the earliest marker for apoptotic cells. Upon apoptosis, ATP levels are reducing as a result of disrupted mitochondrial membrane integrity and flipases can no longer maintain plasma membrane asymmetry. This leads to exposure of phosphatidylserine (PS), which is usually located on the inner site of the plasma membrane and can be stained by AnnexinV (Koopman et al., 1994). PS mediates uptake of apoptotic cells by macrophages and dendritic cells and is also referred as an “eat-me” signal (Koopman et al., 1994).

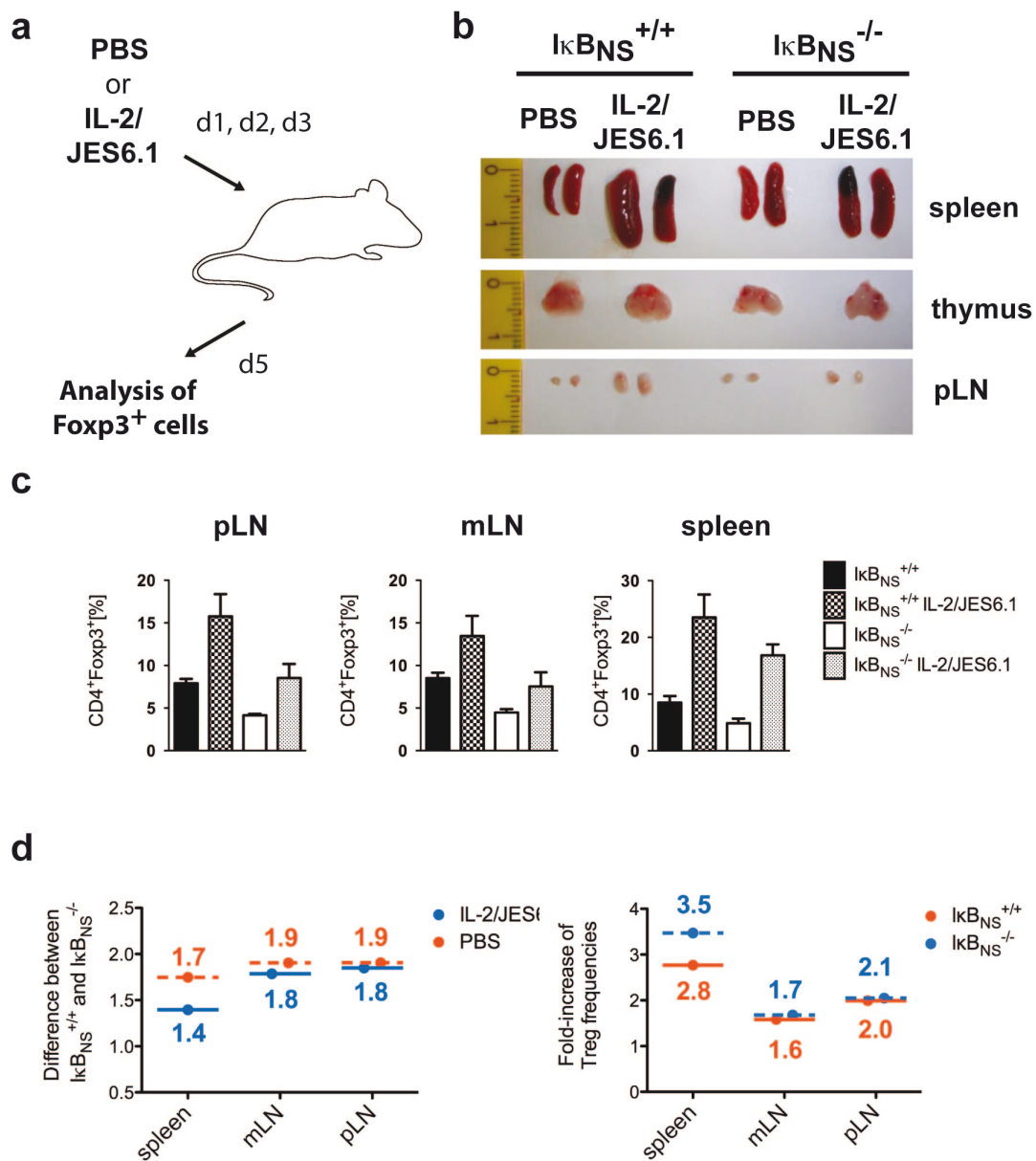


**Figure 22: Tregs proliferate comparably in wildtype and  $IkB_{NS}$ -deficient mice after anti-IL2/IL-2 administration**

**(a)** Schematic overview of Treg expansion *in vivo*. 6 weeks old wildtype and  $IkB_{NS}^{-/-}$  mice of matched gender were injected with 2  $\mu$ g/ml murine IL-2 and 5  $\mu$ g/ml anti IL-2 (JES6.1) or PBS i.p. on three consecutive days. On day five mice were sacrificed and analysed for Treg amplification by flow cytometry. **(b)** Pictures taken from spleens, thymi and peripheral lymph nodes of wildtype and  $IkB_{NS}^{-/-}$  mice injected i.p. with IL-2/anti-IL2 or PBS at day 5. **(c)** Bars of the percentages of CD4<sup>+</sup>Foxp3<sup>+</sup> Tregs in spleens, thymi and peripheral lymph nodes of wildtype and  $IkB_{NS}^{-/-}$  mice injected i.p. with IL-2/anti-IL-2 or PBS at day 5 (n=3; mean  $\pm$  s.d.). **(d)** Relative difference of Treg percentages between wildtype and  $IkB_{NS}^{-/-}$  mice in PBS-injected and IL-2/anti-IL-2 injected animals (left panel; mean). Fold-increase of Tregs in wildtype and  $IkB_{NS}^{-/-}$  mice after IL-2/anti-IL-2 administration (right panel; mean).

Treg frequencies in peripheral blood were assessed by analyses of CD4<sup>+</sup>GFP<sup>+</sup> cells to control if the reporter changed the effect of I $\kappa$ B<sub>NS</sub> deficiency on the Treg compartment (Fig. 23b). I $\kappa$ B<sub>NS</sub><sup>-/-</sup>Foxp3<sup>DTR-eGFP</sup> mice displayed a 50% reduction of Tregs compared to I $\kappa$ B<sub>NS</sub><sup>+/+</sup>Foxp3<sup>DTR-eGFP</sup> mice, heterozygous mice showed an intermediate Treg amount (Fig. 23b). Apoptosis of Treg cells was analyzed by flow cytometry using a combined staining of AnnexinV, which binds to PS exposed to the outer cell membrane and 7AAD, which intercalates into the DNA after disruption of the plasma membrane. Thymic early apoptotic AnnexinV<sup>+</sup>7AAD<sup>-</sup> as well as late apoptotic AnnexinV<sup>+</sup>7AAD<sup>+</sup> Treg cells were nearly identical between I $\kappa$ B<sub>NS</sub><sup>-/-</sup>Foxp3<sup>DTR-eGFP</sup> mice and I $\kappa$ B<sub>NS</sub><sup>+/+</sup>Foxp3<sup>DTR-eGFP</sup> (Fig. 24a and 24b). Comparison of Treg apoptosis in spleen, mesenteric and peripheral lymph nodes did not reveal increased apoptosis upon I $\kappa$ B<sub>NS</sub> deficiency (Fig. 24c).

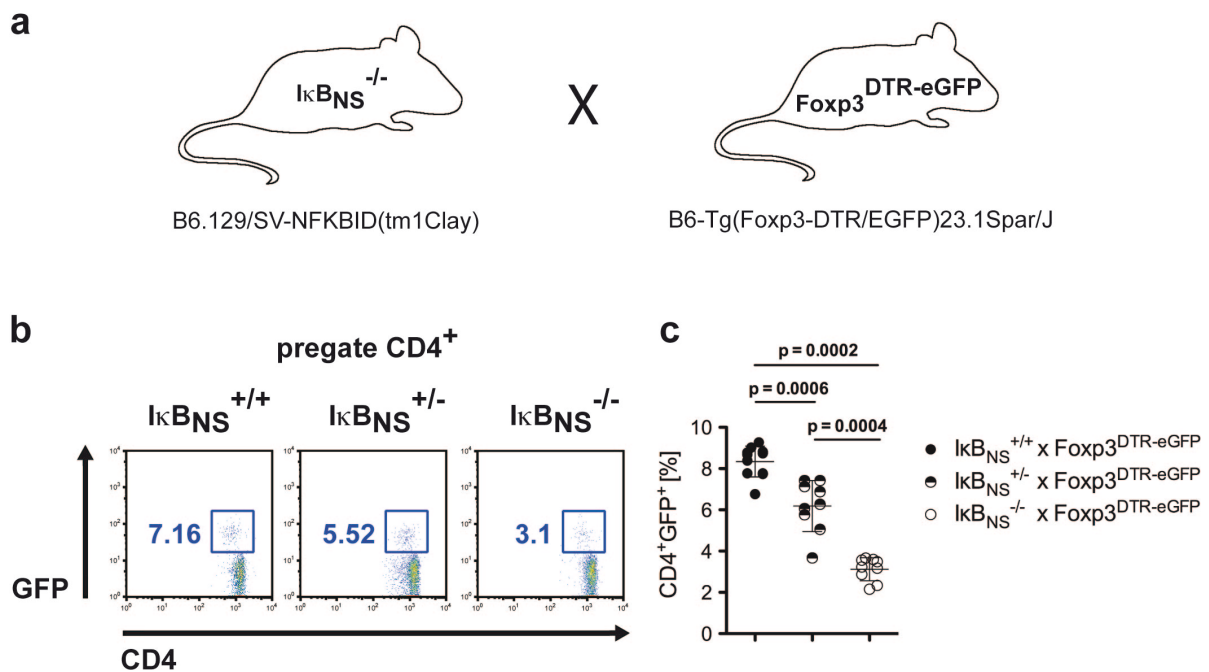


**Figure 23: Generation of I $\kappa$ B<sub>NS</sub><sup>-/-</sup> x Foxp3<sup>DTR-eGFP</sup> reporter mice**

(a) Schematic overview of breeding I $\kappa$ B<sub>NS</sub><sup>-/-</sup> mice (B6.SV-NFKBIDtm1Clay) to Foxp3<sup>DTR-eGFP</sup> reporter mice (B6-TgFoxp3-DTR/EGFP23.1Spar/J). (b) Representative pseudo-color dotblot of CD4<sup>+</sup>GFP<sup>+</sup> Tregs in the peripheral blood from 6 weeks old wildtype, heterozygous and I $\kappa$ B<sub>NS</sub><sup>-/-</sup> Foxp3<sup>DTR-eGFP</sup> littermate reporter mice. Numbers indicate percentages of CD4<sup>+</sup>GFP<sup>+</sup> cells. (c) Scatter dotplot diagram of percentages of CD4<sup>+</sup>GFP<sup>+</sup> Treg cells in the peripheral blood from wildtype, heterozygous and I $\kappa$ B<sub>NS</sub><sup>-/-</sup> Foxp3<sup>DTR-eGFP</sup> reporter mice. Statistical significances were calculated by two-tailed Mann-Whitney tests (n=9; mean  $\pm$  s.d.).

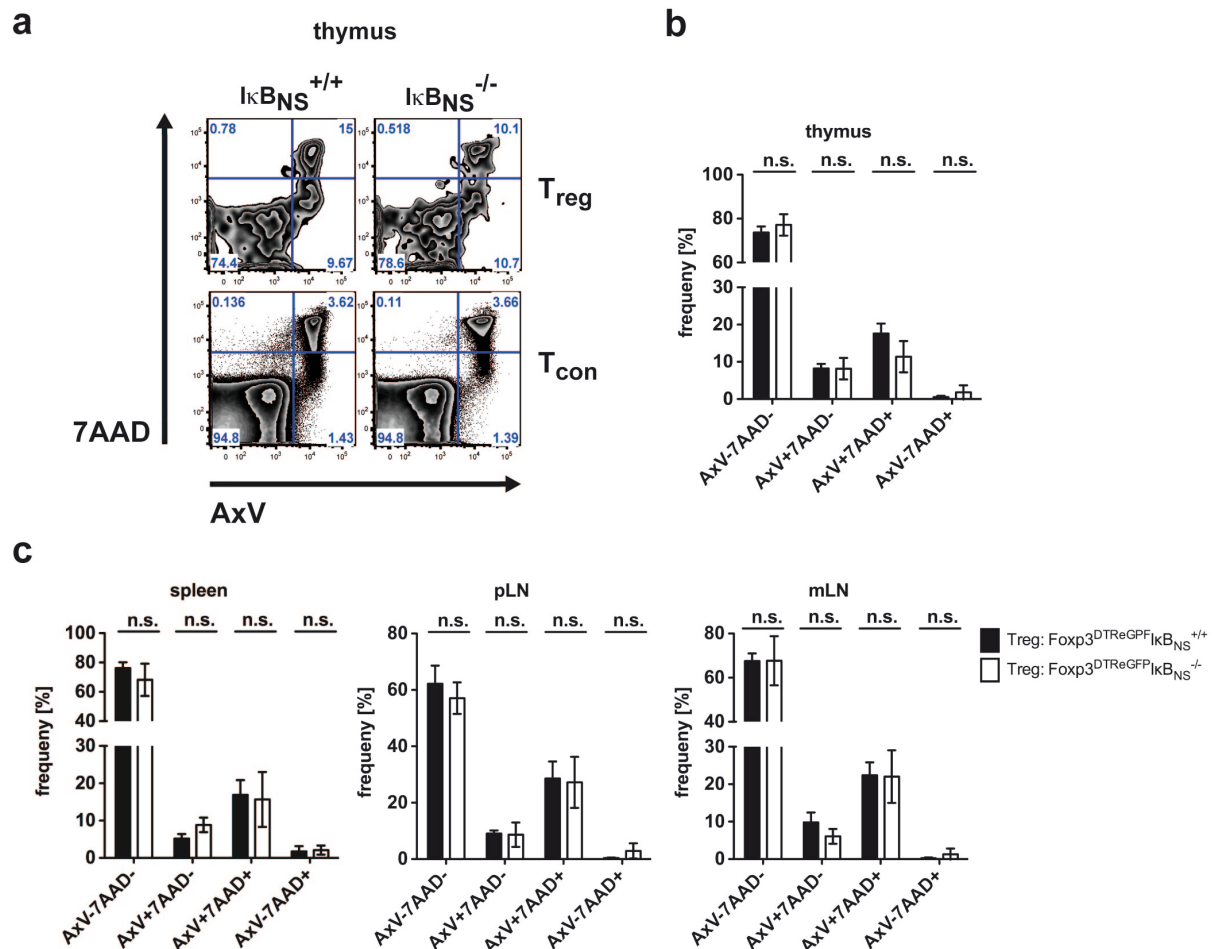


**Figure 24: IkB<sub>NS</sub> deficiency does not alter Treg apoptosis**

(a) Representative zebra-blot analysis of 7AAD and AnnexinV apoptotic cells in the CD4<sup>+</sup>GFP<sup>+</sup> Treg and CD4<sup>+</sup>GFP<sup>-</sup> Tcon compartment in the thymi from wildtype and IkB<sub>NS</sub><sup>-/-</sup> Foxp3<sup>DTR-eGFP</sup> 6 weeks old reporter mice of matched gender. Quadrant numbers indicate the percentages of the indicated populations. (b) Bars of the percentages of living (AxV<sup>-</sup>7AAD<sup>-</sup>), early apoptotic (AxV<sup>+</sup>7AAD<sup>-</sup>), late apoptotic (AxV<sup>-</sup>7AAD<sup>+</sup>) and necrotic (AxV<sup>+</sup>7AAD<sup>+</sup>) CD4<sup>+</sup>GFP<sup>+</sup> Treg cells in the thymi from wildtype and IkB<sub>NS</sub><sup>-/-</sup> Foxp3<sup>DTR-eGFP</sup> reporter mice. (c) Bars of the percentages of living, early apoptotic, late apoptotic and apoptotic/necrotic CD4<sup>+</sup>GFP<sup>+</sup> Treg cells in the spleens, mesenteric and peripheral lymph nodes from wildtype and IkB<sub>NS</sub><sup>-/-</sup> Foxp3<sup>DTR-eGFP</sup> reporter mice. For b and c statistical significances were calculated by two-tailed Mann-Whitney tests (n=9; mean ± s.d.; n.s. = not significant).

In accordance with the AnnexinV/7AAD analyses, no significant difference in early apoptotic Tregs between Foxp3<sup>DTR-eGFP</sup>IkB<sub>NS</sub><sup>+/+</sup> and Foxp3<sup>DTR-eGFP</sup>IkB<sub>NS</sub><sup>-/-</sup> mice was detected by TMRE staining (Fig. 25a and 25b). There was no difference in apoptosis between the two genotypes detected in the CD4<sup>+</sup>Foxp3<sup>-</sup> Tcon compartment as well (Fig. 25b). Remarkably, Tcon cells displayed, independently of the genotype, lower basal apoptosis, indicating that

---

Treg constantly undergo strong apoptosis *in vivo* (Fig. 24a and 25b). In conclusion, the Treg compartment of I $\kappa$ B<sub>NS</sub>-deficient mice undergoes enhanced basal proliferation *in vivo*. Upon injection of an IL-2/ anti-IL-2 complex, I $\kappa$ B<sub>NS</sub>-deficient Tregs displayed mildly enhanced proliferation compared to wildtype mice. Apoptosis of the Treg compartment was not altered as assessed by AnnexinV/7AAD staining and TMRE analysis, but was found stronger compared to Tcon cells, regardless of the genotype.

#### **4.4 Followed from defective Foxp3 induction thymic Treg precursor cells accumulate in I $\kappa$ B<sub>NS</sub>-deficient mice**

According to the current model of thymic Treg development, nTregs originate from autoreactive T cells (Lio and Hsieh, 2008). Since I $\kappa$ B<sub>NS</sub> is expressed by autoreactive thymic T cells, nTreg generation in the thymic CD8<sup>-</sup>CD4<sup>+</sup> compartment was analysed (Fiorini et al., 2002). The so called “two-step” model argues that an early event of nTreg development, which depends on TCR triggering as the first step, is induction of CD25 and GITR (Lio and Hsieh, 2008). The second step – the induction of Foxp3 - is induced in a  $\gamma$  chain cytokine-dependent manner, whereby IL-2 and IL-15 are the most potent mediators of Foxp3 expression (Vang et al., 2008). To control the first step of nTreg development, percentages of CD8<sup>-</sup>CD4<sup>+</sup>CD25<sup>+</sup> T cells in the thymi of wildtype, heterozygous and I $\kappa$ B<sub>NS</sub>-deficient mice were determined. Surprisingly, CD25<sup>+</sup> cells were just marginally reduced in I $\kappa$ B<sub>NS</sub>-deficient mice, which was not statistically significant (Fig. 26a). In contrast, Foxp3<sup>+</sup> Tregs, displayed a dose dependent reduction in the thymi of heterozygous and I $\kappa$ B<sub>NS</sub>-deficient mice (Fig. 26b). Those results indicated accumulation of Foxp3<sup>-</sup> Treg precursors within the CD25<sup>+</sup> compartment of I $\kappa$ B<sub>NS</sub>-deficient mice. To proof this, the distribution of Treg precursors and mature Tregs within the CD8<sup>-</sup>CD4<sup>+</sup>CD25<sup>+</sup>GITR<sup>+</sup> compartment was analysed. Foxp3<sup>+</sup> mature Tregs were dose dependently reduced as expected, whereas Foxp3<sup>-</sup> Treg precursor cells formed the majority of CD25<sup>+</sup>GITR<sup>+</sup> cells by about 85% in I $\kappa$ B<sub>NS</sub>-deficient mice compared to 60% in wildtype mice, which demonstrated impaired transition of immature precursor cells into Foxp3<sup>+</sup> Tregs (Fig. 27a and 27b).

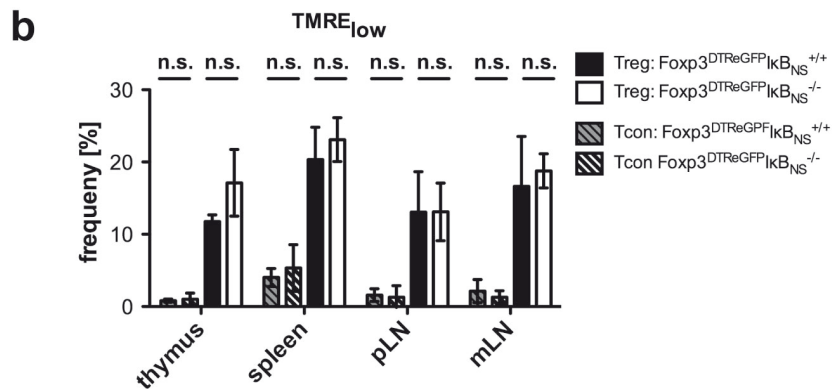
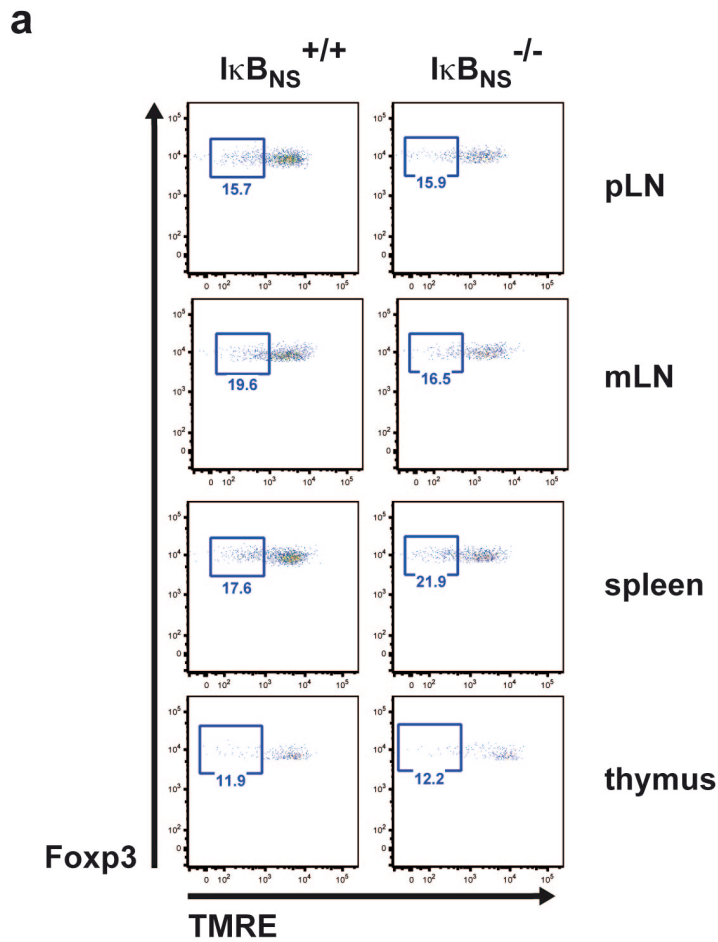


**Figure 25: Mitochondrial membrane integrity of  $I\kappa B_{NS}$ -deficient Tregs remains intact**

(a) Representative pseudo-color dotblots of TMRE and GFP in the CD4 compartment of mesenteric and peripheral lymph nodes, spleens and thymi from wildtype and  $I\kappa B_{NS}^{-/-} Foxp3^{DTR-eGFP}$  6 weeks old littermate reporter mice. Numbers indicate the percentages of CD4<sup>+</sup>GFP<sup>+</sup> Tregs, which lost mitochondrial membrane potential. (b) Bars of the percentages of TMRE<sub>low</sub> Treg and Tcon cells from mesenteric and peripheral lymph nodes, spleens and thymi from wildtype and  $I\kappa B_{NS}^{-/-} Foxp3^{DTR-eGFP}$  6 weeks old littermate reporter mice. Statistical significances were calculated by two-tailed Mann-Whitney tests (n=9; mean ± s.d.; n.s. = not significant).

By pregating to CD25<sup>+</sup>GITR<sup>+</sup> cells the conversion of precursor cells into mature Tregs was analysed, but classically the amount nTreg precursors in the thymus is identified by the percentage of CD25<sup>+</sup>GITR<sup>+</sup> cells pregated to CD8<sup>-</sup>CD4<sup>+</sup>Foxp3<sup>-</sup> cells (Molinero et al., 2009). Using this gating strategy, a mild, but statistical significant enrichment of Treg precursor cells in the thymus of I $\kappa$ B<sub>NS</sub>-deficient mice was found as well (Fig. 28a and 28b). Those data suggested that I $\kappa$ B<sub>NS</sub> deficiency delays Foxp3 induction and thereby, the transition of Treg precursor cells into mature Tregs. This results in accumulation of CD25<sup>+</sup>GITR<sup>+</sup>Foxp3<sup>-</sup> Treg precursor cells.

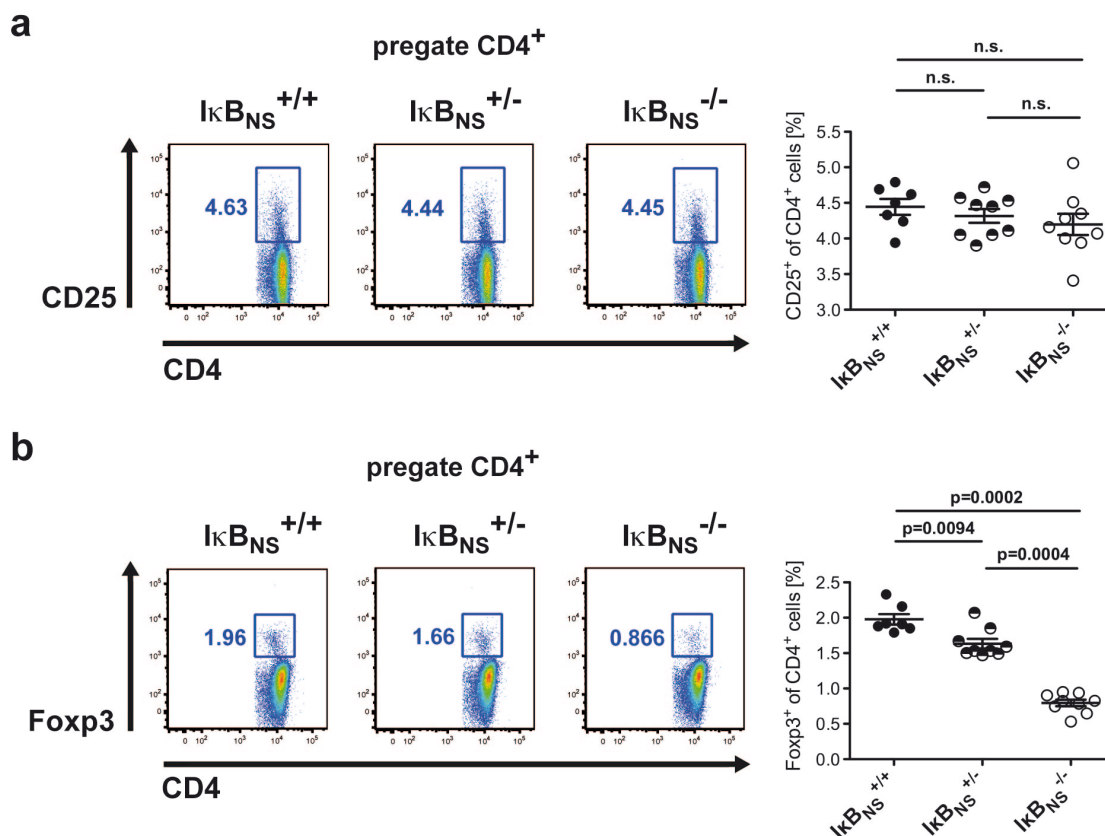


**Figure 26: Thymic CD4<sup>+</sup>CD25<sup>+</sup> are minimally reduced in I $\kappa$ B<sub>NS</sub>-deficient mice in contrast to CD4<sup>+</sup>Foxp3<sup>+</sup> cells**

**(a)** Representative pseudo color dotblots (left panel) and scatter dotblot diagram of CD8<sup>-</sup>CD4<sup>+</sup>CD25<sup>+</sup> T cells in thymi from wildtype, heterozygous and I $\kappa$ B<sub>NS</sub><sup>-/-</sup> 6 weeks old littermate mice. Numbers indicate percentages of CD4<sup>+</sup>CD25<sup>+</sup> cells. **(b)** Representative pseudo color dotblot (left panel) and scatter dotblot diagram of CD8<sup>-</sup>CD4<sup>+</sup>Foxp3<sup>+</sup> T cells in thymi from wildtype, heterozygous and I $\kappa$ B<sub>NS</sub><sup>-/-</sup> 6 weeks old littermate mice. Numbers indicate percentages of CD4<sup>+</sup>Foxp3<sup>+</sup> cells. Statistical significances were calculated by two-tailed Mann-Whitney tests (I $\kappa$ B<sub>NS</sub><sup>+/+</sup> n=7, I $\kappa$ B<sub>NS</sub><sup>+/-</sup> n=9, I $\kappa$ B<sub>NS</sub><sup>-/-</sup> n=9; mean  $\pm$  s.e.m.; n.s. = not significant).

The second step of nTreg development is induced via IL-2 stimulation of Treg precursor cells (Lio and Hsieh, 2008). The previously generated  $\text{Foxp3}^{\text{DTReGFP}} \text{IkB}_{\text{NS}}^{-/-}$  reporter mice (see 4.3) were used to induce conversion of purified nTreg precursor cells *in vitro* by the addition of exogenous IL-2. First, the percentages of these cells were controlled in the thymus of  $\text{Foxp3}^{\text{DTReGFP}}$  and  $\text{IkB}_{\text{NS}}^{-/-} \text{Foxp3}^{\text{DTReGFP}} \text{IkB}_{\text{NS}}^{+/+}$  reporter mice.  $\text{IkB}_{\text{NS}}$  deficiency led to a reduced amount of thymic  $\text{GFP}^+$  Tregs within the  $\text{CD25}^+\text{GITR}^+$  compartment and a concomitant increase of immature  $\text{GFP}^-$  Treg precursor cells to a similar extent found in littermate mice (Fig. 29a and 29b).

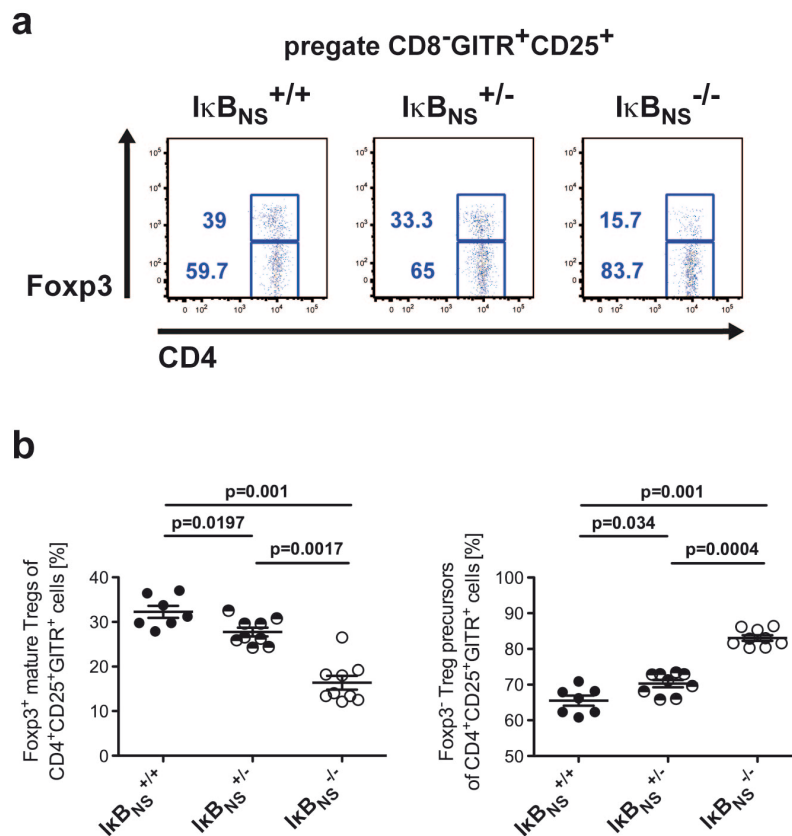


**Figure 27:  $\text{GITR}^+\text{CD25}^+\text{Foxp3}^-$  thymic Treg precursor cells show delayed transition into mature Tregs in  $\text{IkB}_{\text{NS}}$ -deficient mice**

(a) Representative pseudo-color dotblots of  $\text{CD4}^+\text{Foxp3}^-$  and  $\text{CD4}^+\text{Foxp3}^+$  cells within the  $\text{CD8}^-\text{GITR}^+\text{CD25}^+$  compartment in thymi from wildtype, heterozygous and  $\text{IkB}_{\text{NS}}^{-/-}$  weeks old littermate mice. Upper numbers indicate percentages of  $\text{Foxp3}^+$ , lower numbers of  $\text{Foxp3}^-$  cells. (b) Scatter dotblot diagrams of the percentages of  $\text{CD4}^+\text{Foxp3}^-$  Treg precursor cells (right panel) and  $\text{CD4}^+\text{Foxp3}^+$  mature Tregs (left panel) cells within the  $\text{CD8}^-\text{GITR}^+\text{CD25}^+$  compartment in thymi from wildtype, heterozygous and  $\text{IkB}_{\text{NS}}^{-/-}$  6 weeks old littermate mice. Statistical significances were calculated by two-tailed Mann-Whitney tests ( $\text{IkB}_{\text{NS}}^{+/+}$  n=7,  $\text{IkB}_{\text{NS}}^{+/-}$  n=9,  $\text{IkB}_{\text{NS}}^{-/-}$  n=9; mean  $\pm$  s.e.m.; n.s. = not significant).

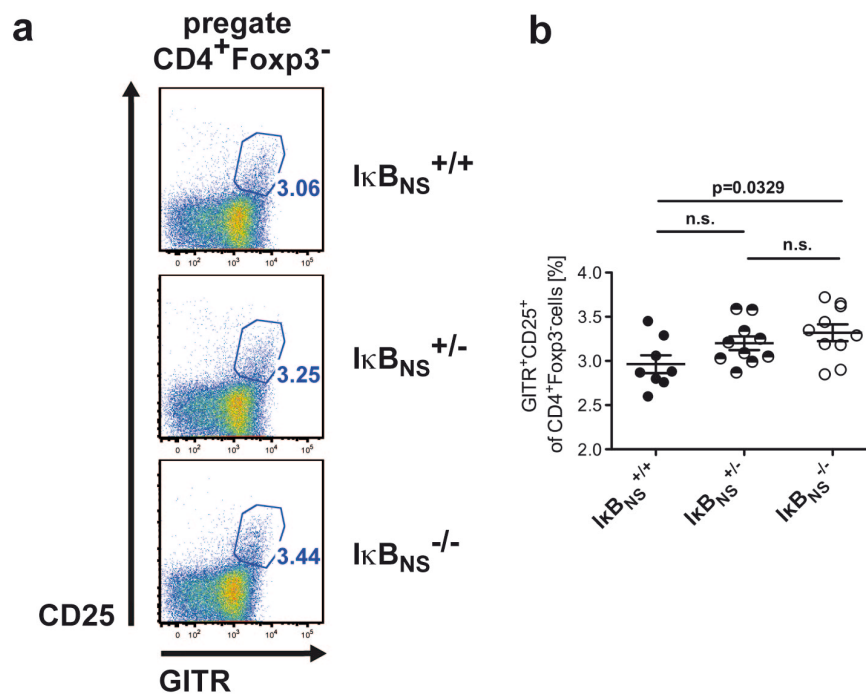


**Figure 28: Foxp3<sup>-</sup> Treg precursor cells accumulate in thymi of IκB<sub>NS</sub>-deficient mice**

(a) Representative pseudo-color dotblots of CD25<sup>+</sup>GITR<sup>+</sup> Treg precursor cells within the CD8<sup>-</sup>CD4<sup>+</sup>Foxp3<sup>-</sup> compartment cells in thymi from wildtype, heterozygous and IκB<sub>NS</sub><sup>-/-</sup> 6 weeks old littermate mice. Numbers indicate percentages of CD25<sup>+</sup>GITR<sup>+</sup>Foxp3<sup>-</sup> Treg precursor cells. (b) Scatter dotplot diagram of the percentages of CD8<sup>-</sup>CD4<sup>+</sup>Foxp3<sup>-</sup>CD25<sup>+</sup>GITR<sup>+</sup> Treg precursor cells in thymi from wildtype, heterozygous and IκB<sub>NS</sub><sup>-/-</sup> 6 weeks old littermate mice. Statistical significances were calculated by two-tailed Mann-Whitney tests (IκB<sub>NS</sub><sup>+/+</sup> n=9, IκB<sub>NS</sub><sup>+/-</sup> n=12, IκB<sub>NS</sub><sup>-/-</sup> n=12 ; mean ± s.e.m.; n.s. = not significant).

Finally, CD8<sup>-</sup>CD4<sup>+</sup>CD25<sup>+</sup>GITR<sup>+</sup>Foxp3<sup>-</sup> precursor cells were purified by flow cytometry and treated with IL-2 or left untreated for 24 hours. Nearly 45% of wildtype precursor cells were converted into GFP<sup>+</sup> Tregs, whereas only 20% of IκB<sub>NS</sub>-deficient cells commenced GFP induction (Fig. 30a and 30b). Thus, the amount of GFP<sup>+</sup> Tregs originated from the wildtype exceeded the percentage of generated IκB<sub>NS</sub>-deficient GFP<sup>+</sup> cells by about 25% (Fig. 30a and 30b).

These experiments demonstrated that IκB<sub>NS</sub> lead to accumulation of immature CD25<sup>+</sup>GITR<sup>+</sup>Foxp3<sup>-</sup> nTreg precursor cells as a result of delayed Foxp3 induction after IL-2 exposure. Thus, the second step in nTreg development, Foxp3 induction upon γ-chain cytokine signaling, is affected by IκB<sub>NS</sub> deficiency.

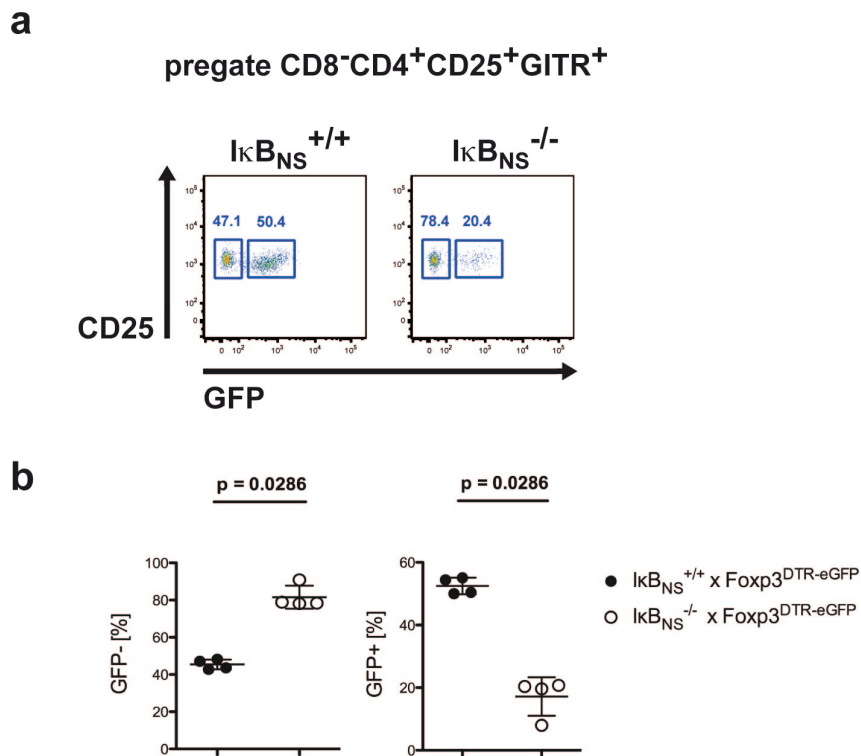


**Figure 29: Thymic Treg precursor cells are reduced in  $I\kappa B_{NS}^{-/-} \times Foxp3^{DTR-eGFP}$  reporter mice**  
**(a)** Representative pseudo-color dotblots of CD25<sup>+</sup>GFP<sup>-</sup> Treg precursor cells and CD25<sup>+</sup>GFP<sup>+</sup> mature Tregs in thymi from wildtype and  $I\kappa B_{NS}^{-/-}$  6 weeks old reporter mice. Left numbers in pseudo-color dotblots indicate percentages of GFP<sup>-</sup> precursor cells, right numbers of GFP<sup>+</sup> mature Tregs. **(b)** Scatter dotplot diagrams of the percentages of GFP<sup>-</sup> precursor cells and of GFP<sup>+</sup> mature Tregs in thymi from wildtype and  $I\kappa B_{NS}^{-/-}$  6 weeks old reporter mice. Statistical significances were calculated by two-tailed Mann-Whitney tests (n=4; ; mean ± s.e.m.).

#### 4.5 $I\kappa B_{NS}$ is expressed during thymic Treg development and interacts with p50 and c-Rel at the regulatory elements CNS2 and CNS3 within the *Foxp3* gene

c-Rel and CARMA1 are proteins of the NF $\kappa$ B signalling pathway, which control *Foxp3* induction in the thymus, and are expressed by nTregs (Isomura et al., 2009; Molinero et al., 2009). As  $I\kappa B_{NS}$  deficiency delays *Foxp3* induction in nTreg precursor cells its expression was analysed in purified GITR<sup>-</sup>CD25<sup>-</sup>, GITR<sup>+</sup>CD25<sup>-</sup> and GITR<sup>+</sup>CD25<sup>+</sup> cells by Western blot (Fig. 31a and 31b). Of note, GITR<sup>+</sup>CD25<sup>+</sup> cells are a mixture of nTreg precursor cells and mature Tregs.  $I\kappa B_{NS}$  was strongly expressed by GITR<sup>+</sup>CD25<sup>-</sup> and GITR<sup>+</sup>CD25<sup>+</sup> cells and hardly detectable in the GITR<sup>-</sup>CD25<sup>-</sup> subset (Fig. 31b). In agreement with recent reports

(Hori, 2010; Isomura et al., 2009), c-Rel was most strongly detected in GITR<sup>+</sup>CD25<sup>+</sup> cells, but also in the GITR<sup>+</sup>CD25<sup>-</sup> subset (Fig. 31b). CARMA1 expression was equal between the isolated populations and Foxp3 was restricted to GITR<sup>+</sup>CD25<sup>+</sup> cells as expected (Fig. 31b). As cell numbers of nTreg precursor cells and fully matured Tregs are too low in the thymus for analyses of the protein level CD4<sup>+</sup>GITR<sup>-</sup>CD25<sup>-</sup>, CD4<sup>+</sup>GITR<sup>+</sup>CD25<sup>-</sup>, CD4<sup>+</sup>GITR<sup>+</sup>CD25<sup>+</sup>Foxp3<sup>-</sup> and CD4<sup>+</sup>GITR<sup>+</sup>CD25<sup>+</sup>Foxp3<sup>+</sup> cells were purified for analyses of mRNA expression (Fig. 31c). RT-PCR revealed strongest expression of I $\kappa$ B<sub>NS</sub> in CD4<sup>+</sup>GITR<sup>+</sup>CD25<sup>-</sup> cells (Fig.31d). Of note, its mRNA was increased in CD25<sup>-</sup> cells, but downregulated upon induction of CD25 (Fig.31d).

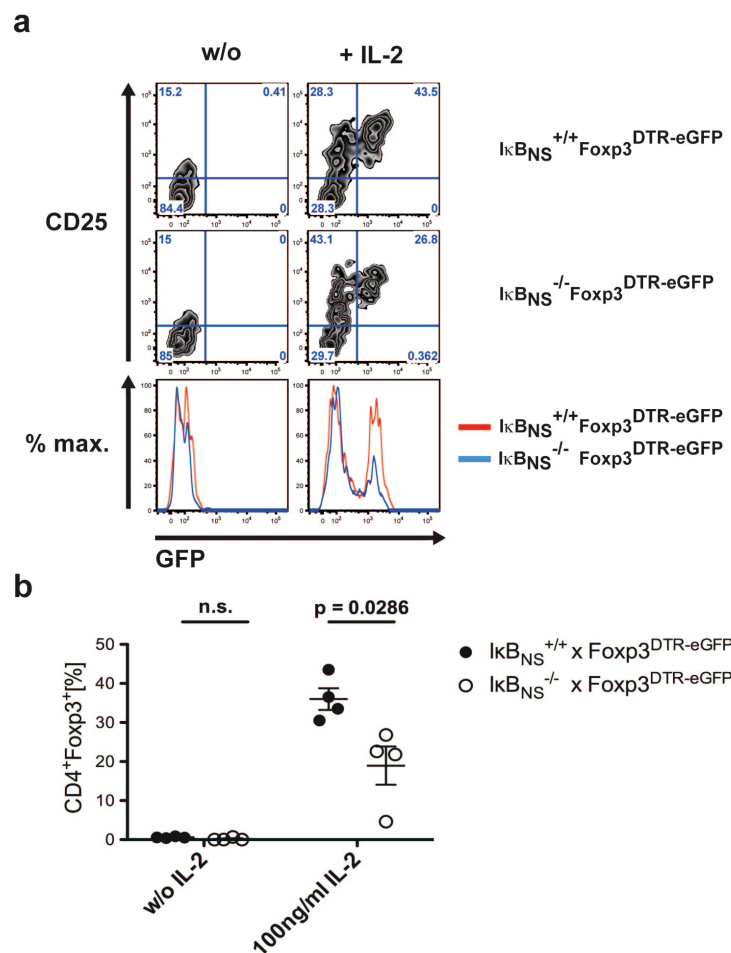


**Figure 30: I $\kappa$ B<sub>NS</sub> deficiency leads to impaired Foxp3 induction in Treg precursor cells after IL-2 exposure**

**(a)** Representative zebra-plot (upper panel) and histogram overlay (lower panel) of GFP expression in purified CD8<sup>-</sup>CD4<sup>+</sup>CD25<sup>+</sup>GITR<sup>+</sup>GFP<sup>-</sup> Treg precursor cells from wildtype and I $\kappa$ B<sub>NS</sub><sup>-/-</sup> 6 weeks old reporter mice of matched gender treated with 100 ng/ml IL-2 or left untreated for 24 hours. GFP<sup>+</sup> cells represent *de novo* induced Tregs. **(b)** Scatter dotplot diagram of the percentages of GFP<sup>+</sup> cells in purified Treg precursor cells from wildtype and I $\kappa$ B<sub>NS</sub><sup>-/-</sup> 6 weeks old reporter mice treated with 100 ng/ml IL-2 or left untreated. Statistical significances were calculated by two-tailed Mann-Whitney tests (n=4; mean  $\pm$  s.e.m.; n.s. = not significant).

Due to the low cell number of Treg precursors, the molecular mechanism by which  $I\kappa B_{NS}$  modulates Foxp3 expression had to be analysed in another cell type. Corresponding to a previous report, *in vitro* expanded  $CD4^+CD25^-$  T cells were used to study the role of  $I\kappa B_{NS}$  for *de novo* Foxp3 induction (Zheng et al., 2010).

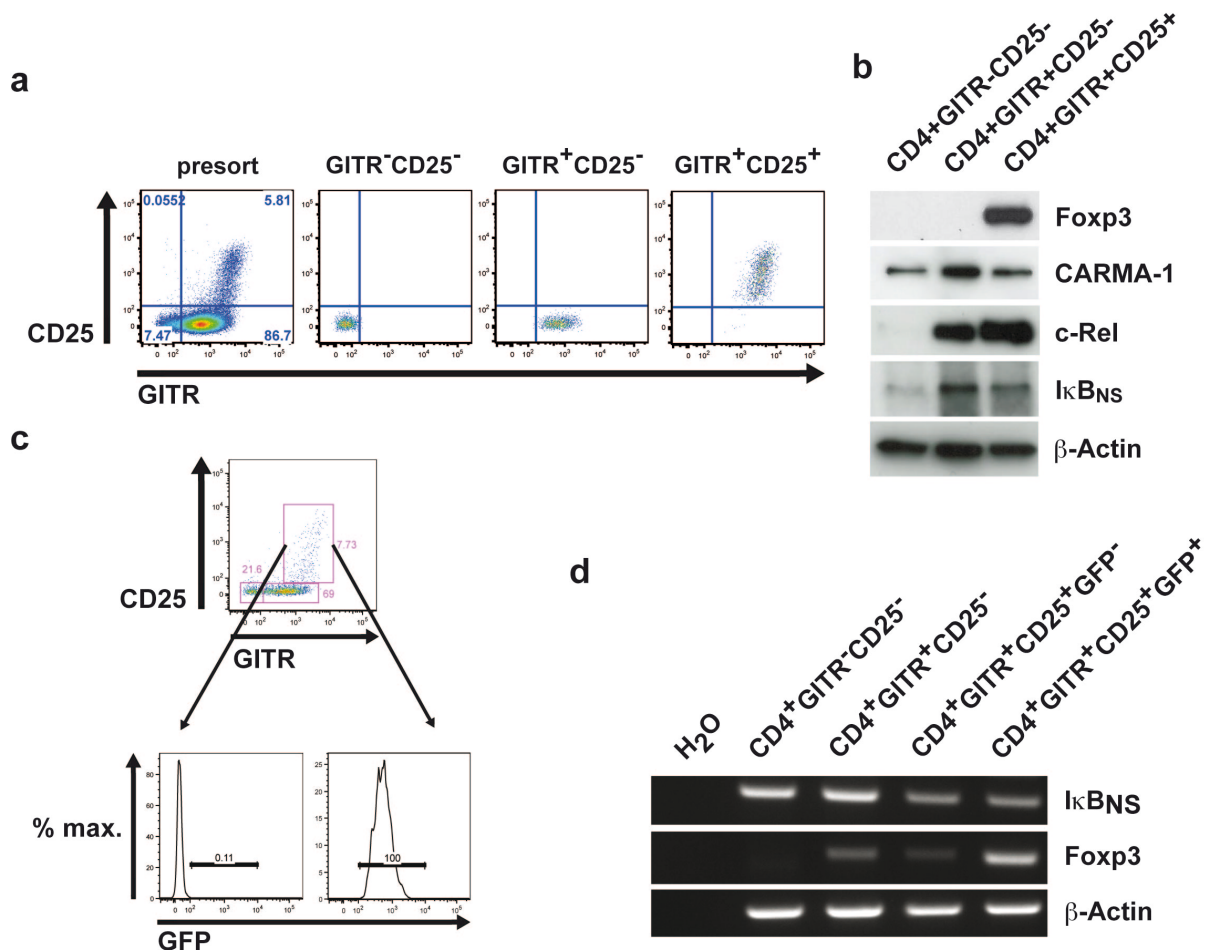


### Figure 31: $I\kappa B_{NS}$ is expressed during thymic Treg maturation

**(a)** Representative pseudo-color dotblots of  $CD25^-GITR^-$ ,  $CD25^-GITR^+$  and  $CD25^+GITR^+$  T cells purified from the  $CD8^+CD4^+$  thymic compartment of 6 weeks old wildtype  $Foxp3^{DTR-eGFP}$  reporter mice. **(b)** Western blot analysis of  $CD25^-GITR^-$ ,  $CD25^-GITR^+$  and  $CD25^+GITR^+$  cells from the  $CD8^+CD4^+$  compartment regarding the expression of Foxp3, CARMA1, c-Rel and  $\beta$ -Actin. **(c)** Representative pseudo-color dotplot and histogram analysis of GFP<sup>-</sup> Treg precursor cells and GFP<sup>+</sup> mature Tregs purified from the  $CD8^+CD4^+GITR^+CD25^+$  thymic compartment of 6 weeks old wildtype  $Foxp3^{DTR-eGFP}$  reporter mice. **(d)** PCR analysis of the expression of  $I\kappa B_{NS}$ , Foxp3 and  $\beta$ -Actin in purified  $CD8^+CD4^+GITR^-CD25^-$  cells,  $CD8^+CD4^+GITR^+CD25^-$  cells,  $CD8^+CD4^+GITR^+CD25^+GFP^-$  Treg precursor cells and  $CD8^+CD4^+GITR^+CD25^+GFP^+$  mature nTregs. Results are representative for 3 independent experiments.

To study the kinetics of I $\kappa$ B<sub>NS</sub> expression in comparison with the other NF $\kappa$ B family members, *in vitro* expanded CD4<sup>+</sup>CD25<sup>-</sup> cells were stimulated with PMA/ ionomycin for the indicated time points and NF $\kappa$ B activation was analysed by fractionised cell lysis (Fig. 32a). The known 35 kDa I $\kappa$ B<sub>NS</sub> isoform was found in the first 2 hours of stimulation in the cytoplasm (Fig. 32a). Two novel, so far undescribed isoforms of about 70 kDa in the nuclear extract within 8 hours of stimulation (Fig. 32a). c-Rel was expressed to a little extent in resting cells, but was enhanced in the cytoplasm upon stimulation and displayed within the first 8 hours a nuclear localisation, correlating with the nuclear signal of the 70 kDa isoforms of I $\kappa$ B<sub>NS</sub> (Fig. 32a). p50 and p65 were constantly strong expressed and even in resting cells a minority of the proteins was localised in the nucleus (Fig. 32a). Increase of p105, the cytoplasmic precursor protein of p50, was observed after 8 hours of stimulation, whereas p65 was just marginally increased in the cytoplasm (Fig. 32a). The amount of nuclear protein was increasing up to 8 hours of stimulation and minimally downregulated after 16 hours, whereas nuclear p65 clearly declined after 4 hours (Fig. 32a).

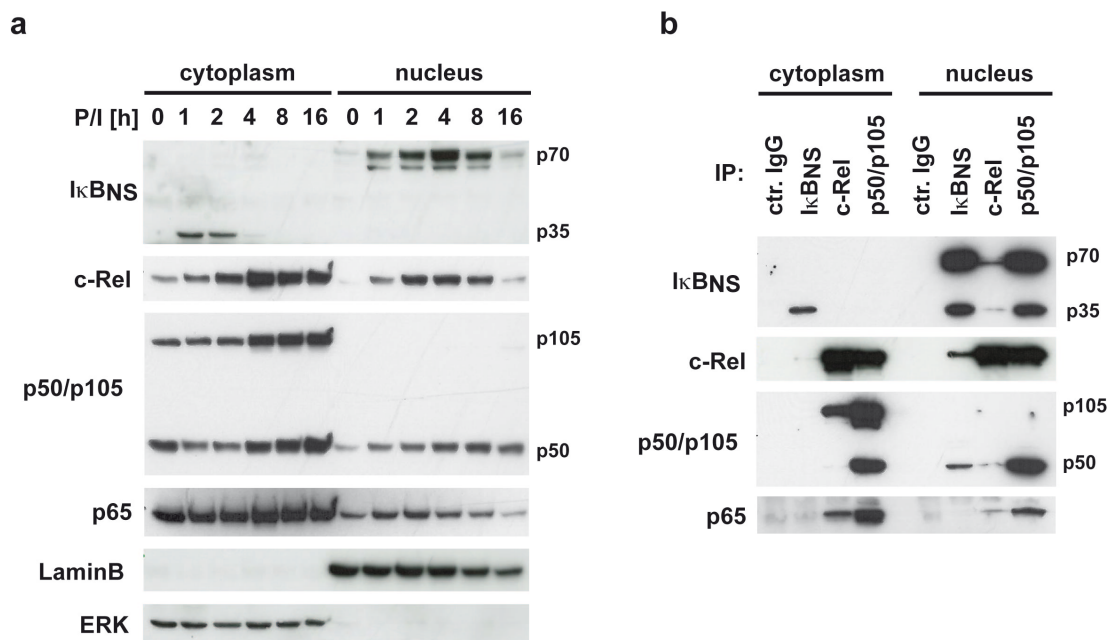


**Figure 32: I $\kappa$ B<sub>NS</sub> interacts with p50 and to a minor extent with c-Rel**

**(a)** Western blot analyses of *in vitro* expanded CD4<sup>+</sup>CD25<sup>-</sup> wildtype T cells stimulated with 20 ng/ml PMA and 1  $\mu$ M ionomycin for the indicated time periods regarding the subcellular localisation of I $\kappa$ B<sub>NS</sub>, c-Rel, p50/p105, p65, LaminB and ERK. **(b)** Western blot analyses of the interaction of I $\kappa$ B<sub>NS</sub>, c-Rel, p50/p105 and p65 by coimmunoprecipitation from cytoplasmic and nuclear extracts of *in vitro* expanded CD4<sup>+</sup>CD25<sup>-</sup> T cells stimulated with 20 ng/ml PMA and 1  $\mu$ M ionomycin for 4 hours. Results are representative for at least 4 independent experiments.

---

Detection of the cytoplasmic MAP-kinase ERK and the nuclear matrix protein LaminB proved the purity of the extracts (Fig. 32a).

To study the interaction pattern of I $\kappa$ B<sub>NS</sub> with NF $\kappa$ B subunits I $\kappa$ B<sub>NS</sub>, c-Rel and p50/p105 were precipitated via rabbit polyclonal antibodies from cytoplasmic and nuclear extracts of PMA/ionomycin stimulated and *in vitro* expanded CD4<sup>+</sup>CD25<sup>-</sup> cells. As all NF $\kappa$ B subunits displayed a distinct cytoplasmic and nuclear fraction after 4 hours of stimulation as described above, this timepoint was used for immunoprecipitation. Remarkably, 35 kDa I $\kappa$ B<sub>NS</sub> did not interact with any NF $\kappa$ B subunit in the cytoplasm (Fig. 32b). Precipitation of c-Rel demonstrated its binding to the precursor protein p105 and to p65, but to p50 (Fig. 32b). Cytoplasmic p50/p105 was proven to interact with p65 and c-Rel as well, whereby the c-Rel signal appeared from its interaction with p105 (Fig. 32b). Precipitated nuclear 35 kDa and 70 kDa isoforms of I $\kappa$ B<sub>NS</sub>, however, interacted most pronounced with p50 and c-Rel, but not p65 (Fig. 32b). Nuclear 70 kDa I $\kappa$ B<sub>NS</sub> was precipitated to a higher extent compared to the 35 kDa isoform as it is present to a higher extent in the nucleus. Nuclear c-Rel was found to interact with both I $\kappa$ B<sub>NS</sub> isoforms and, compared to the cytoplasm to a reduced amount, with p50 and p65 (Fig. 32b). p50 strongly interacted in the nucleus with each analysed nuclear NF $\kappa$ B protein (Fig. 32b).

As the interaction was shown to be most pronounced between I $\kappa$ B<sub>NS</sub>, c-Rel and p50, their binding to  $\kappa$ B sites located within the *Foxp3* locus was determined by DNA pulldown. Using a web based promoter analyses software, provided by the company Genomatix<sup>TM</sup> and the results of chromatin immunoprecipitation from previous studies 9  $\kappa$ B sites and 2 NFAT sites were chosen for the interaction analyses with the indicated NF $\kappa$ B proteins (Fig. 33a) (Floess et al., 2007; Long et al., 2009; Polansky et al., 2008; Ruan et al., 2009; Zheng et al., 2010). 2  $\kappa$ B and both NFAT sites were localised in the *Foxp3* promoter, 6  $\kappa$ B sites in the CNS2 and 1  $\kappa$ B site in the CNS3, but remarkably none in the CNS1 (Fig. 33a). For DNA pulldown analyses *in vitro* expanded CD4<sup>+</sup>CD25<sup>-</sup> cells stimulated with PMA/ionomycin for 4 hours were used.

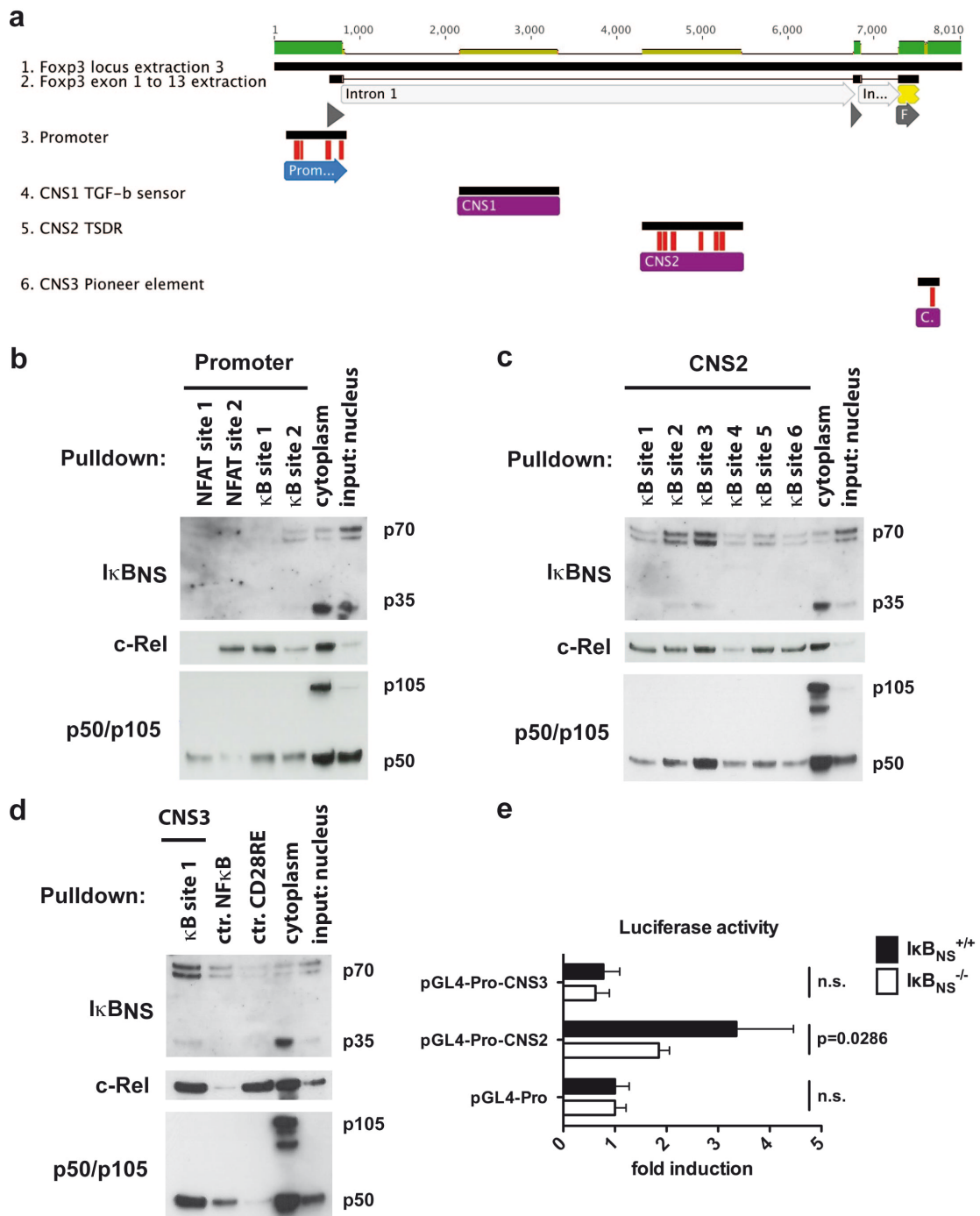


**Figure 33: I $\kappa$ B<sub>NS</sub> interacts with CNS2 and CNS3 and is required for Fcpx3 transcription**

(a) Schematic overview of regulatory elements in the Fcpx3 locus. Red lines mark the positions of possible NF $\kappa$ B binding sites within the regulatory elements. (b-d) DNA-pull-down analyses of the interactions of I $\kappa$ B<sub>NS</sub>, c-Rel and p50/p105 with the indicated  $\kappa$ B-sites of the promoter, CNS2 and CNS3 of the Fcpx3 locus by Western blot of *in vitro* expanded cells, stimulated for 4 hours with PMA/ionomycin. (e) Activity of luciferase constructs containing the Fcpx3 promoter alone, or fused to CNS2 or CNS3 transfected into *in vitro* expanded CD4<sup>+</sup>CD25<sup>-</sup> wildtype and I $\kappa$ B<sub>NS</sub><sup>-/-</sup> T cells. (n=3; mean  $\pm$  s.d.).

---

Nuclear extracts were incubated with 35 bp biotinylated double stranded DNA oligos containing each of the identified sites and as positive controls a classical NF $\kappa$ B site and a CD28 responsive element of the IL-2 promoter were chosen, which were reported to be bound by p50/I $\kappa$ B<sub>NS</sub> and homodimeric c-Rel, respectively (Touma et al., 2007). The controls displayed binding of p50/I $\kappa$ B<sub>NS</sub> to the classical  $\kappa$ B site and c-Rel to the CD28RE of the IL2-promoter as expected (Fig. 33d). Cytoplasmic and nuclear extracts were loaded on the same gel to control T cell stimulation. I $\kappa$ B<sub>NS</sub> did not interact with the Foxp3 promoter, in contrast to c-Rel, which displayed strong binding to NFAT site 2 and  $\kappa$ B site 1 (Fig. 33b). p50, instead, showed strong binding to NFAT site 1 and both  $\kappa$ B sites (Fig. 33b). Binding of 70 kDa I $\kappa$ B<sub>NS</sub>, c-Rel and p50 was observed to  $\kappa$ B site 3 in CNS2 and to a weaker extent to  $\kappa$ B site 2 (Fig. 33c). The other  $\kappa$ B sites displayed minor binding of the indicated proteins, probably reflecting background association to the DNA oligos (Fig. 33c). The most pronounced binding of I $\kappa$ B<sub>NS</sub>, c-Rel and p50, however, was detected to the single  $\kappa$ B site within CNS3 (Fig. 33d). Thus, pulldown analyses indicated binding of I $\kappa$ B<sub>NS</sub> to CNS2 and CNS3. As described above (Fig. 18b), I $\kappa$ B<sub>NS</sub> does not modulate CNS2 demethylation during Treg maturation, since the methylation pattern of I $\kappa$ B<sub>NS</sub>-deficient Tregs was not altered compared to wildtype Tregs (Fig. 18b and 18c). Thus, transcriptional activity of the promoter, CNS2 and CNS3 was analysed by luciferase based reporter gene assays in cooperation with Dipl-Biol. Lisa Schreiber from the department of Experimental Immunology at the HZI (Braunschweig). Luciferase reporter constructs were a gift of Dr. Ye Zheng from the Salk Institute for Biological Studies (La Jolla, CA, USA). Previous publications reported strong luciferase activity only of the CNS2 sequence, but not of the other regulatory elements (Zheng et al., 2010). In line, we found a 3-fold induction of luciferase activity using pGL4-Pro-CNS2 nucleofected into *in vitro* expanded wildtype CD4<sup>+</sup>CD25<sup>-</sup> T cells, but only about 1.8-fold luciferase activity after transfection into identically treated I $\kappa$ B<sub>NS</sub>-deficient cells (Fig. 33e). The pGL4-Prom (promoter only) construct was used for normalisation and, thus, displayed identical luciferase activity in wildtype and I $\kappa$ B<sub>NS</sub>-deficient cells (Fig. 33e). pGL4-Prom-CNS3

---

displayed luciferase activity even below the pure promoter construct and only a marginally reduced activity in I $\kappa$ B<sub>NS</sub>-deficient cells (Fig. 33e).

Those analyses demonstrated that the 35 kDa and two about 70 kDa isoforms of I $\kappa$ B<sub>NS</sub> are induced after T cell activation, with the latter being located in the nucleus within first 8 hours after stimulation, correlating with the strongest nuclear signal of c-Rel. I $\kappa$ B<sub>NS</sub> interacted exclusively in the nucleus with the NF $\kappa$ B proteins p50 and c-Rel and bound to NF $\kappa$ B site 3 within CNS2 and the only  $\kappa$ B site of CNS3. Luciferase activity of pGL4-Prom-CNS2 constructs was markedly reduced in I $\kappa$ B<sub>NS</sub>-deficient T cells compared to wildtype control cells.

#### **4.6 Adoptively transferred I $\kappa$ B<sub>NS</sub>-deficient T cells fail to differentiate in a protective Treg compartment, whereby chronic gut inflammation is exacerbated**

The physiological consequences of impaired Treg development were addressed by a transfer colitis model in cooperation with Dr. Rainer Glauben and Dr. Anja A. Kühl from the Medical Clinic I of the Charité (Berlin). Of note, recent reports demonstrated that gut-associated lymphoid tissues (GALT) constitute a microenvironment, which favors development of induced Tregs (Siddiqui and Powrie, 2008; Sun et al., 2007). Those studies argue that this process might depend on or could be promoted by TGF- $\beta$ . The adoptive transfer of naïve CD4<sup>+</sup>CD25<sup>-</sup> T cells into RAG<sup>-/-</sup> recipients results in massive proliferation of the transplanted T cells and their infiltration into the gut, causing colitis. During this process a Treg compartment is generated *de novo*, which does, however, not protect completely from colitis. Thus, naïve CD25-depleted CD4<sup>+</sup> T cells purified from spleens and peripheral lymph nodes of wildtype and I $\kappa$ B<sub>NS</sub>-deficient mice were adoptively transferred into RAG1<sup>-/-</sup> mice. The disease course was monitored by documentation of wasting disease, diarrhea and rectal bleeding. At the end of the experiment the amount of IFN $\gamma$ <sup>+</sup> T<sub>H</sub>1 and Foxp3<sup>+</sup> Treg cells was determined by flow cytometry and histological analyses of gut sections. Three of the Rag1<sup>-/-</sup> recipients of I $\kappa$ B<sub>NS</sub>-deficient T cells had to be sacrificed before the end of the experiment, because their weight loss exceeded the approved level.

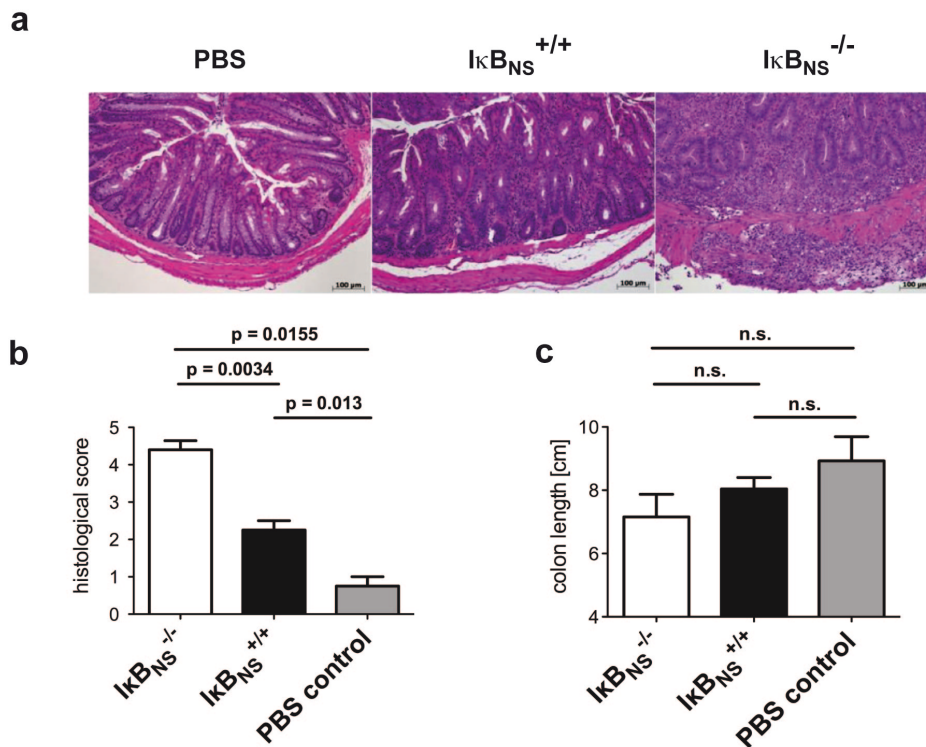


**Figure 34: Adoptive transfer of  $I\kappa B_{NS}$ -deficient  $CD4^+CD25^-$  T cells causes strong inflammation of the colon compared to transfer of wildtype cells**

**(a)** Representative H&E staining of colon section from  $RAG1^{-/-}$  mice injected with PBS or  $CD25^-$  depleted peripheral  $CD4^+$  T cells from wildtype or  $I\kappa B_{NS}$ -deficient mice. **(b)** Bars of the histological severity scores of colon sections from  $RAG1^{-/-}$  mice injected with PBS or  $CD25^-$  depleted peripheral  $CD4^+$  T cells from wildtype or  $I\kappa B_{NS}$ -deficient mice. **(c)** Bars of colon lengths of  $RAG1^{-/-}$  mice injected with PBS or  $CD25^-$  depleted peripheral  $CD4^+$  T cells from wildtype or  $I\kappa B_{NS}$ -deficient mice. For b and c statistical significances were calculated by two-tailed Mann-Whitney tests (PBS  $n=4$ ; wildtype  $n=8$ ;  $I\kappa B_{NS}^{-/-}$   $n=5$ ; mean  $\pm$  s.e.m.).

Colon sections of  $Rag1^{-/-}$  recipient mice, which received  $I\kappa B_{NS}$ -deficient T cells displayed massive infiltration of leukocytes into the colon and severe damage to the epithelial barrier (Fig 34a). The transfer of wildtype T cells resulted in colitis as well, but to a reduced extent and the epithelial barrier was not disrupted (Fig. 34a). PBS-injected mice, which served as a control, did not show abnormally increased leukocytes in gut sections (Fig. 34a). The severity, as seen in histology was scored according to the materials and methods section (3.3.10). The average colitis score of recipients of  $I\kappa B_{NS}$ -deficient T cells was 4.4 on a scale from 0 to 5, whereas wildtype transfer led to a colitis score of about 2.3 (Fig. 34b). Mice, which received PBS, as a negative control did not develop colitis as described above and were consequently scored with about 0.8 (Fig. 34b). Colitis is associated with shortening of

the colon. Thus, the length of colons was assessed as well. Control mice displayed a colon length of about 9 cm, compared to RAG1<sup>-/-</sup> recipients of wildtype T cells, which showed about 8 cm colon length (Fig. 34c). Transfer of I $\kappa$ B<sub>NS</sub>-deficient T cells led to the strongest colon shortening of about 7 cm, corresponding to the colitis score (Fig. 34c).

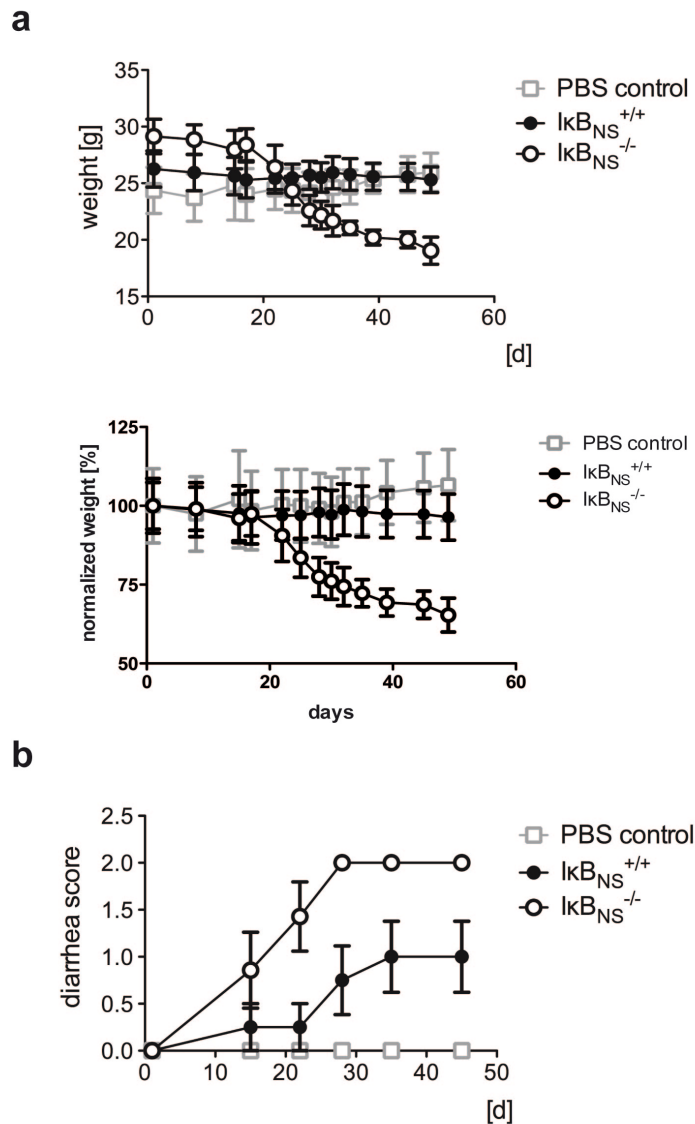


**Figure 35: Transfer of I $\kappa$ B<sub>NS</sub>-deficient CD4<sup>+</sup>CD25<sup>-</sup> T cells leads to an exacerbated disease course in RAG1<sup>-/-</sup> mice**

**(a)** Mean of absolute weight loss (upper panel) and relative weight loss (lower panel), over a period of 50 days of RAG1<sup>-/-</sup> mice injected with PBS or CD25-depleted peripheral CD4<sup>+</sup> T cells from wildtype or I $\kappa$ B<sub>NS</sub>-deficient mice. **(b)** Mean of diarrhea of RAG1<sup>-/-</sup> mice injected with PBS or CD25-depleted peripheral CD4<sup>+</sup> T cells from wildtype or I $\kappa$ B<sub>NS</sub>-deficient mice over a period of 50 days. (PBS n=4; wildtype n=8; I $\kappa$ B<sub>NS</sub><sup>-/-</sup> n=5; mean  $\pm$  s.e.m.).

---

The weight of RAG1<sup>-/-</sup> mice was determined during the experimental course and normalised to the weight at the start of the experiment (Fig. 35a). Recipient mice of I $\kappa$ B<sub>NS</sub>-deficient T cells started losing weight at day 18, weight loss of 25% was observed by day 30, which minimally changed till the end of the experiment at day 50 (Fig. 35a). Remarkably, transfer of wildtype T cells resulted only in minimal loss of weight of about 5% and not to a statistical significant extent when compared to PBS injected control mice (Fig. 35a). The diarrhea was scored according to the materials and methods section (3.3.10). Diarrhea in recipients of I $\kappa$ B<sub>NS</sub>-deficient T cells rapidly increased after the transfer and reached a score of 2 at day 30, whereas wildtype T cells caused diarrhea to a score of 1 at day 35 on a scale between 0 and 3 (Fig. 35b). PBS-injected mice did not develop any signs of diarrhea (Fig. 35b). So, weightloss and diarrhea completely fitted to the histopathology results, showing that I $\kappa$ B<sub>NS</sub> deficiency in adoptively transferred T cells gave rise to exacerbated colitis.

To identify the cellular reasons of enhanced colitis, especially to analyse whether enhanced effector T cell differentiation or decreased Treg induction was responsible, the percentages of Treg cells in sections of the lamina propria were determined by flow cytometry. About 6% of Foxp3<sup>+</sup> regulatory T cells developed from transferred wildtype naïve T cells, whereas between 0.3 and 2% Tregs were detected after the transfer of I $\kappa$ B<sub>NS</sub>-deficient T cells (Fig. 36a). The difference was found to be of statistical significance (Fig. 36a). As the Treg compartment appeared reduced, the amount of IFN $\gamma$  producing T<sub>H</sub>1 cells within the lamina propria was determined. I $\kappa$ B<sub>NS</sub>-deficient IFN $\gamma$ <sup>+</sup> cells were detected with a percentage of about 75% in contrast to 65% IFN $\gamma$  producing wildtype T cells (Fig. 36b). However, the mild increase of IFN $\gamma$  producers, which developed from I $\kappa$ B<sub>NS</sub>-deficient T cells was not statistically significant (Fig. 36b). Those data indicated a relatively normal differentiation of T<sub>H</sub>1 effector cells upon I $\kappa$ B<sub>NS</sub> deficiency, but a massively impaired generation of a protective Treg compartment.

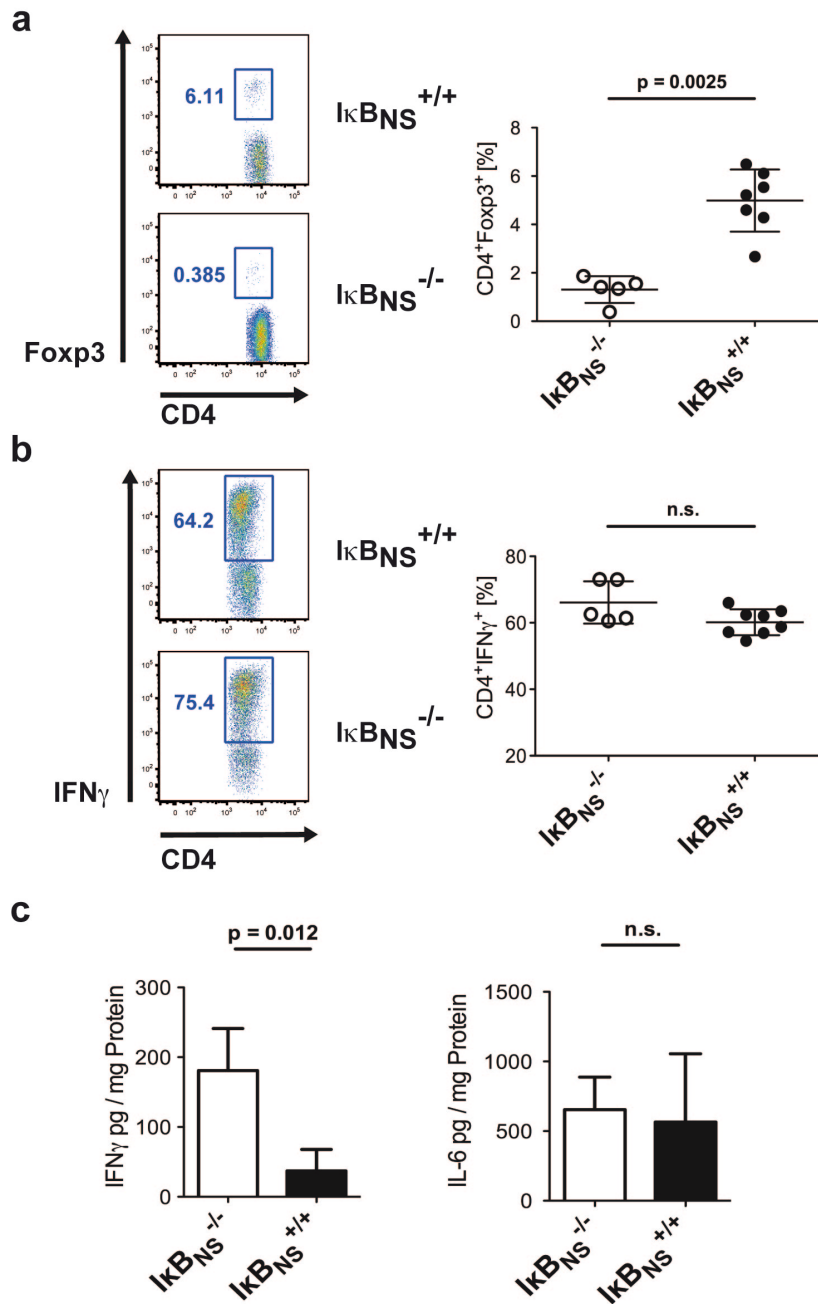


**Figure 36:  $I\kappa B_{NS}$  deficiency impairs generation of a protective Treg compartment during chronic gut inflammation**

**(a)** Representative pseudo-color dot blot (left panel) and scatter dotplot of percentages of CD4<sup>+</sup>Foxp3<sup>+</sup> Tregs in the lamina propria of RAG1<sup>-/-</sup> mice injected with PBS or CD25-depleted peripheral CD4<sup>+</sup> T cells from wildtype or  $I\kappa B_{NS}$ -deficient mice. **(b)** Representative pseudo-color dot blot (left panel) and scatter dotplot of percentages of CD4<sup>+</sup>IFN $\gamma$ <sup>+</sup> T<sub>H</sub>1 cells in the lamina propria of RAG1<sup>-/-</sup> mice injected with PBS or CD25-depleted peripheral CD4<sup>+</sup> T cells from wildtype or  $I\kappa B_{NS}$ -deficient mice. **(c)** Bars of cytometric bead assays of IFN $\gamma$  and IL-6 released from cultivated colon sections of RAG1<sup>-/-</sup> mice injected with PBS or CD25-depleted peripheral CD4<sup>+</sup> T cells from wildtype or  $I\kappa B_{NS}$ -deficient mice. For a-c statistical significances were calculated by two-tailed Mann-Whitney tests (PBS n=4; wildtype n=8;  $I\kappa B_{NS}^{-/-}$  n=5; mean  $\pm$  s.e.m.).

---

The amount of released proinflammatory cytokines was assessed by the incubation of 1 cm colon sections and a subsequent cytometric bead array analyses for secreted IL-6 and IFN $\gamma$ . 180 pg/mg protein of IFN $\gamma$  was detected in sections of RAG1<sup>-/-</sup> mice, which received I $\kappa$ B<sub>NS</sub>-deficient T cells (Fig. 36c). A markedly reduced amount about 40 pg/mg protein of IFN $\gamma$  was detected in control sections, which received wildtype cell (Fig.36c). The amount of released IL-6 remained comparable between the two genotypes at 600 pg/mg protein (Fig. 36c). Taken together I $\kappa$ B<sub>NS</sub> deficiency impairs the development of a protective Treg compartment during chronic inflammation. In the transfer colitis model the reduced amount of Tregs appeared to be responsible for exacerbated colitis. As T<sub>H</sub>1 differentiation was just minimally affected, whereas an increased amount of released IFN $\gamma$  was detected, it is likely that the reduced Treg compartment could not effectively block T<sub>H</sub>1 effector activity.

---

## 5 Discussion

### 5.1 I $\kappa$ B<sub>NS</sub> deficiency results in a massively reduced Treg compartment, comparable to c-Rel deficiency

I $\kappa$ B<sub>NS</sub> was identified in autoreactive T cells undergoing thymic apoptosis in TCR transgenic (TCRtg) mouse models of peptide-induced negative selection (Fiorini et al., 2002). Although I $\kappa$ B<sub>NS</sub> was highly induced in T cells from MHC I-restricted N15 and MHC II-restricted 5CC7 mice upon stimulation of transgenic TCRs with the cognate peptide antigens VSV8 (vesicular stomatitis virus nuclear octapeptide) and PCC (pigeon cytochrome C), respectively, I $\kappa$ B<sub>NS</sub><sup>-</sup> deficient mice did not show signs of altered negative selection or of perturbed distribution of CD4<sup>+</sup> or CD8<sup>+</sup> T cells (Touma et al., 2007). VSV8 stimulation of N15 mice bred to I $\kappa$ B<sub>NS</sub><sup>-</sup> deficient mice did not reveal impaired negative selection compared to N15 mice on a wildtype background (Touma et al., 2007). Moreover, T cells of I $\kappa$ B<sub>NS</sub>-deficient mice displayed normal V $\beta$ -usage (Touma et al., 2007). These findings demonstrated that I $\kappa$ B<sub>NS</sub> is dispensable for negative selection. Thus, the function of its induction in autoreactive T cells in the thymus upon TCR triggering remained enigmatic.

Several groups reported that NF $\kappa$ B activity in immature thymic T cells is essential for the development of regulatory T cells (Hori, 2010; Hsieh, 2009; Isomura et al., 2009; Liou et al., 1999; Molinero et al., 2009). Loss of the NF $\kappa$ B subunit c-Rel was shown to impair Foxp3 expression as the protein directly binds to two unique NFAT sites in the Foxp3 promoter and  $\kappa$ B sites in CNS2 and CNS3 (Isomura et al., 2009; Long et al., 2009). Thereby, c-Rel-deficient mice display a reduction of Treg cells by 50%. Remarkably, I $\kappa$ B<sub>NS</sub> and c-Rel deficiencies cause comparable Treg phenotypes, as Treg cells were reduced by 50% in both mice, demonstrated by intracellular Foxp3 staining (Fig. 10 to 13) (Isomura et al., 2009). Remarkably, c-Rel and I $\kappa$ B<sub>NS</sub> deficiencies only partially reduce Treg frequencies and numbers, whereas intact upstream NF $\kappa$ B signalling is important for the entire Treg generation. Deficiency of proximal signaling events, as described for CARMA1-, IKK2- and TAK1-deficient mice abolishes normal Treg development (Molinero et al., 2009). These

---

phenotypical and molecular observations suggest that the nuclear proteins c-Rel and I $\kappa$ B<sub>NS</sub>, which regulate Treg development, represent two essential downstream targets of the NF $\kappa$ B activators CARMA1, IKK2 and TAK1. It needs to be proven, whether translocation of c-Rel in the nucleus and the induction of I $\kappa$ B<sub>NS</sub> occurs normally in CARMA1-, IKK2- or TAK1-deficient T cells. Loss of these proteins leads to almost entire blocking of the key downstream signaling event, the degradation of I $\kappa$ B $\alpha$ . Therefore, it is unlikely that c-Rel or I $\kappa$ B<sub>NS</sub> are activated without CARMA1, IKK2 or TAK1, as c-Rel is highly induced upon TCR triggering, supposed in a positive f NF $\kappa$ B eedback loop. Since the promoter of I $\kappa$ B<sub>NS</sub> consists of several  $\kappa$ B binding sites as well, suggesting that it is regulated in a comparable manner. A previous study bred mice overexpressing a constitutively active IKK2 under control of the LCK-promoter to CARMA1-deficient mice (Long et al., 2009). Activity of IKK2 was sufficient to restore normal Treg development, compensating the lack of its upstream activator CARMA1 (Long et al., 2009). In a similar vein overexpression of c-Rel and I $\kappa$ B<sub>NS</sub> might restore normal Treg development in CARMA1-, IKK2- or TAK1-deficient mice. One needs to keep in mind that unusual I $\kappa$ B proteins, like I $\kappa$ B<sub>NS</sub>, need an NF $\kappa$ B transcription factor, which is already associated to the DNA to trigger gene expression. Therefore, it might be necessary to overexpress I $\kappa$ B<sub>NS</sub> in combination with other transcription factor subunits of the Rel-family like c-Rel to rescue Treg development.

Of note, a reduced Treg compartment is not the only corresponding phenotype of I $\kappa$ B<sub>NS</sub>- and c-Rel-deficient mice. Previous studies reported impaired IL-2 production and reduced proliferation of CD4 and CD8 T cells from c-Rel- and I $\kappa$ B<sub>NS</sub>-deficient mice as well (Liou et al., 1999; Touma et al., 2007; Touma et al., 2011). Moreover, both mice lack intraperitoneal B1 B cells (Touma et al., 2011). Although these studies did not compare both genotypes directly, c-Rel and I $\kappa$ B<sub>NS</sub> obviously share several functional properties of T cell homeostasis and B cell development indicating cooperative or parallel functioning. Data from ChIP sequencing analyses using anti-I $\kappa$ B<sub>NS</sub> and anti-c-Rel antibodies would allow determination of the amount of cooperatively regulated genes. Taken together, I $\kappa$ B<sub>NS</sub> deficiency causes a

---

reduced Treg compartment of about 50%, which is comparable to c-Rel deficiency. The generation of Foxp3 positive cells *in vitro* was affected as well (Fig. 14). Aside from impaired IL-2 and IFN $\gamma$  expression by isolated T cells, this is a further common observation of I $\kappa$ B<sub>NS</sub><sup>-</sup> and c-Rel-deficient mice. Although there is no experimental proof, the phenotypes of CARMA1-, TAK1- IKK2-, c-Rel-, and I $\kappa$ B<sub>NS</sub>-deficient mice suggest that these proteins are activating a common NF $\kappa$ B signaling event, which forces Foxp3 induction.

## 5.2 Treg precursor accumulation follows from delayed Foxp3 induction

Thymic nTregs develop according to the “two-step” model from CD8<sup>-</sup>CD4<sup>+</sup>CD25<sup>+</sup>GITR<sup>+</sup>Foxp3<sup>-</sup> Treg precursor cells (Lio and Hsieh, 2008). This population arises from an initial strong TCR triggering in the thymus, which requires the expression of autoreactive TCRs (Lio and Hsieh, 2008). It is thought that this initial TCR stimulation induces binding of a c-Rel containing enhanceosome, which remodels the chromatin of the Foxp3 locus to a relaxed condensation status, which mediates responsiveness to other signaling cascades. The next step, the transition of Foxp3<sup>-</sup> precursors into Foxp3<sup>+</sup> cells, depends on  $\gamma$ -chain cytokine signaling mediated by IL-2 and IL-15 (Lio and Hsieh, 2008; Vang et al., 2008). Combining these observations, a recent report demonstrated that IL-2 responsiveness of c-Rel-deficient CD25<sup>+</sup>GITR<sup>+</sup>Foxp3<sup>-</sup> precursors is impaired, as fewer Foxp3<sup>+</sup> cells were induced upon IL-2 treatment of Treg precursor cells *in vitro* (Grigoriadis et al., 2011). Remarkably, not only transition into Foxp3<sup>+</sup> cells in c-Rel-deficient mice was impaired, but the amount of immature Treg precursor cells was massively reduced as well (Grigoriadis et al., 2011). This indicates that NF $\kappa$ B activity regulate both steps of Treg development, precursor induction and  $\gamma$ c-cytokine responsiveness.

Remarkably, I $\kappa$ B<sub>NS</sub>-deficient mice display accumulation of thymic nTreg precursor cells, rather than reduced generation as reported for c-Rel- and CARMA1-deficient mice (Fig. 26 to 28). It appears that the observed precursor accumulation is a result of decelerated Foxp3 induction, meaning transition of Foxp3<sup>-</sup> into Foxp3<sup>+</sup> cells. As this second step of Treg development is mediated by  $\gamma$ c-cytokine signals, I $\kappa$ B<sub>NS</sub> might regulate phosphorylation of

---

STAT5, or its binding to the Foxp3 promoter, probably by remodeling of the chromatin to an open conformation as part of the c-Rel enhanceosome. This idea is further emphasized by the impaired Foxp3 induction upon IL-2 treatment of purified I $\kappa$ B<sub>NS</sub>-deficient Treg precursor cells *in vitro* (Fig. 30). Moreover, interactions between unusual I $\kappa$ Bs and histone modifying enzymes were described previously for BCL-3, which recruits TIP60 to the IL-6 locus, and I $\kappa$ B $\zeta$ , which might bind to HDAC-4 or HDAC-5 (Dechend et al., 1999; Totzke et al., 2006). An alternative explanation, which mediates reduced transition of precursor cells into Foxp3<sup>+</sup> Tregs by impaired levels of IL-2 in I $\kappa$ B<sub>NS</sub>-deficient mice was ruled out by two experimental approaches. On the one hand by the *ex vivo* treatment of precursor cells with identical amounts of IL-2 and on the other hand by the generation of mixed bone marrow chimeric mice (Fig. 15), which demonstrated that the I $\kappa$ B<sub>NS</sub> protein intrinsically modulates Foxp3 expression.

It needs to be explained, why c-Rel-deficient mice display reduction of Treg precursors, whereas I $\kappa$ B<sub>NS</sub>-deficient mice show accumulation of these cells. A possible explanation is the direct regulation of CD25 by c-Rel (Liou et al., 1999). Microarray data from stimulated CD4<sup>+</sup> T cells did not show that I $\kappa$ B<sub>NS</sub> targets CD25, in contrast to c-Rel (Touma et al., 2007). It can also not completely excluded, that the Treg precursor population in the thymus is contaminated with activated effector cells. To this end no marker exist, which allows distinguishing between CD25<sup>+</sup>GITR<sup>+</sup>Foxp3<sup>-</sup> Treg precursors and activated effector T cells.

### **5.3 I $\kappa$ B<sub>NS</sub> –deficient Tregs undergo enhanced proliferation**

Remarkably, I $\kappa$ B<sub>NS</sub>-deficient Treg cells displayed an increased cycling assessed by BrdU incorporation and Ki67 staining, but apoptosis analysed by AnnexinV/7AAD and TMRE was not affected (Fig. 20 to 25). Obviously, these results seem to conflict with the reduced number of Treg cells in I $\kappa$ B<sub>NS</sub>-deficient mice. It was previously reported that I $\kappa$ B<sub>NS</sub> is suppressed by mature Treg cells (Marson et al., 2007), therefore a direct regulation of Treg proliferation appears unlikely. The turnover rate of the Treg compartment is apparently very strong, as seen in *in vivo* apoptosis and cell death analyses (Fig. 24 and 25). As Treg cells

---

are generated to a reduced extent in I $\kappa$ B<sub>NS</sub>-deficient mice in the thymus, they have to undergo enhanced homeostatic proliferation, to compensate their minimal thymic generation, but fail to compensate impaired generation entirely. As for c-Rel and CARMA1 no corresponding analyses were performed, it is not possible to compare these data with other studies. Nevertheless, it is conceivable that the few generated c-Rel- and CARMA1-deficient Tregs display enhanced basal proliferation as well.

#### **5.4 Nuclear p50 and c-Rel interacts with 70 kDa and 35 kDa I $\kappa$ B<sub>NS</sub>**

Via interaction to NF $\kappa$ B transcription factors on the DNA unusual I $\kappa$ B proteins modulate gene transcription as demonstrated by binding of BCL-3 and I $\kappa$ B $\zeta$  to p65 and p50 (Dechend et al., 1999; Totzke et al., 2006). Although unusual I $\kappa$ B proteins functionally act in the nucleus, they are shortly localized in the cytoplasm, but migrate immediately after translation into the nucleus (Fig. 32a). Pulldown analyses from cytoplasmic and nuclear protein extracts from stimulated T cells using GST-tagged recombinant I $\kappa$ B<sub>NS</sub> demonstrated its predominant interaction with nuclear p50 and p52, and to a reduced extent with c-Rel and p65, but exclusively with nuclear proteins (Fiorini et al., 2002). A prominent interaction with p65 as described for BCL-3 and I $\kappa$ B $\zeta$  was not identified.

To study interaction of endogenous proteins I $\kappa$ B<sub>NS</sub>, p50 and c-Rel were immunoprecipitated from cytoplasmic and nuclear extracts of stimulated CD4<sup>+</sup>CD25<sup>-</sup> T cells. This cell type was introduced previously as a suitable model system to study early events of *de novo* Foxp3 induction (Zheng et al., 2010). In the cytoplasm, no interaction of I $\kappa$ B<sub>NS</sub> with any NF $\kappa$ B subunit was detected, in contrast to the nucleus, where the protein associated to p50 and c-Rel. Interactions between p65 and I $\kappa$ B<sub>NS</sub> as seen in pulldown analyses were not detected (Fig. 32b). These data are in line with the mentioned pulldown analyses in terms that I $\kappa$ B<sub>NS</sub> did not interact with cytoplasmic but nuclear NF $\kappa$ B proteins (Fiorini et al., 2002). It is conceivable that either block of the I $\kappa$ B binding site within cytoplasmic NF $\kappa$ B subunits by other I $\kappa$ B proteins or posttranslational modification of NF $\kappa$ B during its activation lead to binding of I $\kappa$ B<sub>NS</sub>. Because the pulldowns from cytoplasmic and nuclear fractions were done

---

with identical recombinant I $\kappa$ B<sub>NS</sub> proteins, a different interaction pattern is hardly the reason of post translational modification of I $\kappa$ B<sub>NS</sub>. Although, one cannot entirely rule out that a posttranslational modification of the recombinant protein occurs *in vitro* by an enzyme from the nuclear extract.

The kinetic to identify the optimal timepoint of NF $\kappa$ B activity revealed two novel isoforms of I $\kappa$ B<sub>NS</sub> of about 70 kDa, which were not detected in stimulated I $\kappa$ B<sub>NS</sub>-deficient T cells, arguing against crossreactivity of the used anti-I $\kappa$ B<sub>NS</sub> antibody. Unspecificity of the used antibody appears more unlikely as these isoforms were detected using four different rabbit polyclonal sera and one IgG2b mouse monoclonal antibody, each raised independently. Moreover, screening of cDNA libraries and RACE-PCR reported only a mRNA of 985 bp, which encode for the 35 kDa isoform, making alternative splicing as an explanation for the different I $\kappa$ B<sub>NS</sub> protein sizes highly unlikely (Fiorini et al., 2002). Additionally, the I $\kappa$ B<sub>NS</sub> locus is too short to encode a 70 kDa protein. Therefore, one can assume that the 70 kDa isoforms originate from posttranslational modifications. Unpublished data from Prof. Linda K. Clayton (Dana Farber Cancer Institute, Harvard Medical School, Boston, USA) suggest that the upper of both nearly 70 kDa isoforms is the result of phosphorylation, since treatment of protein extracts with alkaline phosphatases led to disappearance of its signal. However, as phosphatases have also protease activities the results require further validation for example by *in vitro* phosphorylation assays. It is also possible, that Ubiquitin, or small ubiquitin-like modifiers (Hirotsani et al.) are responsible for the shift in the molecular weight of I $\kappa$ B<sub>NS</sub>, as poly-ubiquitin modification of nuclear BCL-3 was recently reported, which regulates its DNA binding activity (Ghosh and Hayden, 2008; Massoumi et al., 2006). Alternatively the doubled molecular weight might indicate a homodimer of I $\kappa$ B<sub>NS</sub> generated in the nucleus, which stays stable in SDS-Page and Western blot. Clearly, mass spectrometry analyses of purified 70 kDa I $\kappa$ B<sub>NS</sub> is needed to identify the kind of I $\kappa$ B<sub>NS</sub> modification. It needs to be addressed, whether or not the 70 kDa or 35 kDa isoform in the nucleus might have different functional properties or might even represent active or inactive isoforms, especially since 35 kDa as well as 70 kDa I $\kappa$ B<sub>NS</sub> bind to p50 and c-Rel. However, as 70 kDa I $\kappa$ B<sub>NS</sub> is the most prominent isoform in the

---

nucleus it is conceivable that this protein variant is of higher significant functional importance than its 35 kDa homolog.

### **5.5 CNS2 and CNS3 are targeted by I $\kappa$ B<sub>NS</sub>**

Both I $\kappa$ B<sub>NS</sub> isoforms displayed interaction with c-Rel and p50 in the nucleus suggesting that these proteins interact at the Foxp3 locus to regulate its transcriptional activity. An early study suggested that p50 controls development of regulatory T cells (Jana et al., 2009). These results were obtained from *in vitro* differentiation experiments, but conditional p50-deficient mice and analyses in mixed bone marrow chimeric mice demonstrated that p50 is dispensable for Treg development *in vivo* (Ruan et al., 2009). Additionally, the *in vitro* differentiation data await confirmation by an independent study. As already mentioned the role of c-Rel was extensively investigated. The protein binds to two unique NFAT sites in the Foxp3 promoter, one  $\kappa$ B binding site in CNS2, and the single  $\kappa$ B site in CNS3 (Hori, 2010; Isomura et al., 2009; Liou et al., 1999). So far, the combination of the c-Rel containing NF $\kappa$ B dimer remains unknown and both, interactions with p50 and p65, were suggested (Hori, 2010; Hsieh, 2009; Isomura et al., 2009).

CNS2, which is bound by I $\kappa$ B<sub>NS</sub> is the only regulatory sequence that displays transcriptional activity in luciferase-based reporter gene assay. Its induction was significantly reduced using I $\kappa$ B<sub>NS</sub>-deficient *in vitro* expanded primary CD4<sup>+</sup>CD25<sup>-</sup> T cells (Fig. 33e). So, I $\kappa$ B<sub>NS</sub> has a direct impact on the transcriptional activity of CNS2. This sequence was also described as the Treg specific demethylation region (TSDR), which undergoes demethylation during Treg maturation in order to ensure stable Foxp3 expression (Huehn et al., 2009; Polansky et al., 2008). In luciferase assays a non-methylated construct was transfected into the cells, which corresponds to the opened locus in Treg cells. Since its methylation pattern appeared identical between purified wildtype and I $\kappa$ B<sub>NS</sub>-deficient CD4<sup>+</sup>CD25<sup>+</sup> Tregs, I $\kappa$ B<sub>NS</sub> seems to regulate exclusively its transcriptional activity, but not its demethylation during Treg development. Previous studies reported that CNS2 demethylation in c-Rel-deficient Tregs was not altered compared to wildtype Tregs and transcriptional activity was reduced as well

---

(Hori, 2010; Hsieh, 2009). Of note, none of the sites, which were bound by  $I\kappa B_{NS}$  or c-Rel are localized within a single CpG.

CNS3 is thought to function as a pioneer element in Treg development and its only  $\kappa B$  site was bound by c-Rel, p50 and  $I\kappa B_{NS}$  in pulldown analyses (Fig. 33d). According to the literature, this element did not display luciferase activity (Zheng et al., 2010). The identical reduction of Treg cells from c-Rel- and  $I\kappa B_{NS}$ -deficient mice, and reduced responsiveness of Treg precursors to exogenous IL-2 suggest that both proteins modulate Foxp3 expression by a commonly regulated mechanism. As discussed above interaction of c-Rel with  $I\kappa B_{NS}$  might cooperatively recruit a histone modifying enzyme to the Foxp3 locus and thereby relaxing the chromatin and allow binding for other transcription factors. The idea that c-Rel modifies the Foxp3 locus follows from the observation that IL-2 expression is regulated by a comparable mechanism, which mediated chromatin remodeling in a c-Rel-dependent manner. In case of IL-2 expression, however, c-Rel does not directly associate to  $I\kappa B_{NS}$ . It binds along with p50 to a classical  $\kappa B$  site localized about 150 bp downstream of a CD28 responsive element occupied by a c-Rel homodimer. Nevertheless another  $I\kappa B$  protein like BCL-3 or  $I\kappa B\zeta$  might bind to c-Rel at the CD28 responsive element to mediate chromatin remodeling (Touma et al., 2007).

Collectively,  $NF\kappa B$  activity modulates Foxp3 expression by direct binding of the effector proteins c-Rel and  $I\kappa B_{NS}$  to CNS2, but does not regulate Foxp3 via its demethylation. Their combined binding to CNS3 might regulate opening of the locus by chromatin remodeling via recruitment of an unknown acetyltransferase. As deletion of the genomic sequence massively abolished Foxp3 induction, its role is highly important for Treg generation, although it does not display transcriptional activity, as previously reported (Zheng et al., 2010).

---

## 5.6 I $\kappa$ B<sub>NS</sub> deficiency does not alter Treg functioning, but affects Treg generation during chronic gut inflammation

The phenotype of mature Tregs remained unaffected by I $\kappa$ B<sub>NS</sub> deficiency. The lack of difference of Treg functioning and homeostasis between wildtype and I $\kappa$ B<sub>NS</sub>-deficient Tregs assessed by *in vitro* suppression assays, demethylation of CNS2 and expression of Foxp3, CD25, GITR, CD122 and intracellular CTLA-4 assessed by mean fluorescent intensities points out that I $\kappa$ B<sub>NS</sub> is dispensable for mature Tregs (Fig. 17 to 19). c-Rel-deficient Tregs do also not display differences in suppressive capacity or CNS2 demethylation. As neither c-Rel- nor I $\kappa$ B<sub>NS</sub>-deficient mice display signs of autoimmunity, the functional Treg compartment, albeit reduced in size, might sufficiently protect those mice against activation of autoreactive T cells. Of note, I $\kappa$ B<sub>NS</sub> and c-Rel also force proliferation and IL-2 secretion of effector T cells (Liou et al., 1999; Touma et al., 2007). Thus, the lack of autoimmunity in c-Rel- and I $\kappa$ B<sub>NS</sub>-deficient mice might as well arise from both an impaired Treg compartment and diminished Tcon activation. This idea is further emphasized by the lack of difference in Tcon activation status between wildtype and I $\kappa$ B<sub>NS</sub>-deficient mice and the strong induction of I $\kappa$ B<sub>NS</sub> after TCR triggering in conventional T cells.

To assess the physiological consequences of decreased Foxp3 induction *in vivo*, a model system of chronic gut inflammation was chosen as the microbial microflora of the gut favours Treg induction as previously demonstrated (Harada et al., 1995; Sun et al., 2007). Fewer Tregs originated from transferred I $\kappa$ B<sub>NS</sub>-deficient naïve T cells verifying its impact on Foxp3 induction even during colitis. (Fig. 36a). Thus, I $\kappa$ B<sub>NS</sub> regulates Treg development under inflammatory conditions as well, verifying its role as an essential component of *de novo* Foxp3 expression. Since migration and activation of I $\kappa$ B<sub>NS</sub>-deficient and wildtype IFN $\gamma$  producers was not impaired it appeared unlikely that I $\kappa$ B<sub>NS</sub>-deficiency regulated T<sub>H</sub>1 development *in vivo* as well, although it was reported that proliferation and IFN $\gamma$  secretion is impaired upon I $\kappa$ B<sub>NS</sub> deficiency.

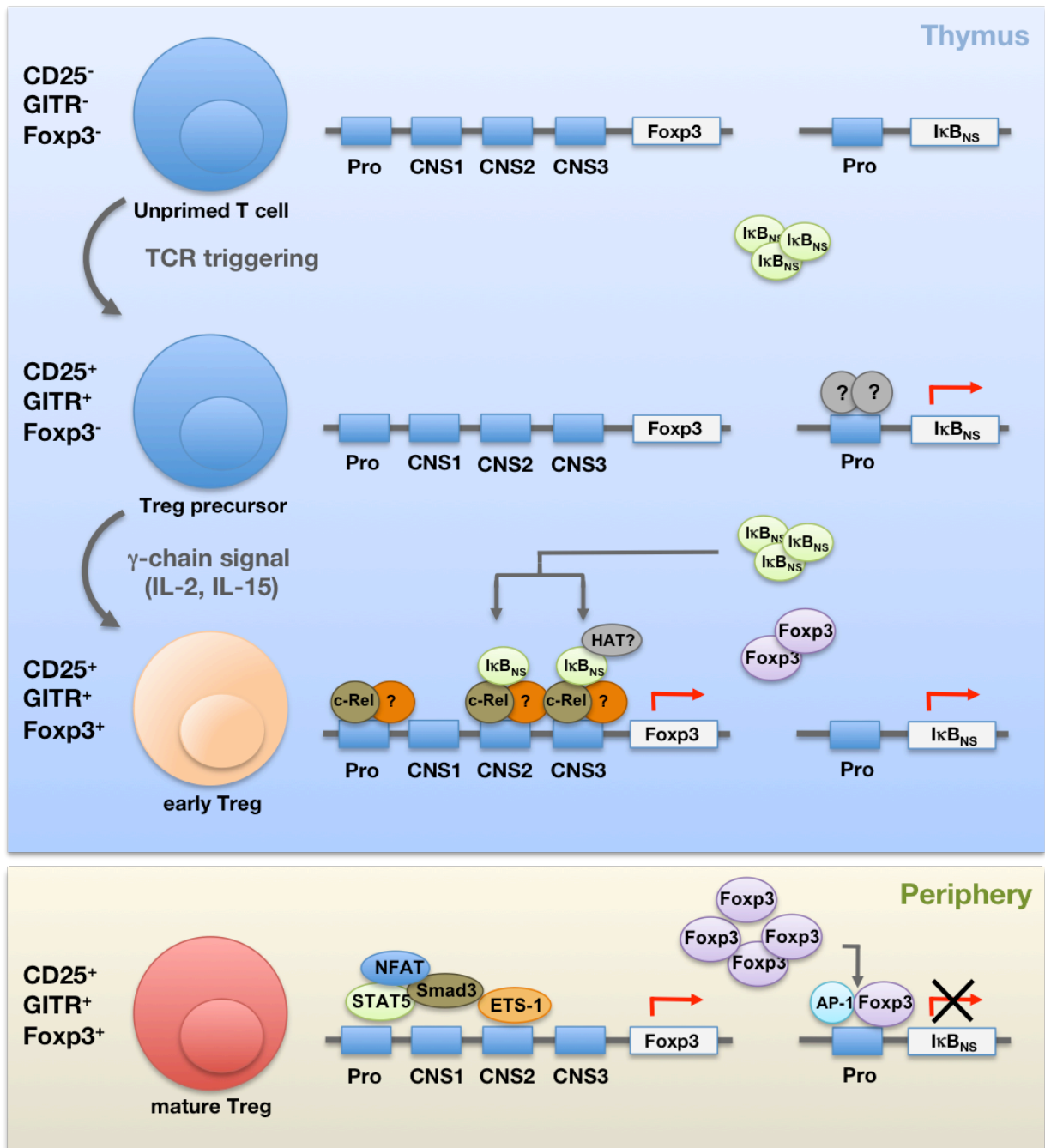


**Figure 37: Regulation of *de novo* Foxp3 induction by IκB<sub>NS</sub>**

Overview of the molecular role of IκB<sub>NS</sub> during Foxp3 induction as a model is shown. The initial TCR triggering of CD4<sup>+</sup>CD8<sup>-</sup>GITR<sup>-</sup>CD25<sup>-</sup>Foxp3<sup>-</sup> T cells leads to expression of IκB<sub>NS</sub> in CD4<sup>+</sup>CD8<sup>-</sup>GITR<sup>+</sup>CD25<sup>+</sup>Foxp3<sup>-</sup> Treg precursor cells. Foxp3 is induced by γc-signaling from IL-2 and IL-15 and forced by an IκB<sub>NS</sub> and c-Rel containing NFκB complex associated to CNS2 and CNS3, which might recruit an unknown histone acetyl transferase to CNS3. Once Foxp3 is induced the protein downregulates IκB<sub>NS</sub>-expression in cooperation with AP-1 in a negative feedback loop.

---

Alternatively, Treg induction in the gut could have been studied using  $I\kappa B_{NS}$ -deficient bred to OT-II mice and their following oral feeding via drinking water with OVA-peptide. The incorporated OVA would have led to Treg induction in the gut. Although this is a widely accepted model, it shapes TCR specificity to a singly epitope. The effect of a polyclonal background is more close to the real physiological situation of Treg development.

$CD4^+$  T cells led only to minimal signs of colitis (Fig. 35). However, three of seven RAG1-deficient mice, which were injected with  $I\kappa B_{NS}$ -deficient T cells had to be sacrificed before the end of the experiment as their weight loss exceeded the approved level. Stronger conditions could have led to the complete loss of this group. Adoptive transfer colitis experiments were not done with c-Rel-deficient T cells, thus it is not possible to compare the data to a possible effect of c-Rel. It was only proven, that cotransfer of c-Rel-deficient Tregs to wildtype effector cells protects from development of colitis *in vivo* as efficient as wildtype Tregs (Grigoriadis et al., 2011; Isomura et al., 2009).

Conclusively, a physiological relevance of the reduced Treg compartment in  $I\kappa B_{NS}$ -deficient mice in form of spontaneously developing autoimmunity does not arise under pathogen-free conditions. Upon massive gut inflammatory, however, the markedly reduced Treg development is associated with a strong disease course.

## **5.7 Concluding remarks and model**

Taken together, this thesis demonstrated an important role of  $I\kappa B_{NS}$  in the development of regulatory T cells. Together with c-Rel,  $I\kappa B_{NS}$  is the only nuclear  $NF\kappa B$  components described so far, which regulate Foxp3 expression.  $I\kappa B_{NS}$  deficiency leads to a significant reduction of the Treg compartment, which is comparable to the degree of impairment in c-Rel-deficient mice. The combination of published and novel cellular and molecular data suggests a model, in which  $I\kappa B_{NS}$  is induced after the initial TCR triggering of developing T cells in the thymus (Fig. 37). Instead of modulating the clonal deletion of autoreactive thymocytes,  $I\kappa B_{NS}$  binds to CNS2 and CNS3 within the Foxp3 locus in  $CD4^+CD8^-CD25^+GITR^+Foxp3^-$  Treg precursor cells, whereby it forces Foxp3 expression and

---

transition of precursor cells into mature Tregs (Fig. 37). The early Foxp3<sup>+</sup> Treg cells leave the thymus and Foxp3 downregulates I $\kappa$ B<sub>NS</sub> via direct repression through an AP-1/Foxp3 complex in the fashion of a negative feedback loop (Fig. 37). Thereby, I $\kappa$ B<sub>NS</sub> is crucial for *de novo* Foxp3 induction, but not maintenance or suppressive function of mature Treg cells. As I $\kappa$ B<sub>NS</sub> forces transition of precursor cells into mature Tregs, its deficiency leads to an accumulation of immature Treg precursor cells in the thymus. The importance of I $\kappa$ B<sub>NS</sub> for Foxp3 induction was demonstrated by a transfer colitis model as Treg generation under inflammatory conditions was impaired upon I $\kappa$ B<sub>NS</sub> deficiency as well.

On the molecular level some aspects of the induction model require further investigation. If indeed histone modification is regulated through an I $\kappa$ B<sub>NS</sub>-containing NF $\kappa$ B complex, one need to identify the acetyl transferase or histone deacetylase, which is recruited by I $\kappa$ B<sub>NS</sub> to the Foxp3 locus. It is also unknown, whether c-Rel and I $\kappa$ B<sub>NS</sub> act in a simultaneous or sequential order. Thus, the phenotype of c-Rel/I $\kappa$ B<sub>NS</sub> double knockout mice regarding the amount of Treg cells would provide additional functional insight into regulation of Foxp3 by NF $\kappa$ B. Considering the recent report that mice deficient for the BCL-3 class protein I $\kappa$ B $\zeta$  are completely protected from EAE (Okamoto et al., 2010), unusual I $\kappa$ B proteins could regulate the development of distinct T helper cell subsets. Detailed analyses of the impact of BCL-3, I $\kappa$ B $\zeta$ , I $\kappa$ B $\eta$  and I $\kappa$ B<sub>NS</sub> on the development of individual T cell subsets could provide profound new insights into NF $\kappa$ B dependent T cells generation and might clarify whether unusual I $\kappa$ B proteins represent suitable pharmacological targets for the treatment of chronic inflammatory diseases and cancer.

---

## 6. Abbreviations

7AAD	7-aminoactinomycin D
AIRE	Autoimmune regulator
AP-1	Activating protein 1
APC	Antigen presenting cells
APS-1	Autoimmune polyendocrinopathy syndrome type 1
BCL-2	B cell lymphoma protein 2
BCL-3	B cell lymphoma protein 3
BCL-10	B cell lymphoma protein 10
BrdU	5' bromodeoxyuridine
cAMP	Cyclic adenosin monophosphat
CARD	Caspase-recruitment domain
CARMA1	CARD containing MAGUK protein 1
CD28RE	CD28 responsive element
CDK	Cyclin dependent kinase
CNS	Conserved non-coding sequence
CTLA-4	Cytotoxic T-lymphocyte antigen 4
DC	Dendritic cell
DD	Death domain
DN	Double negative (CD4 <sup>-</sup> CD8 <sup>-</sup> )
DNA	Desoxyribonucleic acid
DP	Double positive (CD4 <sup>+</sup> CD8 <sup>+</sup> )
dsRNA	Double stranded ribonucleic acid
EAE	Experimental induced encephalomyelitis
<i>Ebi3</i>	<i>Eppstein-Barr virus induced gene 3</i>
Flip	Flice-inhibitory protein
Foxp3	Forkhead box protein 3
GALT	Gut-associated lymphoid tissues

---

GITR	Glycocorticoid-induced TNF receptor
HAT	Histone acetyl transferase
HDAC	Histone deacetylase
IBD	Inflammatory bowel disease
ICAM-1	Intercellular adhesion molecule 1
IDO	Indolamin-2,3-Dioxygenase
Ig	Immunoglobulin
I $\kappa$ B	Inhibitor of NF $\kappa$ B protein
IL-1	Interleukin-1
IL-2	Interleukin-2
IL-6	Interleukin-6
IL-10	Interleukin-10
IL-12	Interleukin-12
IL-15	Interleukin-15
IL-35	Interleukin-35
i.p.	intra peritoneal
IP-10	Interferon $\gamma$ -induced protein 10
IPEX	Immudysregulation polyendocrinopathy X-linked syndrom
i.v.	intra venous
Lag-3	Lymphocyte activation gene 3
LPS	Lipopolysaccharide
MAGUK	Matrix-associated guanylate kinase
MALT1	Mucosa-associated lymphoid tissue protein 1
MAPK	Mitogen-activated protein kinase
MFI	Mean fluorescent intensity
MHC	Major histocompatibility complex
mTEC	Medullary thymic epithelial cell

---

NFAT	Nuclear factor of activated T cells
NF $\kappa$ B	Nuclear factor $\kappa$ B
NLS	Nuclear localisation signal
NP-1	Neuropilin-1
OVA	Ovalbumin
PAMP	Pathogen associated molecular pattern
PCC	Pigeon cytochrome C
PCR	Polymerase chain reaction
RAG1	Recombination activating gene 1
RAG2	Recombination activating gene 2
RACE-PCR	Rapid amplification of cDNA-ends with PCR
RANTES	Regulated upon Activation, Normal T-cell expressed and presumably secreted
RHD	REL-homology domain
SH3	src-homology domain 3
Smad3	Mothers against decapentaplegic homolog 3
STAT5	Signal transducer and activator of transcription 5
SUMO	Small ubiquitin-like modifiers
TAD	Transactivation domain
TAK1	TGF- $\beta$ activated kinase 1
TCR	T cell receptor
TGF- $\beta$	Transforming growth factor- $\beta$
TMRE	Tetramethylrhodamine ethyl ester
TNF- $\alpha$	Tumor necrosis factor $\alpha$
Treg	Regulatory T cell
TSDR	Treg specific demethylation region
VSV8	Vesicular stomatitis virus nuclear octapeptide

---

## 7. References

- Abd Elrazek, E., Thornton, M., and Lannigan, A. (2010). Effective awake thoracic epidural anesthetic for major abdominal surgery in two high-risk patients with severe pulmonary disease--a case report. *Middle East J Anesthesiol* 20, 891-895.
- Alam, S.M., Travers, P.J., Wung, J.L., Nasholds, W., Redpath, S., Jameson, S.C., and Gascoigne, N.R. (1996). T-cell-receptor affinity and thymocyte positive selection. *Nature* 381, 616-620.
- Apostolou, I., Sarukhan, A., Klein, L., and von Boehmer, H. (2002). Origin of regulatory T cells with known specificity for antigen. *Nat Immunol* 3, 756-763.
- Aschenbrenner, K., D'Cruz, L.M., Vollmann, E.H., Hinterberger, M., Emmerich, J., Swee, L.K., Rolink, A., and Klein, L. (2007). Selection of Foxp3+ regulatory T cells specific for self antigen expressed and presented by Aire+ medullary thymic epithelial cells. *Nat Immunol* 8, 351-358.
- Barnes, M.J., Krebs, P., Harris, N., Eidenschenk, C., Gonzalez-Quintal, R., Arnold, C.N., Crozat, K., Sovath, S., Moresco, E.M., Theofilopoulos, A.N., *et al.* (2009). Commitment to the regulatory T cell lineage requires CARMA1 in the thymus but not in the periphery. *PLoS Biol* 7, e51.
- Bennett, C.L., Christie, J., Ramsdell, F., Brunkow, M.E., Ferguson, P.J., Whitesell, L., Kelly, T.E., Saulsbury, F.T., Chance, P.F., and Ochs, H.D. (2001). The immune dysregulation, polyendocrinopathy, enteropathy, X-linked syndrome (IPEX) is caused by mutations of FOXP3. *Nat Genet* 27, 20-21.
- Bennett, C.L., and Ochs, H.D. (2001). IPEX is a unique X-linked syndrome characterized by immune dysfunction, polyendocrinopathy, enteropathy, and a variety of autoimmune phenomena. *Curr Opin Pediatr* 13, 533-538.
- Bensing, S., Fetissov, S.O., Mulder, J., Perheentupa, J., Gustafsson, J., Husebye, E.S., Oscarson, M., Ekwall, O., Crock, P.A., Hokfelt, T., *et al.* (2007a). Pituitary autoantibodies in autoimmune polyendocrine syndrome type 1. *Proc Natl Acad Sci U S A* 104, 949-954.
- Bensing, S., Hulting, A.L., Hoog, A., Ericson, K., and Kampe, O. (2007b). Lymphocytic hypophysitis: report of two biopsy-proven cases and one suspected case with pituitary autoantibodies. *J Endocrinol Invest* 30, 153-162.
- Boller, T., and Felix, G. (2009). A renaissance of elicitors: perception of microbe-associated molecular patterns and danger signals by pattern-recognition receptors. *Annu Rev Plant Biol* 60, 379-406.

- 
- Bours, V., Franzoso, G., Azarenko, V., Park, S., Kanno, T., Brown, K., and Siebenlist, U. (1993). The oncoprotein Bcl-3 directly transactivates through kappa B motifs via association with DNA-binding p50B homodimers. *Cell* 72, 729-739.
- Bruder, D., Probst-Kepper, M., Westendorf, A.M., Geffers, R., Beissert, S., Loser, K., von Boehmer, H., Buer, J., and Hansen, W. (2004). Neuropilin-1: a surface marker of regulatory T cells. *Eur J Immunol* 34, 623-630.
- Brunkow, M.E., Jeffery, E.W., Hjerrild, K.A., Paepfer, B., Clark, L.B., Yasayko, S.A., Wilkinson, J.E., Galas, D., Ziegler, S.F., and Ramsdell, F. (2001). Disruption of a new forkhead/winged-helix protein, scurfy, results in the fatal lymphoproliferative disorder of the scurfy mouse. *Nat Genet* 27, 68-73.
- Burchill, M.A., Yang, J., Vogtenhuber, C., Blazar, B.R., and Farrar, M.A. (2007). IL-2 receptor beta-dependent STAT5 activation is required for the development of Foxp3+ regulatory T cells. *J Immunol* 178, 280-290.
- Chen, C., Rowell, E.A., Thomas, R.M., Hancock, W.W., and Wells, A.D. (2006). Transcriptional regulation by Foxp3 is associated with direct promoter occupancy and modulation of histone acetylation. *J Biol Chem* 281, 36828-36834.
- Chen, L.F., and Greene, W.C. (2004). Shaping the nuclear action of NF-kappaB. *Nat Rev Mol Cell Biol* 5, 392-401.
- Chen, W., Jin, W., Hardegen, N., Lei, K.J., Li, L., Marinos, N., McGrady, G., and Wahl, S.M. (2003). Conversion of peripheral CD4+CD25- naive T cells to CD4+CD25+ regulatory T cells by TGF-beta induction of transcription factor Foxp3. *J Exp Med* 198, 1875-1886.
- Chen, Z.J. (2005). Ubiquitin signalling in the NF-kappaB pathway. *Nat Cell Biol* 7, 758-765.
- Chiba, T., Matsuzaka, Y., Warita, T., Sugoh, T., Miyashita, K., Tajima, A., Nakamura, M., Inoko, H., Sato, T., and Kimura, M. (2011a). NFKBIL1 confers resistance to experimental autoimmune arthritis through the regulation of dendritic cell functions. *Scand J Immunol* 73, 478-485.
- Chiba, T., Miyashita, K., Sugoh, T., Warita, T., Inoko, H., Kimura, M., and Sato, T. (2011b). IkappaBL, a novel member of the nuclear IkappaB family, inhibits inflammatory cytokine expression. *FEBS Lett* 585, 3577-3581.
- Claudio, E., Brown, K., and Siebenlist, U. (2006). NF-kappaB guides the survival and differentiation of developing lymphocytes. *Cell Death Differ* 13, 697-701.
- Crimeen-Irwin, B., Scalzo, K., Gloster, S., Mottram, P.L., and Plebanski, M. (2005). Failure of immune homeostasis -- the consequences of under and over reactivity. *Curr Drug Targets Immune Endocr Metabol Disord* 5, 413-422.

- 
- Davis, C.B., Killeen, N., Crooks, M.E., Raulet, D., and Littman, D.R. (1993). Evidence for a stochastic mechanism in the differentiation of mature subsets of T lymphocytes. *Cell* 73, 237-247.
- Davis, M.M., and Bjorkman, P.J. (1988). T-cell antigen receptor genes and T-cell recognition. *Nature* 334, 395-402.
- Dechend, R., Hirano, F., Lehmann, K., Heissmeyer, V., Ansieau, S., Wulczyn, F.G., Scheidereit, C., and Leutz, A. (1999). The Bcl-3 oncoprotein acts as a bridging factor between NF-kappaB/Rel and nuclear co-regulators. *Oncogene* 18, 3316-3323.
- Fiorini, E., Schmitz, I., Marissen, W.E., Osborn, S.L., Touma, M., Sasada, T., Reche, P.A., Tibaldi, E.V., Hussey, R.E., Kruisbeek, A.M., *et al.* (2002). Peptide-induced negative selection of thymocytes activates transcription of an NF-kappa B inhibitor. *Mol Cell* 9, 637-648.
- Floess, S., Freyer, J., Siewert, C., Baron, U., Olek, S., Polansky, J., Schlawe, K., Chang, H.D., Bopp, T., Schmitt, E., *et al.* (2007). Epigenetic control of the foxp3 locus in regulatory T cells. *PLoS Biol* 5, e38.
- Fu, S., Zhang, N., Yopp, A.C., Chen, D., Mao, M., Zhang, H., Ding, Y., and Bromberg, J.S. (2004). TGF-beta induces Foxp3 + T-regulatory cells from CD4 + CD25 - precursors. *Am J Transplant* 4, 1614-1627.
- Germain, R.N. (2002). T-cell development and the CD4-CD8 lineage decision. *Nat Rev Immunol* 2, 309-322.
- Gerondakis, S., Grossmann, M., Nakamura, Y., Pohl, T., and Grumont, R. (1999). Genetic approaches in mice to understand Rel/NF-kappaB and IkappaB function: transgenics and knockouts. *Oncogene* 18, 6888-6895.
- Ghosh, S., and Hayden, M.S. (2008). New regulators of NF-kappaB in inflammation. *Nat Rev Immunol* 8, 837-848.
- Goldrath, A.W., and Bevan, M.J. (1999). Selecting and maintaining a diverse T-cell repertoire. *Nature* 402, 255-262.
- Gregersen, P.K., and Behrens, T.W. (2006). Genetics of autoimmune diseases--disorders of immune homeostasis. *Nat Rev Genet* 7, 917-928.
- Grigoriadis, G., Vasanthakumar, A., Banerjee, A., Grumont, R., Overall, S., Gleeson, P., Shannon, F., and Gerondakis, S. (2011). c-Rel Controls Multiple Discrete Steps in the Thymic Development of Foxp3 CD4 Regulatory T Cells. *PLoS One* 6, e26851.
- Harada, M., Matsunaga, K., Oguchi, Y., Iijima, H., Ito, O., Tamada, K., Kimura, G., and Nomoto, K. (1995). The involvement of transforming growth factor beta in the impaired antitumor T-cell response at the gut-associated lymphoid tissue (GALT). *Cancer Res* 55, 6146-6151.

- 
- Hayden, M.S., and Ghosh, S. (2008). Shared principles in NF-kappaB signaling. *Cell* 132, 344-362.
- Hayden, M.S., and Ghosh, S. (2011). NF-kappaB in immunobiology. *Cell Res* 21, 223-244.
- Hayden, M.S., and Ghosh, S. (2012). NF-kappaB, the first quarter-century: remarkable progress and outstanding questions. *Genes Dev* 26, 203-234.
- Heino, M., Peterson, P., Kudoh, J., Nagamine, K., Lagerstedt, A., Ovod, V., Ranki, A., Rantala, I., Nieminen, M., Tuukkanen, J., *et al.* (1999). Autoimmune regulator is expressed in the cells regulating immune tolerance in thymus medulla. *Biochem Biophys Res Commun* 257, 821-825.
- Hirotsu, T., Lee, P.Y., Kuwata, H., Yamamoto, M., Matsumoto, M., Kawase, I., Akira, S., and Takeda, K. (2005). The nuclear IkappaB protein IkappaBNS selectively inhibits lipopolysaccharide-induced IL-6 production in macrophages of the colonic lamina propria. *J Immunol* 174, 3650-3657.
- Hogquist, K.A., Baldwin, T.A., and Jameson, S.C. (2005). Central tolerance: learning self-control in the thymus. *Nat Rev Immunol* 5, 772-782.
- Hori, S. (2010). c-Rel: a pioneer in directing regulatory T-cell lineage commitment? *Eur J Immunol* 40, 664-667.
- Hori, S., Nomura, T., and Sakaguchi, S. (2003). Control of regulatory T cell development by the transcription factor Foxp3. *Science* 299, 1057-1061.
- Hsieh, C.S. (2009). Kickstarting Foxp3 with c-Rel. *Immunity* 31, 852-853.
- Hsieh, C.S., Liang, Y., Tzgnik, A.J., Self, S.G., Liggitt, D., and Rudensky, A.Y. (2004). Recognition of the peripheral self by naturally arising CD25+ CD4+ T cell receptors. *Immunity* 21, 267-277.
- Huehn, J., Polansky, J.K., and Hamann, A. (2009). Epigenetic control of FOXP3 expression: the key to a stable regulatory T-cell lineage? *Nat Rev Immunol* 9, 83-89.
- Isomura, I., Palmer, S., Grumont, R.J., Bunting, K., Hoyne, G., Wilkinson, N., Banerjee, A., Proietto, A., Gugasyan, R., Wu, L., *et al.* (2009). c-Rel is required for the development of thymic Foxp3+ CD4 regulatory T cells. *J Exp Med* 206, 3001-3014.
- Jana, S., Jailwala, P., Haribhai, D., Waukau, J., Glisic, S., Grossman, W., Mishra, M., Wen, R., Wang, D., Williams, C.B., *et al.* (2009). The role of NF-kappaB and Smad3 in TGF-beta-mediated Foxp3 expression. *Eur J Immunol* 39, 2571-2583.
- Kanno, T., and Siebenlist, U. (1996). Activation of nuclear factor-kappaB via T cell receptor requires a Raf kinase and Ca<sup>2+</sup> influx. Functional synergy between Raf and calcineurin. *J Immunol* 157, 5277-5283.

- 
- Kingeter, L.M., Paul, S., Maynard, S.K., Cartwright, N.G., and Schaefer, B.C. (2010). Cutting edge: TCR ligation triggers digital activation of NF-kappaB. *J Immunol* *185*, 4520-4524.
- Kitamura, H., Kanehira, K., Okita, K., Morimatsu, M., and Saito, M. (2000). MAIL, a novel nuclear I kappa B protein that potentiates LPS-induced IL-6 production. *FEBS Lett* *485*, 53-56.
- Klages, K., Mayer, C.T., Lahl, K., Loddenkemper, C., Teng, M.W., Ngiow, S.F., Smyth, M.J., Hamann, A., Huehn, J., and Sparwasser, T. (2010). Selective depletion of Foxp3+ regulatory T cells improves effective therapeutic vaccination against established melanoma. *Cancer Res* *70*, 7788-7799.
- Koopman, G., Reutelingsperger, C.P., Kuijten, G.A., Keehnen, R.M., Pals, S.T., and van Oers, M.H. (1994). Annexin V for flow cytometric detection of phosphatidylserine expression on B cells undergoing apoptosis. *Blood* *84*, 1415-1420.
- Krappmann, D., and Scheidereit, C. (2005). A pervasive role of ubiquitin conjugation in activation and termination of IkappaB kinase pathways. *EMBO Rep* *6*, 321-326.
- Kuwata, H., Matsumoto, M., Atarashi, K., Morishita, H., Hirotani, T., Koga, R., and Takeda, K. (2006). IkappaBNS inhibits induction of a subset of Toll-like receptor-dependent genes and limits inflammation. *Immunity* *24*, 41-51.
- Kyewski, B., and Klein, L. (2006). A central role for central tolerance. *Annu Rev Immunol* *24*, 571-606.
- Lahl, K., Loddenkemper, C., Drouin, C., Freyer, J., Arnason, J., Eberl, G., Hamann, A., Wagner, H., Huehn, J., and Sparwasser, T. (2007). Selective depletion of Foxp3+ regulatory T cells induces a scurfy-like disease. *J Exp Med* *204*, 57-63.
- Lawrence, T., Bebien, M., Liu, G.Y., Nizet, V., and Karin, M. (2005). IKKalpha limits macrophage NF-kappaB activation and contributes to the resolution of inflammation. *Nature* *434*, 1138-1143.
- Lederberg, J. (1959). Genes and antibodies. *Science* *129*, 1649-1653.
- Leithauser, F., Krajina, T., Trobonjaca, Z., and Reimann, J. (2002). Early events in the pathogenesis of a murine transfer colitis. *Pathobiology* *70*, 156-163.
- Li, Q., and Verma, I.M. (2002). NF-kappaB regulation in the immune system. *Nat Rev Immunol* *2*, 725-734.
- Lio, C.W., and Hsieh, C.S. (2008). A two-step process for thymic regulatory T cell development. *Immunity* *28*, 100-111.
- Liou, H.C., Jin, Z., Tumang, J., Andjelic, S., Smith, K.A., and Liou, M.L. (1999). c-Rel is crucial for lymphocyte proliferation but dispensable for T cell effector function. *Int Immunol* *11*, 361-371.

- 
- Liston, A., Lesage, S., Gray, D.H., Boyd, R.L., and Goodnow, C.C. (2005). Genetic lesions in T-cell tolerance and thresholds for autoimmunity. *Immunol Rev* 204, 87-101.
- Long, M., Park, S.G., Strickland, I., Hayden, M.S., and Ghosh, S. (2009). Nuclear factor-kappaB modulates regulatory T cell development by directly regulating expression of Foxp3 transcription factor. *Immunity* 31, 921-931.
- Mantel, P.Y., Ouaked, N., Ruckert, B., Karagiannidis, C., Welz, R., Blaser, K., and Schmidt-Weber, C.B. (2006). Molecular mechanisms underlying FOXP3 induction in human T cells. *J Immunol* 176, 3593-3602.
- Marie, J.C., Letterio, J.J., Gavin, M., and Rudensky, A.Y. (2005). TGF-beta1 maintains suppressor function and Foxp3 expression in CD4+CD25+ regulatory T cells. *J Exp Med* 201, 1061-1067.
- Marson, A., Kretschmer, K., Frampton, G.M., Jacobsen, E.S., Polansky, J.K., MacIsaac, K.D., Levine, S.S., Fraenkel, E., von Boehmer, H., and Young, R.A. (2007). Foxp3 occupancy and regulation of key target genes during T-cell stimulation. *Nature* 445, 931-935.
- Massoumi, R., Chmielarska, K., Hennecke, K., Pfeifer, A., and Fassler, R. (2006). Cxcl12 inhibits tumor cell proliferation by blocking Bcl-3-dependent NF-kappaB signaling. *Cell* 125, 665-677.
- May, M.J., and Ghosh, S. (1998). Signal transduction through NF-kappa B. *Immunol Today* 19, 80-88.
- Molinero, L.L., Yang, J., Gajewski, T., Abraham, C., Farrar, M.A., and Alegre, M.L. (2009). CARMA1 controls an early checkpoint in the thymic development of FoxP3+ regulatory T cells. *J Immunol* 182, 6736-6743.
- Mucida, D., Kutchukhidze, N., Erazo, A., Russo, M., Lafaille, J.J., and Curotto de Lafaille, M.A. (2005). Oral tolerance in the absence of naturally occurring Tregs. *J Clin Invest* 115, 1923-1933.
- Mueller, D.L. (2010). Mechanisms maintaining peripheral tolerance. *Nat Immunol* 11, 21-27.
- Munn, D.H., Zhou, M., Attwood, J.T., Bondarev, I., Conway, S.J., Marshall, B., Brown, C., and Mellor, A.L. (1998). Prevention of allogeneic fetal rejection by tryptophan catabolism. *Science* 281, 1191-1193.
- Okamoto, K., Iwai, Y., Oh-Hora, M., Yamamoto, M., Morio, T., Aoki, K., Ohya, K., Jetten, A.M., Akira, S., Muta, T., *et al.* (2010). IkappaBzeta regulates T(H)17 development by cooperating with ROR nuclear receptors. *Nature* 464, 1381-1385.

- 
- Ostanin, D.V., Bao, J., Koboziev, I., Gray, L., Robinson-Jackson, S.A., Kosloski-Davidson, M., Price, V.H., and Grisham, M.B. (2009). T cell transfer model of chronic colitis: concepts, considerations, and tricks of the trade. *Am J Physiol Gastrointest Liver Physiol* 296, G135-146.
- Pahl, H.L. (1999). Activators and target genes of Rel/NF-kappaB transcription factors. *Oncogene* 18, 6853-6866.
- Park, H.B., Paik, D.J., Jang, E., Hong, S., and Youn, J. (2004). Acquisition of anergic and suppressive activities in transforming growth factor-beta-costimulated CD4+CD25- T cells. *Int Immunol* 16, 1203-1213.
- Pasparakis, M., Luedde, T., and Schmidt-Supprian, M. (2006). Dissection of the NF-kappaB signalling cascade in transgenic and knockout mice. *Cell Death Differ* 13, 861-872.
- Pearse, M., Wu, L., Egerton, M., Wilson, A., Shortman, K., and Scollay, R. (1989). A murine early thymocyte developmental sequence is marked by transient expression of the interleukin 2 receptor. *Proc Natl Acad Sci U S A* 86, 1614-1618.
- Perkins, N.D. (2007). Integrating cell-signalling pathways with NF-kappaB and IKK function. *Nat Rev Mol Cell Biol* 8, 49-62.
- Polansky, J.K., Kretschmer, K., Freyer, J., Floess, S., Garbe, A., Baron, U., Olek, S., Hamann, A., von Boehmer, H., and Huehn, J. (2008). DNA methylation controls Foxp3 gene expression. *Eur J Immunol* 38, 1654-1663.
- Raetz, C.R., and Whitfield, C. (2002). Lipopolysaccharide endotoxins. *Annu Rev Biochem* 71, 635-700.
- Ramsey, C., Winqvist, O., Puhakka, L., Halonen, M., Moro, A., Kampe, O., Eskelin, P., Pelto-Huikko, M., and Peltonen, L. (2002). Aire deficient mice develop multiple features of APECED phenotype and show altered immune response. *Hum Mol Genet* 11, 397-409.
- Ray, P., Yang, L., Zhang, D.H., Ghosh, S.K., and Ray, A. (1997). Selective up-regulation of cytokine-induced RANTES gene expression in lung epithelial cells by overexpression of IkappaBR. *J Biol Chem* 272, 20191-20197.
- Ruan, Q., Kameswaran, V., Tone, Y., Li, L., Liou, H.C., Greene, M.I., Tone, M., and Chen, Y.H. (2009). Development of Foxp3(+) regulatory t cells is driven by the c-Rel enhanceosome. *Immunity* 31, 932-940.
- Ruefli-Brasse, A.A., French, D.M., and Dixit, V.M. (2003). Regulation of NF-kappaB-dependent lymphocyte activation and development by paracaspase. *Science* 302, 1581-1584.

- 
- Ruland, J., Duncan, G.S., Elia, A., del Barco Barrantes, I., Nguyen, L., Plyte, S., Millar, D.G., Bouchard, D., Wakeham, A., Ohashi, P.S., *et al.* (2001). Bcl10 is a positive regulator of antigen receptor-induced activation of NF-kappaB and neural tube closure. *Cell* 104, 33-42.
- Sakaguchi, S., Ono, M., Setoguchi, R., Yagi, H., Hori, S., Fehervari, Z., Shimizu, J., Takahashi, T., and Nomura, T. (2006a). Foxp3+ CD25+ CD4+ natural regulatory T cells in dominant self-tolerance and autoimmune disease. *Immunol Rev* 212, 8-27.
- Sakaguchi, S., Sakaguchi, N., Asano, M., Itoh, M., and Toda, M. (1995). Immunologic self-tolerance maintained by activated T cells expressing IL-2 receptor alpha-chains (CD25). Breakdown of a single mechanism of self-tolerance causes various autoimmune diseases. *J Immunol* 155, 1151-1164.
- Sakaguchi, S., Sakaguchi, N., Shimizu, J., Yamazaki, S., Sakihama, T., Itoh, M., Kuniyasu, Y., Nomura, T., Toda, M., and Takahashi, T. (2001). Immunologic tolerance maintained by CD25+ CD4+ regulatory T cells: their common role in controlling autoimmunity, tumor immunity, and transplantation tolerance. *Immunol Rev* 182, 18-32.
- Sakaguchi, S., Setoguchi, R., Yagi, H., and Nomura, T. (2006b). Naturally arising Foxp3-expressing CD25+CD4+ regulatory T cells in self-tolerance and autoimmune disease. *Curr Top Microbiol Immunol* 305, 51-66.
- Sakaguchi, S., Wing, K., and Miyara, M. (2007). Regulatory T cells - a brief history and perspective. *Eur J Immunol* 37 *Suppl* 1, S116-123.
- Sato, S., Sanjo, H., Tsujimura, T., Ninomiya-Tsuji, J., Yamamoto, M., Kawai, T., Takeuchi, O., and Akira, S. (2006). TAK1 is indispensable for development of T cells and prevention of colitis by the generation of regulatory T cells. *Int Immunol* 18, 1405-1411.
- Schluter, C., Duchrow, M., Wohlenberg, C., Becker, M.H., Key, G., Flad, H.D., and Gerdes, J. (1993). The cell proliferation-associated antigen of antibody Ki-67: a very large, ubiquitous nuclear protein with numerous repeated elements, representing a new kind of cell cycle-maintaining proteins. *J Cell Biol* 123, 513-522.
- Schmidt-Suppran, M., Courtois, G., Tian, J., Coyle, A.J., Israel, A., Rajewsky, K., and Pasparakis, M. (2003). Mature T cells depend on signaling through the IKK complex. *Immunity* 19, 377-389.
- Schmitz, M.L., and Krappmann, D. (2006). Controlling NF-kappaB activation in T cells by costimulatory receptors. *Cell Death Differ* 13, 834-842.
- Scholzen, T., and Gerdes, J. (2000). The Ki-67 protein: from the known and the unknown. *J Cell Physiol* 182, 311-322.

- 
- Schwarz, B.A., and Bhandoola, A. (2006). Trafficking from the bone marrow to the thymus: a prerequisite for thymopoiesis. *Immunol Rev* 209, 47-57.
- Sen, R., and Baltimore, D. (1986). Inducibility of kappa immunoglobulin enhancer-binding protein Nf-kappa B by a posttranslational mechanism. *Cell* 47, 921-928.
- Shortman, K. (1992). Cellular aspects of early T-cell development. *Curr Opin Immunol* 4, 140-146.
- Siddiqui, K.R., and Powrie, F. (2008). CD103+ GALT DCs promote Foxp3+ regulatory T cells. *Mucosal Immunol* 1 *Suppl* 1, S34-38.
- Siebenlist, U., Brown, K., and Claudio, E. (2005). Control of lymphocyte development by nuclear factor-kappaB. *Nat Rev Immunol* 5, 435-445.
- Sprent, J., and Kishimoto, H. (2001). The thymus and central tolerance. *Philos Trans R Soc Lond B Biol Sci* 356, 609-616.
- Stewart, I., Schluter, P.J., and Shaw, G.R. (2006). Cyanobacterial lipopolysaccharides and human health - a review. *Environ Health* 5, 7.
- Sun, C.M., Hall, J.A., Blank, R.B., Bouladoux, N., Oukka, M., Mora, J.R., and Belkaid, Y. (2007). Small intestine lamina propria dendritic cells promote de novo generation of Foxp3 T reg cells via retinoic acid. *J Exp Med* 204, 1775-1785.
- Takikawa, O. (2005). Biochemical and medical aspects of the indoleamine 2,3-dioxygenase-initiated L-tryptophan metabolism. *Biochem Biophys Res Commun* 338, 12-19.
- Tavares, G.A., Panepucci, E.H., and Brunger, A.T. (2001). Structural characterization of the intramolecular interaction between the SH3 and guanylate kinase domains of PSD-95. *Mol Cell* 8, 1313-1325.
- Terzidou, V., Blanks, A.M., Kim, S.H., Thornton, S., and Bennett, P.R. (2011). Labor and inflammation increase the expression of oxytocin receptor in human amnion. *Biol Reprod* 84, 546-552.
- Thome, M. (2004). CARMA1, BCL-10 and MALT1 in lymphocyte development and activation. *Nat Rev Immunol* 4, 348-359.
- Thornton, A.M., Korty, P.E., Tran, D.Q., Wohlfert, E.A., Murray, P.E., Belkaid, Y., and Shevach, E.M. (2010). Expression of Helios, an Ikaros transcription factor family member, differentiates thymic-derived from peripherally induced Foxp3+ T regulatory cells. *J Immunol* 184, 3433-3441.
- Toker, A., and Huehn, J. (2011). To be or not to be a treg cell: lineage decisions controlled by epigenetic mechanisms. *Sci Signal* 4, pe4.
- Tonegawa, S. (1983). Somatic generation of antibody diversity. *Nature* 302, 575-581.

- 
- Totzke, G., Essmann, F., Pohlmann, S., Lindenblatt, C., Janicke, R.U., and Schulze-Osthoff, K. (2006). A novel member of the I kappa B family, human I kappa B-zeta, inhibits transactivation of p65 and its DNA binding. *J Biol Chem* 281, 12645-12654.
- Touma, M., Antonini, V., Kumar, M., Osborn, S.L., Bobenchik, A.M., Keskin, D.B., Connolly, J.E., Grusby, M.J., Reinherz, E.L., and Clayton, L.K. (2007). Functional role for I kappa BNS in T cell cytokine regulation as revealed by targeted gene disruption. *J Immunol* 179, 1681-1692.
- Touma, M., Keskin, D.B., Shiroki, F., Saito, I., Koyasu, S., Reinherz, E.L., and Clayton, L.K. (2011). Impaired B cell development and function in the absence of I kappa BNS. *J Immunol* 187, 3942-3952.
- Tran, D.Q., Ramsey, H., and Shevach, E.M. (2007). Induction of FOXP3 expression in naive human CD4+FOXP3 T cells by T-cell receptor stimulation is transforming growth factor-beta dependent but does not confer a regulatory phenotype. *Blood* 110, 2983-2990.
- Uren, A.G., O'Rourke, K., Aravind, L.A., Pisabarro, M.T., Seshagiri, S., Koonin, E.V., and Dixit, V.M. (2000). Identification of paracaspases and metacaspases: two ancient families of caspase-like proteins, one of which plays a key role in MALT lymphoma. *Mol Cell* 6, 961-967.
- van Santen, H.M., Benoist, C., and Mathis, D. (2004). Number of T reg cells that differentiate does not increase upon encounter of agonist ligand on thymic epithelial cells. *J Exp Med* 200, 1221-1230.
- Vang, K.B., Yang, J., Mahmud, S.A., Burchill, M.A., Vegoe, A.L., and Farrar, M.A. (2008). IL-2, -7, and -15, but not thymic stromal lymphopoietin, redundantly govern CD4+Foxp3+ regulatory T cell development. *J Immunol* 181, 3285-3290.
- Verhagen, J., and Wraith, D.C. (2010). Comment on "Expression of Helios, an Ikaros transcription factor family member, differentiates thymic-derived from peripherally induced Foxp3+ T regulatory cells". *J Immunol* 185, 7129; author reply 7130.
- Vignali, D. (2008). How many mechanisms do regulatory T cells need? *Eur J Immunol* 38, 908-911.
- Vignali, D.A., Collison, L.W., and Workman, C.J. (2008). How regulatory T cells work. *Nat Rev Immunol* 8, 523-532.
- von Boehmer, H. (1991). Positive and negative selection of the alpha beta T-cell repertoire in vivo. *Curr Opin Immunol* 3, 210-215.
- von Boehmer, H., Teh, H.S., and Kisielow, P. (1989). The thymus selects the useful, neglects the useless and destroys the harmful. *Immunol Today* 10, 57-61.

- 
- Wan, Y.Y., Chi, H., Xie, M., Schneider, M.D., and Flavell, R.A. (2006). The kinase TAK1 integrates antigen and cytokine receptor signaling for T cell development, survival and function. *Nat Immunol* 7, 851-858.
- Waubant, E. (2006). Biomarkers indicative of blood-brain barrier disruption in multiple sclerosis. *Dis Markers* 22, 235-244.
- Wildin, R.S., Ramsdell, F., Peake, J., Faravelli, F., Casanova, J.L., Buist, N., Levy-Lahad, E., Mazzella, M., Goulet, O., Perroni, L., *et al.* (2001). X-linked neonatal diabetes mellitus, enteropathy and endocrinopathy syndrome is the human equivalent of mouse scurfy. *Nat Genet* 27, 18-20.
- Yamauchi, S., Ito, H., and Miyajima, A. (2010). IkappaBeta, a nuclear IkappaB protein, positively regulates the NF-kappaB-mediated expression of proinflammatory cytokines. *Proc Natl Acad Sci U S A* 107, 11924-11929.
- Zheng, Y., Josefowicz, S., Chaudhry, A., Peng, X.P., Forbush, K., and Rudensky, A.Y. (2010). Role of conserved non-coding DNA elements in the Foxp3 gene in regulatory T-cell fate. *Nature* 463, 808-812.
- Zuniga-Pflucker, J.C. (2004). T-cell development made simple. *Nat Rev Immunol* 4, 67-72.

---

## 8. Declaration of originality

Marc Patrick Schuster

Franz-Liszt-Straße 40

38106 Braunschweig

Hiermit erkläre ich, dass die eingereichte Dissertation mit dem Titel

### **The unusual NF $\kappa$ B inhibitor I $\kappa$ B<sub>NS</sub> regulates Foxp3 expression**

von mir selbständig verfasst wurde, nicht schon als Dissertation verwendet wurde und benutzte Hilfsmittel und Quellen vollständig angegeben wurden.

Weiterhin erkläre ich, dass ich weder diese noch eine andere Arbeit zur Erlangung des akademischen Grades doctor rerum naturalium (Dr. rer. nat.) an anderen Einrichtungen eingereicht habe.

Magdeburg, den 24.2.2012

Marc Patrick Schuster

---

## 9. Curriculum vitae

Name: Marc Patrick Schuster

Geburt: 02 Juli 1982 in Wuppertal

Familienstand: ledig

Nationalität: deutsch-österreich

### Schule und Ausbildung:

1989-1993 Städt. Grundschule Donarstrasse, Wuppertal  
1993-2002 Wilhelm-Dörpfeld-Gymnasium, Wuppertal  
06/2002 Allgemeine Hochschulreife (Abitur)  
09/2002-03/2007 Studium der Biologie an der Heinrich-Heine-Universität, Düsseldorf  
06/2006-03/2007 Diplomarbeit am Institut für Molekulare Medizin bei PD Dr. Ingo Schmitz, Heinrich-Heine-Universität, Düsseldorf  
03/2007 Erwerb des akademischen Grades Diplom-Biologe

### Berufstätigkeit:

08/2001-06/2002 Programmierer der Firma Osthoff-Senge, GmbH, Wuppertal  
07/2002-06/2006 Werksstudent der Firma Morét und Partner, Haan

### Wissenschaftliche Tätigkeit:

03/2007 Erwerb des Fachkundenachweises gem. §9 des Tierschutzgesetzes  
03/2007-03/2009 Beginn der Doktorarbeit am Institut für Molekulare Medizin, Düsseldorf bei PD. Dr. Ingo Schmitz  
03/2009-09/2009 Fortsetzung der Doktorarbeit am Institut für Medizinische Mikrobiologie und Krankenhaushygiene, Düsseldorf bei PD. Dr. Ingo Schmitz  
seid 09/2009 Fortsetzung der Doktorarbeit am Helmholtz-Zentrum für Infektionsforschung, Braunschweig bei Prof. Dr. Ingo Schmitz

### Sonstiges:

2001-2004 Kommissarischer Jugendwart des TSC 95 Haan e.V.  
2004-2006 Pressewart des TSC 95 Haan e.V.

### Originalarbeiten:

- 1) Ueffing N, **Schuster M**, Keil E, Schulze-Osthoff K, Schmitz I "Upregulation of c-FLIP<sub>short</sub> by NFAT contributes to apoptosis resistance of short-term activated T cells". Blood 2008 Aug 1;112(3):690-8.
- 2) Brandt S, Beuter-Gunia C, **Schuster M**, Hausser A, Schmitz I, Beer-Hammer S "The nucleo-cytoplasmic protein SLy2 targets the SAP30/HDAC1 complex" Int J Biochem Cell Biol. 2010 Sep;42(9):1472-81.
- 3) Ewald F, Ueffing N, Brockmann L, Hader C, Telieps T, **Schuster M**, Schulz WA, Schmitz I "The role of c-FLIP variants in urothelial tumours". Cell Death Dis. 2011 Dec 22;2:e245